# THE CALCULATION OF THE LIFT DISTRIBUTION AND THE NEAR VORTEX WAKE BEHIND HIGH AND LOW ASPECT RATIO WINGS IN SUBSONIC FLOW

Josef Rom, et al

Technion - Israel Institute of Technology

Prepared for:

Air Force Office of Scientific Research

January 1973

S.R. No. 2.

JANUARY 1973

Technion Research &
Development Foundation
Haifa, Israel



SCIENTIFIC REPORT No. 2

# THE CALCULATION OF THE LIFT DISTRIBUTION AND THE NEAR VORTEX WAKE BEHIND HIGH AND LOW ASPECT RATIO WINGS IN SUBSONIC FLOW

BY

JOSEF ROM and CARLOS ZOREA



Department of Aeronautical Engineering
Technion — Israel Institute of Technology,
Haifa, Israel



T. A. E. REPORT No. 168

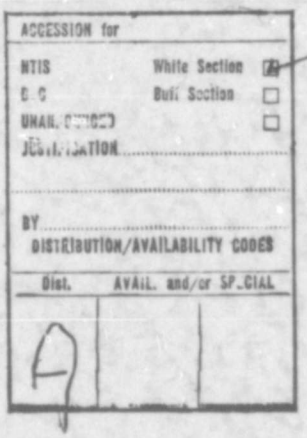


Qualified requestors may obtain additional copies from the Defense Documentation Center; all others should apply to the Clearinghouse for Federal Scientific and Technical Information.

DOCUMENT CONTROL DATA - R & D

(Security classification of title, body of abstract and indexing annotation must be entered when the overall report is classified)

1. ORIGINATING ACTIVITY (Corporate author)
TECHNION RESEARCH AND DEVELOPMENT FOUNDATION
AERONAUTICAL ENGINEERING DEPARTMENT
HAIFA, ISRAEL

2a. REPORT SECURITY CLASSIFICATION
UNCLASSIFIED

2b. GROUP

3. REPORT TITLE
THE CALCULATION OF THE LIFT DISTRIBUTION AND THE NEAR VORTEX WAKE BEHIND HIGH AND LOW ASPECT RATIC WINGS IN SUBSONIC FLOW

4. DESCRIPTIVE NOTES (Type of report and inclusive dates)
Scientific Interim

5. AUTHOR(S) (First name, middle initial, last name)
JOSEF ROM CARLOS ZOREA

| 6. REPORT DATE | 7a. TOTAL NO. OF PAGES | 7b. NO. OF REFS |
|---|---|---|
| Jan 1973 | 94 | 41 |

| 8a. CONTRACT OR GRANT NO. | 9a. ORIGINATOR'S REPORT NUMBER(S) |
|---|---|
| AFOSR-71-2145 | TAE Rpt No. 168 |
| b. PROJECT NO. 9781-01 | Sci Rpt No. 2 |
| c. 61102F | 9b. OTHER REPORT NO(S) (Any other numbers that may be assigned this report) AFOSR - TR - 73 - 0652 |
| d. 681307 | |

10. DISTRIBUTION STATEMENT
Approved for public release; distribution unlimited.

| 11. SUPPLEMENTARY NOTES | 12. SPONSORING MILITARY ACTIVITY |
|---|---|
| TECH, OTHER | AF Office of Scientific Research (NAM)<br>1400 Wilson Blvd.<br>Arlington, Va. 22209 |

13. ABSTRACT

A method is presented for the combined calculation of the lift, and lift distribution on a wing and also of the trailing vortex flow behind the wing. It is assumed that the lift of a wing is generated by a system of vortices distributed over the complete wing planform and shed away from each elemental area on the planform. Using the concepts of the vortex lattice method, it is assumed in the linear lift variation case, that the vortices are aligned on the wing planform and are shed away from the trailing edges. Due to this interaction between the vortices on the wing and in the trailing wake the well known rolled up vortex sheet is obtained. When the vortices from each element on the planform are allowed to be shed locally into the flow, the interactions between these free vortices and the bound vortices on the wing results in a nonlinear lift variation. Vortex line interaction calculations for the trajectories of these vortex lines are now being programmed. As a result, the leading edge lift vortices which are obtained on slender wings can now be handled. This report contains a description of the numerical method. It is suggested numerical difficulties in representing a vortex sheet by discrete line vortices can be avoided by proper selection of the vortex spacing. The calculation based on the present method result in good estimation of the lift coefficients (both the linear and nonlinear cases) for wings of any aspect ratio when conpared to available experimental data. The vortex sheet shape calculated for the high aspect ratio wings is qualitatively in agreement with experimental data. Quantitative evaluation is hampered by the fact that the accuracy of the experimental data due to effects of wing tunnel and instrumentation interferences has not been resolved.

DD FORM 1 NOV 65 1473



UNCLASSIFIED
Security Classification

| 14. KEY WORDS | LINK A | | LINK B | | LINK C | |
|---|---|---|---|---|---|---|
| | ROLE | WT | ROLE | WT | ROLE | WT |
| CALCULATION OF LIFT | | | | | | |
| NEAR VORTEX WAKE | | | | | | |
| HIGH ASPECT RATIO WINGS | | | | | | |
| LOW ASPECT RATIO WINGS | | | | | | |
| SUBSONIC FLOWS | | | | | | |
| TRAILING VORTEX | | | | | | |



UNCLASSIFIED

Security Classification

[redacted]

JANUARY 1973.

S.R. No. 2.

SCIENTIFIC REPORT No. 2.

# THE CALCULATION OF THE LIFT DISTRIBUTION AND THE NEAR VORTEX WAKE BEHIND HIGH AND LOW ASPECT RATIO WINGS IN SUBSONIC FLOW.

by

JOSEF ROM and CARLOS ZOREA
Department of Aeronautical Engineering
Technion - Israel Institute of Technology,
Haifa, Israel.

T.A.E. REPORT No. 168



[redacted]

The research reported in this paper has been sponsored in part by the Air Force Office of Scientific Research (AFSC), United States Air Force under Grant AFOSR 71-2145.

## ABSTRACT

This report presents a method for the combined calculation both of the lift, and lift distribution on a wing and also of the trailing vortex flow behind the wing. It is assumed that the lift of a wing is generated by a system of vortices distributed over the complete wing planform and shed away from each elemental area on the planform. Using the concepts of the vortex lattice method, it is assumed in the linear lift variation case, that the vortices are aligned on the wing planform and are shed away from the trailing edges. Due to this interaction between the vortices on the wing and in the trailing wake the well known rolled up vortex sheet is obtained. When the vortices from each element on the planform are allowed to be shed locally into the flow, the interaction between these free vortices and the bound vortice on the wing results in the nonlinear lift variation. The completion of the vortex line interaction calculations for the trajectories of these vortex lines which are now being programmed will result in a rolled up vortex sheet starting from the leading edges; that is, the leading edge lift vortices which are obtained on slender wings should now be simulated.

The present report contains the description of the numerical method. It is suggested that the numerical difficulties in representing a vortex sheet by discrete line vortices may be due to the use of potential vortices which introduce velocity singularities at their centers. These problems can be avoided by proper selection of the vortex spacing. The

calculations based on the present method result in good estimation of the lift coefficients (both the linear and nonlinear cases) for wings of any aspect ratio when compared to available experimental data. The vortex sheet shape calculated for the high aspect ratio wings is qualitatively in agreement with experimental data. Quantitative evaluation is hampered by the fact that the accuracy of the experimental data due to effects of wind tunnel and instrumentation interferences has not been resolved. The vortex sheet shape over slender wings is still being calculated by the present method and results will be presented in a future report.

## TABLE OF CONTENTS

## LIST OF SYMBOLS

| | |
|---|---|
| AR | aspect ratio |
| b | wing span |
| $c_i$ | local chord |
| C | chord - rectangular wing |
| $c_\ell$ | two-dimensional lift coefficient |
| $C_L$ | lift coefficient |
| $C_{L_\alpha}$ | lift slope coefficient |
| $C_M$ | moment coefficient |
| h | distance between a point and the line vortex |
| [H] | geometry influence matrix |
| k | vortex strength |
| [K] | vortex strength matrix |
| $\ell_x, \ell_y$ | distances from bound wing vortex cells to a line passing through the wing apex |
| M | number of steps in the vortex interactions calculation |
| N | number of discrete vortices used in the vortex sheet representation |
| $Q_j$ | components of the induced velocity vector (in the three dimensional case) at point (j) |
| x,y,z | space coordinates (the origin at the mid span trailing edge) |
| $x_{c.p.}$ | longitudinal center of pressure |
| $y_{c.p.}$ | lateral center of pressure |
| s | wing area |

| | |
|---|---|
| $U$ | free stream velocity |
| $v_i$ | components of the induced velocity at point (i) ( in the two-dimensiona case) |
| $[V]$ | velocity matrix |
| $\alpha$ | angle of attack |
| $\alpha_i$ | |
| $\beta_i$ | angles formed between vortex segment and a point in space |
| $\Gamma$ | calculation |

## LIST OF FIGURES

## LIST OF FIGURES (CONT'D)

## LIST OF TABLES

TABLE No.

## LIST OF TABLES (CONT'D)

TABLE No.

## 1. INTRODUCTION

Every aircraft in flight trails behind it a region of disturbed flow. At subsonic speeds this flow is influenced mainly by the vortex system generated by the wing lift. The strength of these vortices increases as the wing lift is increased. Furthermore, the vortices tend to persist for great distances behind the wing since the viscous dissipation is weak at flight Reynolds numbers.

It is known that the vortex layer behind the wing tips and the trailing edges is unstable and rolls up into two well defined vortices. For some large aircraft the measured tangential velocities at the edges of the cores of these trailing vortices reach values of 200 to 300 ft. per second[1,2]. These velocities are large enough to become a serious technological problem (illustrated in Fig. 1) in the determination of airplane spacing around busy airports and in flight corridors. The overall circulation around the cores is fixed by the maximum wing chordwise circulation, which is normally at center span, and, since the span-loading distributions of wings do not vary much in shape under normal circumstances, the circulation is proportional to the wing lift with approximately the same constant of proportionality in all cases. Any significant change in this constant can only be brought about by drastic modifications to the normal wing geometry, inevitably resulting in a considerable loss of efficiency. However, the diameter of the cores, and hence the maximum velocities near their edges may be amenable to more subtle treatment. Before we can contemplate how to do this, we must know more about how the wake is

influenced by the details of the wing geometry and how the rolling-up process occurs.

Another possibility for reducing the effects of the trailing vortices is to try and increase dissipation. This viscous dissipation at flight Reynolds numbers is generally rather weak, and, barring any other effects, the trailing vortices may persist for a distance which is of the order of many thousands of wing spans, i.e., a considerable number of miles behind a large airplane. One mechanism by means of which the dissipation is accelerated is by the breakup of the trailing vortex pair into small ring vortices. This breakup is due to the instability of the system caused by the amplification of oscillatory disturbances[2]. This instability may be triggered earlier by oscillatory variation of the wing lift or it may be affected by variation of wing lift distribution. Therefore, either of the two ways of affecting the trailing vortices requires a knowledge of the relationship between the lift distribution on the wing and the trailing vortex flow field.

This report presents a method for the combined calculation both of the lift distribution on the wing planform and the trailing vortex flow field behind a wing. The lift of a wing is generated by a system of vortices which are then shed into a vortex sheet behind the wing. For a high aspect ratio wing, these vortices roll up into the well known tip vortices[3,4,5,6]. A seemingly different flow structure is observed on low aspect ratio wings[7,8,9], where the vortices seem to be shed from the leading edges and the wing tips and in this case an additional lift

is obtained (the nonlinear lift). In the present analysis we assume that the vortices which are generated at the tips and the trailing edges of the high aspect-ratio wing should be similar in nature to those which are generated by the leading edges and tips of the low aspect-ratio wing. Although the appearance of the leading-edge vortices is associated with the boundary layer separation it has been shown [8,9,10,11,12,13,14] that the lift generated can be obtained without direct calculation of the boundary layer separation. This formulation enables the setting up of a vortex distribution on the wing planform regardless of whether it is a low aspect-ratio or a high aspect-ratio wing. Therefore, it should be possible to obtain the correct lift distribution by a unified method for any wing in subsonic flow.

The lift of a wing is obtained by adding the contributions of the vortices distributed over the wing planform. There are various analytical and numerical methods for the calculation of this lift distribution. The vortex lattice method [15,16] used in the lift calculations is selected as being best suited for our purpose. In the classical vortex lattice method the vortex lines are assumed to remain straight after being shed from the wing. It can be shown that this approximation gives reasonable results for lift distribution on a high aspect-ratio wing. However, in the case of low aspect-ratio wings, particularly at high angles of attack, one must include the effects of the interactions between the vortices. These interactions change the trajectories of the vortices and the result is a rolled up vortex sheet. This new shape of the vortex wake must be included in the calculation of the lift. Therefore a calculation

scheme that includes a vortex lattice on the wing planform and trajectories of the shedded vortices and their mutual interactions will yield a single procedure for the generalized calculation of lift for all types of wings. A numerical method for the calculation of the lift distribution by a scheme including the interactions between the vortices is developed. In the present calculation the effect of the non planar rolled up wake is considered. The results of these lift and vortex-wake calculations are being compared with availabe experimental results.

In the present report all the calculations are applicable only to incompressible flows. Therefore, the results are applicable only for wings at low speed. There are various ways of including effects of compressibility, these however have not been used as yet for the vortex roll-up calculations.

## 2. OUTLINE OF THE ANALYTICAL MODELS USED IN THE CALCULATIONS

The analytical models used in the calculations of the lift distribution and the rolling up of the vortex sheet are presented in graphical form in Figs. 2,3 and 4.

### 2.1. The Elliptic Lift Distribution

The basic approximation is in the representation of the distributed vorticity on the wing planform and in the trailing vortex sheet by discrete line vortices. This approximation was introduced by Westwater[4] in 1936. He represented the elliptical lift distribution by twenty discrete line vortices. In his model, the line vortices extended to infinity in both directions and the effect of the bound vortex was neglected. This is shown as model (a) in Fig. 2. Using this model, Westwater showed that due to mutual interactions the line vortices will roll up into two concentrated tip vortices. Initially the line vortices are in a plane and therefore this is a two-dimensional model which can be called the "elliptic, two-dimensional, rolled-up vortex wake". Some numerical problems are encountered in the calculations using these discrete vortex lines. These will be discussed in Part (3.2) where the numerical procedure is presented.

An improved calculation is obtained by including the effect of the bound vortex and eliminating the upstream portion of the line vortices from $-\infty$ to the wing bound vortex line. This is presented as model (b) in Fig. 2. In this model the elliptic lift distribution is still used, however the introduction of the bound vortex in the wing planform results in a simplified three-dimensional vortex system when the wing is held at an

angle of attack. This model will be called the "elliptic, three-dimensional rolled-up vortex wake".

## 2.2. Lift Distribution Based on the Vortex Lattice Method

Models using a more realistic lift distribution on the wing planform are presented in Fig. 3. These models are limited to linear variation of the lift with angle of attack. There are several methods for the calculation of the lift distribution on the wing planform. The vortex lattice method has been selected here as being the most suitable for the numerical calculations of the vortex wake roll up. These calculations are carried out using the steps shown in Fig. 3.

**Step 1**

Calculation of the lift on the wing planform by the vortex lattice method (VLM). The wing is subdivided in both the spanwise and chordwise directions,into a number of elemental areas and the circulation distribution is calculated assuming a planar wake.

**Step 2**

The calculated spanwise circulation distribution is placed on the wing trailing edge. A two-dimensional vortex interaction calculation is now performed, from which the rolled-up wake is obtained.

**Step 3**

The original VLM lift distribution, obtained in Step 1, is now combined with the two-dimensional rolled-up vortex wake obtained in Step 2. Calculating their mutual interactions results in a new rolled-up vortex wake. This solution is called the"VLM-3D rolled-up wake".

Step 4

The mutual interaction of the VLM lift distribution and the three-dimensional rolled-up wake which was determined in step 3 results in a new lift distribution which is calculated by an iteration procedure. The method is called "the modified vortex-lattice method" (MVLM).

Step 5

The lift distribution determined in the MVLM calculation is now used to modify the three-dimensional rolled-up wake to obtain the"MVLM 3D rolled-up wake"

## 2.3. The Non-Linear Lift Distribution

The VLM calculations are based on variations of lift with angle of attack and therefore are applicable mainly to high-aspect-ratio wings. The non-linear lift variation, that is of particular interest for low-aspect ratio wings, is obtained by the procedure which is shown in Fig. 4, using the following steps:

Step 1.

The non-linear lift distribution is calculated by dividing the wing planform in the spanwise and chordwise directions. The values of the circulation at each of the resulting cells is calculated assuming straight vortex lines to be shed from each one of the cells at a prescribed angle to the flow direction.

Step 2.

The straight line vortices shed from each cell are allowed to interact and their new trajectories are obtained. This calculation results in a three-dimensional, non-linear, rolled-up wake.

Step 3.

The calculations of steps 1 and 2 are repeated until convergence is obtained for the vortex strength in each one of the cells. This calculation results in the final shape of the three-dimensional, non-linear, rolled-up wake. Thus this calculation results in the evaluation of the distribution of lift on the wing planform and also the shape of the rolled-up vortex sheet.

This method is called the NLMVLM-3D method ("Non-Linear, Modified Vortex-Lattice Method in Three Dimensions").

## 3. OUTLINE OF THE NUMERICAL PROCEDURES

### 3.1. The Representation of the Vortex Sheet by Discrete Vortices

The numerical method for the representation of the wing vortex sheet utilizes a finite number of line vortices. The early work of Westwater[4] showed that the vortex sheet so represented will roll up at the edges. This formulation results in a two-dimensional problem for the location of the individual line vortices at each plane. Performing this calculation on a digital computer was hampered by various numerical difficulties. It is stated in Ref. 17 that the approximation of replacing a vortex sheet by an array of line vortices has inherent problems due to the trajectories of the outer vortices. Furthermore it is shown that these difficulties cannot be avoided by increasing the subdivisions used.

The discrete vortices used in the work of Westwater[4] and discussed in Ref. 17 have a velocity singularity at their centers. Therefore as the distance between a pair of vortex lines diminishes numerical problems arise. This problem can be avoided if we remember that when dealing with discrete vortices, we must specify a minimum distance of approach between two vortices, that is, specify a core radius. When two vortices are in such close proximity that their cores are in contact then we specify that they combine to a single vortex whose strength equals the sum of the two vortices. The new core area may be assumed to be proportional to the total circulation. This hypothesis must limit the number of discrete vortices which can be obtained over a wing span.

This procedure may be justified also by the fact that in previous calculations reasonable results were obtained only when a limited number of discrete vortices were used.

Our first numerical solutions did not include the finite core model just discussed. Therefore, the various numerical problems which are associated with the discrete potential vortices were excluded by varying the number of vortices and the number of segments into which each vortex was divided until the numerical difficulty disappeared.

3.2. Two-Dimensional Trailing Vortex Calculations

In the simplified approximation,discussed in 2.1, the circulation on the wing is assumed to be elliptic:

$$\Gamma = \Gamma_o[1 - y^2/(b/2)^2]^{1/2} \tag{1}$$

This circulation is divided into a number of discrete vortices. The commonly used divisions are either equal strength vortices or equally spaced ones. The induced velocity is derived from the Biot-Savart Law:

$$v_i = -\frac{1}{2\pi} \sum_{j=1}^{n} \frac{K_n(y_j - y_n)}{(x_j-x_n)^2+(y_j-y_n)^2} \quad n \neq j \tag{2}$$

$$w_i = \frac{1}{2\pi} \sum_{j=1}^{n} \frac{K_n(x_j-x_n)}{(x_j-x_n)^2-(y_j-y_n)^2} \quad n \neq j \tag{3}$$

The displacement of a line vortex is then obtained

$$dy = v_i dt = v_i \frac{dx}{V} \tag{4}$$

$$dz = w_i dt = w_i \frac{dx}{V} \tag{5}$$

The vortex system center of gravity for the elliptic distribution is

$$y_{cg} = \frac{\int_0^{b/2} y \frac{d\Gamma}{dy} dy}{\int_0^{b/2} \frac{d\Gamma}{dy} dy} = \frac{\pi}{4} (b/2) \tag{6}$$

$$z_{cg} = 0$$

The numerical calculation based on these relations indicated three problems, which are the manifestation of the difficulties discussed in 3.1. These are: firstly, the "escaping" of the vortex near the tip,(Fig.5). Secondly, the vortex lines cross over each other (physically impossible in real flow) and thirdly, the cross-section of the vortex sheet becomes irregular when many vortices and many steps in the calculation are used. These difficulties are illustrated in Figures 6 and (7).

The first problem is due to the short distance between the two vortices at the tip. As discussed in 3.1. this difficulty is due to the difference between the real velocity distribution as shown in sketch (a), and the potential vortex used in the relations (2) and (3) shown on sketch (b).

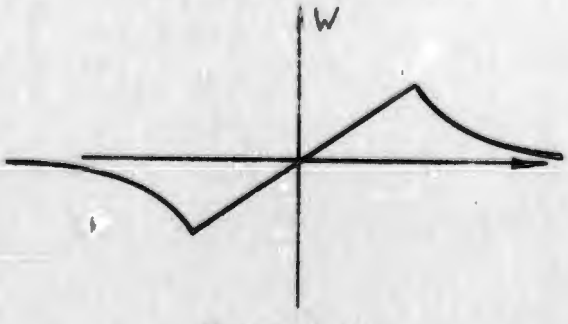


Sketch (a)

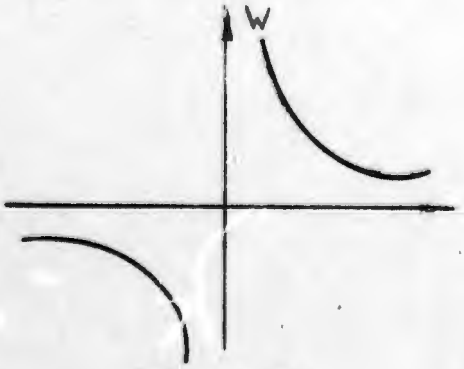


Sketch (b)

The initial spacing between the vortices in the tip zone is larger in the equally spaced case than in the equal strength one. This numerical difficulty is thus less severe in the equally spaced distribution which is therefore adopted in this work.

The problem of crossover of the vortex lines is eliminated by selecting the number of vortices and the number of steps in the calculation. The problem of irregular shape of the cross-section of the vortex sheet is caused by a large number of vortices or very short streamwise steps in the calculation. This problem again can be avoided by selecting a proper combination of the number of vortices and the number of steps.

Calculations were performed with a wide range of variables. These calculations indicate that the combinations of N = 5 with M = 16,32,64, 104; N = 10, M = 16,32,64; N = 20, M = 32, result in well behaved solutions as shown in the two-dimensional case in Figure 8.. The center of gravity of the tip vortex for all these cases remains in the original position, as required by Betz's theorems[18].

### 3.3. The Vortex Wake Modified by the Bound Vortex

A more realistic model for the vortex wake of a wing can be obtained by inclusion of the effects of the bound vortex and the substraction of the effect of the upstream vortices from the simplified two dimensional model. The first iteration starts with the vortex pattern obtained in the previous calculation described in 3.2. The solution is obtained by substracting the induced velocities due to the upstream vortices extending from $-\infty$ to 0, and by adding the effect of the bound vortex at 0.25C.

The sections of the trailing vortices from the trailing edge to this bound vortex are also added as seen in Fig. (2b). The velocity field is now calculated by the relation

$$Q_j = \sum_{i=1}^{n} \frac{k_i}{4\pi h_i} (\cos\alpha_i + \cos\beta_i) \qquad n \neq j \qquad (7)$$

The system is solved by an iteration procedure until the velocities of successive calculations converge to within a predetermined tolerance. The result of the trailing vortex calculation is shown in Figure 8, and is compared there with the two-dimensional calculation. It is clearly seen that the bound vortex does affect the flow field although qualitatively both solutions are similar. A somewhat similar solution was presented by Hacket and Evans[19]. In Reference 19 the Westwater solution is modified in the cross flow plane allowing for the influence of the wing bound vortex. The calculation is based on a known spanwise lift distribution and it is shown that a vortex grouping is obtained at the tip. However, in this calculation the vortex sheet does sometimes cross itself. An additional calculation based on a similar method is presented by Butter and Hancock[20]. A method is developed for the prediction of the spatial distribution of the trailing vortices during the rolling up process, giving the overall downwash field behind the wing. The method extends Westwater's model to include the effect of the wing bound vortex and the three-dimensional pattern of trailing vortices. In this calculation the swept wing is replaced by a single lifting bound vortex which represents the circulation distribution around the wing while the trailing vortex sheet is

approximated by a number of discrete line vortices. Starting with a nearly planar system and following a step by step calculation working downstream aft of the wing trailing edge, the deformation of the trailing vortex sheet is determined. A further iteration procedure, keeping the same spanwise load distribution on the wing checks out the results. It has been found in Ref. (19) (as in our work) that using equally spaced vortices avoids many of the numerical problems which are found when vortices of equal strength are used. Numerical aspects and the accuracy of representing the wing by a single bound vortex are not discussed in Ref. 20.

It can be noted that since the entire vortex pattern consists of straight line segments the calculation of the downwash and sidewash at any point is based on the Biot Savart-Law. The principal factors limiting the accuracy of the results are the step length and the number and position of the vortices chosen to represent the trailing vortex sheet.

### 3.4. The Modified Vortex Lattice Method

A more realistic approximation to the wing lift distribution can be obtained by the use of the vortex lattice method where the wing surface is divided into a large number of cells, where each of the cells is treated as a lifting surface. Therefore, each cell is represented by a single horseshoe vortex with its bound vortex at the 1/4 cell chord and the trailing vortices are assumed to be straight lines trailing to infinity. The vortices are determined so that the

velocity boundary condition at the 3/4 chord line of each cell due to the total wing circulation is satisfied. The method was first developed by Falkner in Ref. 21, 22, 23.

The induced velocity field and the circulation distribution at the various cells are related by a matrix equation

$$[V] = [H][K]$$

where [H] is the influence matrix, determined from the wing planform and its subdivision.

From the calculated [K] matrix, the lift, moment and aerodynamic center ($x_{c.p.}$, $y_{c.p.}$) location can be evaluated by the following relations:

$$C_L = \frac{1}{S}\int_{-b/2}^{b/2} c_i c_{\ell_i}\, dy = \frac{2b}{U.N_s.S}\sum_{i=1}^{N_s}\sum_{j=1}^{N_c} K_{ij}$$

where

$$\sum_{j=1}^{N_c} K_{ij} = \Gamma_i = \frac{U c_i c_{\ell_i}}{2}$$

for a rectangular wing

$$C_L = \frac{2}{U N_s C}\sum_{i=1}^{N_s}\sum_{j=1}^{N_c} K_{ij}$$

The pitching moment can be estimated by

$$C_M = C_L \cdot \frac{x_{c.p.}}{C}$$

where:

$$x_{c.p.} = \frac{\sum_{i=1}^{N_s}\sum_{j=1}^{N_c} c_{\ell_{ij}} \cdot \ell_{x_{ij}}}{C_L} = \frac{\sum_{i=1}^{N_s}\sum_{j=1}^{N_c} K_{ij}\, \ell_{x_{ij}}}{\sum_{i=1}^{N_s}\sum_{j=1}^{N_c} K_{ij}}$$

$$y_{cp} = \frac{\sum_{i=1}^{N_s}\sum_{j=1}^{N_c} c_{\ell_{ij}}\, \ell_{y_{ij}}}{C_L} = \frac{\sum_{i=1}^{N_s}\sum_{j=1}^{N_c} K_{ij}\, \ell_{y_{ij}}}{\sum_{i=1}^{N_s}\sum_{j=1}^{N_c} K_{ij}}$$

Since in this model the trailing vortices are assumed to remain in their original straight line positions, this model cannot be used to evaluate the shape of the trailing vortex. Furthermore, the effect of the interference of the rolled up vortex sheet on the wing lift cannot be obtained by this approach. With the use of the presently available large digital computers it is possible to account for the interactions of the bound and trailing vortices of each cell and therefore obtain the shape of the rolled-up vortex sheet behind the wing. Once the rolled-up sheet is calculated, it is possible also to calculate the effect of the induced velocity field due to this trailing vortex wake on the strength of the vortices at each cell. This calculation requires an iterative procedure as presented in 2.2 and 2.3 where it is referred to as the "Modified Vortex Lattice Method (MVLM)". (In the nonlinear lift case this program is denoted by "(NLMVLM)".

### 3.5. The Linear Lift Variation Modified Vortex Lattice Method - MVLM

The numerical procedure for the case of linear lift variation is presented in 2.2. However, there are three considerations that must be checked. These are: firstly, the shape of the bound vortex in each

cell, secondly, the location of the bound vortex and the location of the control point in the cell and thirdly, the number of the chordwise subdivision $N_c$, and the spanwise subdivision $N_s$, needed to obtain a reasonable solution.

One alternative for the shape of the bound vortex in each cell is to place this vortex perpendicular to the wing axis. This system was adopted originally by Falkner (22), Robinson and Zlotnick (24) and more recently by Blackwell (26) and is illustrated in sketch (a). The other alternative is to place an inclined bound vortex aligned on constant percentage chordlines as in the works of Hedman (26), Fox (27) and Margason and Lamar (15) and as illustrated in sketch (b).

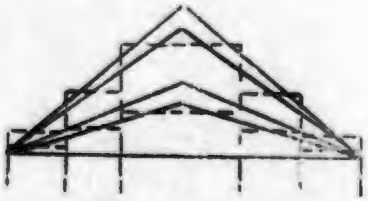

Sketch (a)

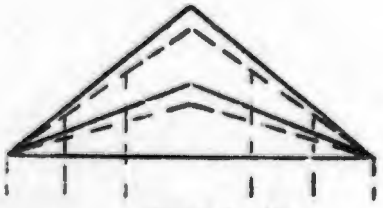

Sketch (b)

In the two-dimensional case the bound vortex position and the control point position can be selected so that the vortex lattice calculation results in the same lift and pitching moment as does the thin airfoil theory. The corresponding positions are at 0.25C for the bound vortex and 0.75C for the control point. It should be noted that in the case of a square cell this position of the control point is

equidistant from the bound and streamwise vortices (sketch (c)).

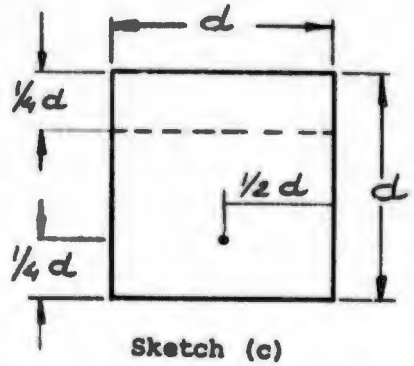


Sketch (c)

The effect of the subdivisions on the results of the calculations was checked for the cases of rectangular and delta wings. The lift coefficient is calculated for AR = 5.33 rectangular wing for various $N_c$ and $N_s$ subdivisions and the results are presented in Table Ia. It is seen that two chordwise stations give adequate results. Twenty spanwise stations, $N_s$, result in an error of less than 2% in the value of $C_{L_\alpha}$ with respect to the asymptotic value. These results are in agreement with those of Ref. 15. Lift coefficients of various AR, rectangular wings are shown in Table Ib.

The effect of chordwise and spanwise subdivisions on the lift coefficients of delta wings with AR = 0.5 to 5 and AR = 3 cropped delta wings is presented in Tables II and III.

3.6. <u>Non-Linear, Modified Vortex-Lattice Method - NLMVLM</u>

The wind tunnel studies of sharp leading-edge low aspect-ratio wings have shown that even at relatively low angles of attack the flow separates from the leading edge and rolls up into two cone-shaped vortex sheets. An increase in lift at a given angle of attack results, and it is this increase that is usually refer ed to

as the nonlinear (or vortex) lift. The vortex lift also changes the distribution of the lift on the wing planform. Because of the flow separation at the leading edge the pressure peaks predicted by the potential flow theory are not developed.

Various methods have been developed for the estimation of the lift due to the separated vortex sheets. These can be grouped as follows: (a) Empirical approximations-Locke (28), Poisson-Quinton (29) Bergessen and Porter (30). (b) Betzes' Theory -The lift increment equals the normal force developed because of the cross flow (Ref. (18)); (c) Polhamus's Theory: based on a leading edge suction analogy (Ref. (7)); (d) In the 4th group the two spiral vortex sheets are replaced by two concentrated line vortices above the wing and two feeding vortex sheets connecting the wings' leading edges and the line vortices. In these methods several approximations to the shape of the real spiral vortex sheets have been made. Brown and Michael (12) for example, use isolated vortices and planar feeding sheets. Mangler and Smith (8,10,11) have improved on this model by calculation of an approximate form of the vortex sheet between the wing leading edge and a point not too distant from the center of the vortex spiral.

Bollay in Ref. (13), assumes that the vorticity shed ahead of the trailing edge of a rectangular wing is inclined at one half the angle of attack relative to the flight direction. This lower inclination of the vortex lines reduces the downwash induced at the wing surface and thereby requires additional circulation in order to maintain the boundary condition of tangential flow at the wing surface. The application to arbitrary planform wings has been carried out by Gersten (14). In Ref.

(14) the wing is repalced by infinitesimal lifting elements. In this case Bollay's mathematical model is applied to each lifting element and is solved for the surface load distribution which is required to satisfy the boundary conditions.

In our present work we try to combine Gersten's theory and the vortex lattice method. The wing is divided into a finite number of cells as in the linear VLM. However it is assumed in this case that the free vortices leave the cells at an angle of $\alpha/2$. The matrix equation is solved as in the linear case and the nonlinear circulation is obtained. This circulation is used for the rolled up vortex sheet calculation. In this method (because of the lack of previous calculations) it is of special importance to check the position of the bound vortex in each cell i.e. perpendicular or inclined. For rectangular wings there is no difference between the two ways of dividing the wing planform. Results of the present method for the AR = 1/30 rectangular wing are shown in Fig. 9 and are compared with the experimental results of Winter as presented in Ref. (13).

For wings of non rectangular shape the results indicate that the effect of the inclination of the bound vortex is large. It is found that the perpendicular bound vortex results in a better agreement with the experimental results than the inclined one.

## 4. THE COMPUTER PROGRAMS

Computer programs are prepared for carrying out the calculations discussed in the previous Sections. The programs are written in Fortran IV for the IBM 370/165 computer. The calculations have been performed in the computer center of the Technion-Israel Institute of Technology.

The outline of the programs in the form of flow charts are presented in the Appendices A to F.

The flow chart for the computation of the rolled up wake for two-dimensional and three-dimensional elliptic distributions using equally spaced vortices is presented in Appendix A and that for the equal strength vortices case in Appendix B. The flow chart for the calculation of the linear aerodynamic coefficients by the vortex lattice method (VLM) is presented in Appendix C. The flow chart for the calculatior of the linear aerodynamic lift coefficients and the shape of the rolled up wake based on the vortex lattice method is presented in Appendix D. The flow chart for the modified vortex lattice method (MVLM), that includes the results of the interactions between the lift distribution on the wing and the rolled up wake is presented in Appendix E.

Computer programs for the non-linear lift cases are being developed. The program for the nonlinear aerodynamic coefficients assuming straight vortices in the wake at $\alpha/2$ inclination is presented in Appendix F. The programs for the rolled up vortex wake and the complete non-linear wing aerodynamics (corresponding to those presented in Appendices D and E for the linear case) are being developed at present.

## 5. RESULTS OF THE CALCULATIONS

### 5.1. The Calculations of Aerodynamic Coefficients

The aerodynamic coefficients of wings are obtained from the calculations based on the vortex lattice method by the program presented in Appendix C, and by the modified VLM presented in Appendix E. The nonlinear coefficients are calculated in this report by the simplified program described in Appendix F. The calculated aerodynamic coefficients of the various wings are compared with those obtained by other methods, and with experimental values.

For rectangular wings the evaluation of the lift curve slope by the VLM is in good agreement with experimental values as seen in Fig. 10, (where the experimental results are summarized from References 31 and 32). The effect of various subdivisions of the wing is presented in Table 1a for an aspect ratio 5.33 wing and in Table 1b for rectangular wings of AR between 0.5 and 6.

Nonlinear results are obtained for rectangular wings of various aspect ratios. The nonlinear contribution is indicated in Fig. 11. It is seen that for wings with aspect ratio below 3 the additional nonlinear lift is considerable. Of particular interest is the AR = 1/30 rectangular wing for which the nonlinear lift was estimated by Bollay (13) and the experimental measurements of Winters (cited in Ref.13) are available. The results of the present calculation which are in excellent agreement with the data are presented in Fig. 9. Some additional data for the nonlinear lift of rectangular wings is included in Ref. 33. The lift coefficient of AR 1 and 2 straight rectangular wings is presented in Figs. 12a and 12b respectively.

The results for rectangular wings with $45^{\circ}$ sweep are presented in Figs. 13a and 13b for wings of AR 1 and 2 respectively. The calculations of the lift coefficient, $C_L$, and the lift curve slope, $C_{L_\alpha}$, for delta wings of various aspect-ratio have been performed by the linear VLM and MVLM. These are compared with results of other methods as well as with the experimental values. The calculated values of $C_{L_\alpha}$ at $\alpha = 0$ are compared with the data of Reference 41 in Figure 14. The nonlinear lift calculated by the simplified NLVLM is compared with the VLM calculation for delta wings at $\alpha = 10^{\circ}$ in Fig. 15. The particularly high values of the nonlinear lift for wings of aspect ratio less than 2 are evident.

The nonlinear lift of low aspect ratio delta wings is evaluated by the simplified NLVLM program. Calculation of the lift coefficients of delta wings of AR = 0.5 and AR = 2 are presented in Figures 16a and 16b respectively, included are the experimental results from Refs. 35 and 36. The experimental results for a cropped delta wing (from Ref. 14) are compared with our calculated values in Fig. 17. In all these cases the agreement between the calculated results by the NLVLM are in very good agreement with the experimental data.

5.2. The Rolled up Vortex Sheet Calculations

The shape of the rolled up vortex sheet behind the wing is calculated by the programs of Appendix A for elliptic lift distribution, Appendix D for the VLM distribution and Appendix E for the MVLM distribution.

The computer plotted vortex sheet shapes behind a rectangular wing of AR = 3 at $\alpha = 10^{\circ}$ are presented in Fig. 8 for the elliptic lift distribution, in Fig. 18 for the VLM case and in Fig. 19 for the MVLM case.

In the case of the elliptic lift distribution the vortex sheet has been calculated with 16, 32 and 64 steps while in the VLM 3D and MVLM cases with 16 and 32 steps. It was found that these step sizes are all adequate and only very small variation of the shape of the vortex sheet as the calculation steps are increased are found. These can be seen in Table IV where values of the lift coefficients and the vortex center trajectories are listed for the various calculation steps.

Calculations of the VLM and MVLM vortex sheet shape were performed also for the AR = 5.33 wing at angle of attack of $12^{\circ}$. Some measurements on the vortex center trajectory are reported in Ref.36 and the results are plotted in Fig. 20.

## 6. DISCUSSION

The early models for the lift generation on a wing, developed by Lancaster and Prandtl, associated the lift of the wing with a vortex pattern which is shed from the trailing edge and tips downstream of the wing and rolls up to the so called "tip vortices". In the present report, we follow a new model for the generation of lift on any wing by considering that the lift generating vortices are distributed over the complete wing planform and are shed away from each elemental area on the planform. These infinitesimal vortices then join into the well known "tip vortices" for the high aspect ratio wing or join into the leading edge and tips lift vortices which are found on the low aspect ratio wings. This is a generalization of the model of the lift on delta wings which was suggested by a number of authors. A more definite proposal of such a model for generation of lift and the rolling up of the vortex sheet is presented by R. Legendre in Ref. 37 and some numerical results based on this approach are presented in Ref. 38. However, in this model the tip vortices are shed only from the tip chord profile's leading edge. In our model the vortex sheet of the complete wing planform is involved. Therefore we obtain a unified model which enables a single numerical program for any wing of any aspect ratio. The generation of vortices over the complete wing planform suggests the use of a method which is based on a vortex lattice distributed over the wing's planform. We therefore adopted the VLM procedures for this purpose. An example of another approach for wing lift representation may bethe use of the Panel Methods developed at Boeing and at NLR and reviewed in References 39 and 40.

Proceeding with the vortex lattice method, we may allow the vortices to stay on the wing planform and be shed from the trailing edge only. In this case we obtain the linear lift variation with angle of attack and the vortex sheet shape is obtained by the numerical calculations presented in Sections 3.3, 3.4 and 3.5 and the computer programs in Appendices D and E. These calculations result in reasonable results for high aspect ratio wings (AR > 3) as seen in Figures 10 & 14 for rectangular and triangular wings respectively.

In the case when we allow the vortices from each cell to be shed locally into the flow, we obtain free vortices over the wing planform and due to the vortex interaction a nonlinear lift variation with angle of attack is obtained. For high aspect ratio wings the effects of these interactions are small and the results are almost equal to the case when the vortices stay in the wing planform and are shed from the trailing edge only. However as the aspect ratio of the wing is reduced the effect of the free vortices over the wing becomes large. This effect is clearly seen in the comparison between the VLM and the NLVLM calculations presented in Figures 11 and 15 ; The calculation of the lift of low aspect ratio wings by the NLVLM is in remarkable agreement with the experimental data as is evident from Figs. 9, 12a,12b,13a,13b,16a,16b and 17. It now remains to complete the calculation of the nonlinear vortex sheet shape, that is-steps 2 and 3 in Fig. 4, to obtain the complete flow pattern, as well as the aerodynamic coefficients of these wings.

A basic problem in the numerical method is the representation of the vortex sheet by discrete line vortices. This problem is discussed in

Section 3.1 where it is suggested that the difficulties discussed by Moore in Ref. 17 are due to the use of the potential vortex model for each line vortex. This model introduces a velocity singularity at each vortex origin and therefore results in difficulties when the vortices approach each other. A simple way to avoid this problem is to use wide spread vortices - i.e. the equal distance division. A more refined approach is to replace the vortices by a real vortex model with a finite core radius as suggested in Section 3.1. This model is now being programmed. Using the present numerical programs we find good convergence of the computer calculations as is evident from the tabulated results (Tables Ia, Ib, II and III).

The shape of the vortex sheet obtained by the VLM and MVLM calculations is certainly in good qualitative agreement with the experimentally observed vortex pattern of high aspect ratio wings. The very few experimental results for the vortex pattern right behind the wing, such as those of Ref. 37, indicate that the calculated results are probably a good approximation to the actual flow pattern. The really interesting results will be obtained when the vortex pattern over the wing planform will be computed by the NLVLM program. We hope to report this result in a future report.

## REFERENCES


1. Wetmore, J.W., and Reeder, J.P., Aircraft vortex wakes in relation to terminal operations, NASA TN D-1777, April 1963.
2. Wetmore, J.W., Aircraft trailing vortices - A hazard to operations, Aeronautics and Astronautics, Dec. 1964, pp. 44-51.
3. Kaden, H., Aufwiklung eines unstabilen Unstetigkeitsflasche. Ing.-Archiv. Bd. II, Helft 2, May 1931, pp.140-168.
4. Westwater, F.L., Rolling up of the surface of discontinuity behind an aerofoil, on finite span. British A.R.C., R & M 1692, 1935.
5. Spreiter J.R., and Sacks, A.H., The rolling up of the trailing vortex sheet and its effect on the downwash behind wings. Journal of the Aeronautical Sciences, Vol. 18, No. 1, Jan. 1951, pp.21-32.
6. Olsen, J.H., Goldburg, A., and Rogers, M., Aircraft wake turbulence and its detection, Plenum Press, N.Y. London, 1971.
7. Polhamus, E.C., A concept of the vortex lift of sharp-edge delta wings based on a leading edge suction analogy. NASA TN D-3767, December, 1966.
8. Mangler, K.W., and Smith, J.H.B., A theory of slender wings with leading edge separation. Proc. Royal Soc., London, Series A. Vol. 251, 1959.
9. Maltby, R.L., The development of the slender delta concept. Aircraft Engineering, March 1968, pp. 12 - 17.
10. Mangler, K.W., and Smith, J.H.B., A theory for slender delta wings with leading edge separation, R.A.E. Tech. Note No. Aero. 2442, April 1956.
11. Mangler, K.W., And Smith, J.H.B., Calculation of the flow past slender delta wings with leading edge separation. R.A.E. Report No. Aero. 2593, May 1957.

12. Brown, C., and Michael, W., Jr., On slender wings with leading edge separation. NACA TN 3430, April 1955.

13. Bollay, W., A theory for rectangular wings of small aspect ratio. Journal of the Aeronautical Sciences, Vol. 4, Part 1, Jan. 1937, pp.294-296.

14. Gersten, K., A non-linear lifting surface theory especially for low aspect ratio wings, AIAA Journal, Vol. 1, No. 4, 1963, pp.924-925.

15. Margason, R.J. and Lamar, J.E., Vortex lattice fortran program for estimating subsonic aerodynamic characteristics of complex planforms. NASA TN D 6142, Feb. 1971.

16. Kalman, T.P., Giesing, J.P., and Rodden, W.P., Spanwise distribution of induced drag in subsonic flow by the vortex lattice method. Journal of Aircraft, Vol. 7, No. 6, Nov-Dec. 1970. pp. 574-576.

17. Moore, D.W., The discrete vortex approximation of a finite vortex sheet, AFOSR-1804-69, TR 72-0034, Oct. 1971.

18. Betz, A. Applied aerofoil theory, Aerodynamic Theory (Vol. IV), W.F. Durand, Berlin 1935.

19. Hackett, J.E. and Evans, M.R. Vortex wakes behind high-lift wings, AIAA Paper No. 69-740. CASI/AIAA Subsonic Aero and Hydro-Dynamics Meeting, July 1969.

20. Butter, D.J., and Hancock, G.J., A numerical method for calculating the trailing vortex system behind a swept wing at low speed. The , Aeronautical Journal of the Royal Aeronautical Society, August, 1971, pp.564-568.

21. Falkner, V.M., The calculation of aerodynamic loading on surfaces of any shape, British A.R.C. R & M 1910, 1943.

22. Falkner, V.M., The solution of lifting plane problems by vortex lattice theory. British A.R.C. R & M 2591, London, 1947.

23. Falkner, V.M., Calculated leadings due to incidence of a number of straight and swept back wings. British A.R.C. R & M 2596, London, 1948.

24. Robinson, S.W. and Zlotnick, M., A method for calculating the aerodynamic loading on wing-tip-tank combinations in subsonic flow, NACA RM L53-B18, 1953.

25. Blackwell, J.A. A finite step method for calculation of theoretical load distributions for arbitrary lifting-surface arrangements at subsonic speeds. NASA TN D 5335, July 1969.

26. Hedman, S.G., Vortex lattice method for calculation of quasi-steady state loadings on thin elastic wings in subsonic flow. The Aeronautical Research Institute of Sweden, FFA Rep. 105, 1966.

27. Fox, C.H., Prediction of lift and drag for slender sharp-edge delta wings in ground proximity. NASA TN D-4891, Jan. 1969.

28. Locke, F.W.S. (Jr.), An empirical study of low aspect ratio lifting surfaces with particular regard to planning craft. Journal of the Aeronautical Sciences, Vol. 16, No. 3, 1949, pp.184-188.

29. Poisson-Quinton, P., and Erlich, E., Hyperlift and balancing of slender wings. NASA TT F-9523, August, 1965.

30. Bergessen, A.J., and Porter, J.D., An investigation of the flow around slender delta wings with leading edge separation. O.N.R. Report No. 510. Princeton Univ. May 1960.

31. Thwaites, B., Incompressible Aerodynamics, Fig. VIII,28A, Oxford Press, 1960.

32. Jones, R.T., in the Princeton Series on High Speed Aerodynamics, Vol. 7, Part A. Fig. A7t, Princeton Press, 1960.

33. Garner H.C. and Lehrian, D.E., Non-linear theory of steady forces on wings with leading-edge flow separation. British A.R.C., R & M, 3375, 1964.

34. Tosti, L.P., Low-speed static stability and damping-in-roll characteristics of some swept and unswept low-aspect ratio wings. NACA TN 1468, 1947.

35. Bartlet, G.E., and Vidal, R.J., Experimental investigation of influence of edge shape on the aerodynamic characteristics of low aspect ratio wings at low speeds, Journal of the Aeronautical Sciences, Vol. 22, No. 8, Aug. 1955, pp.517-533,588.

36. Chigier, N.A., and Corsiglia, V.R., Wind-Tunnel Studies of Wing Wake Turbulence, American Inst. of Aeronautics and Astronautics, Paper 72-41, 10th Aerospace Sciences Meeting, San Diego, California, January 17-19, 1972. Also NASA TMX 62,148, May 1972.

37. Legendre, R., Effect of wing tip shape on vortex sheet rolling up. ONERA, La Recherche Aerospatiale, Brevés Informations, July-August 1971, 227-228.

38. Rehbach, C., Numerical study of the influence of the wing tip shape on the vortex sheet rolling up. ONERA, La Recherche Aerospatiale, Brevés Informations, Nov.-Dec. 1971, pp.367-368.

39. Woodward, F.A., Analysis and design of wing-body combinations at subsonic and supersonic speeds. Journal of Aircraft, Vol. 5, No. 6, 1968, pp.528-534.

40. Nieuwland G.Y., Choice and balance, a research programme in aerodynamics in perspective. ICAS Paper No. 72-01, The 8th ICAS Congress, Amsterdam, August 28th-Sept. 2nd, 1972.

41. Razur, K. and Snyder, M., A review of the planform effects on the low speed aerodynamic characteristics of triangular and modified triangular wings, NASA CR 421, April 1966.

## APPENDIX A: FLOW CHART FOR PROGRAM OF ELLIPTIC DISTRIBUTION - EQUAL SPACED VORTICES.

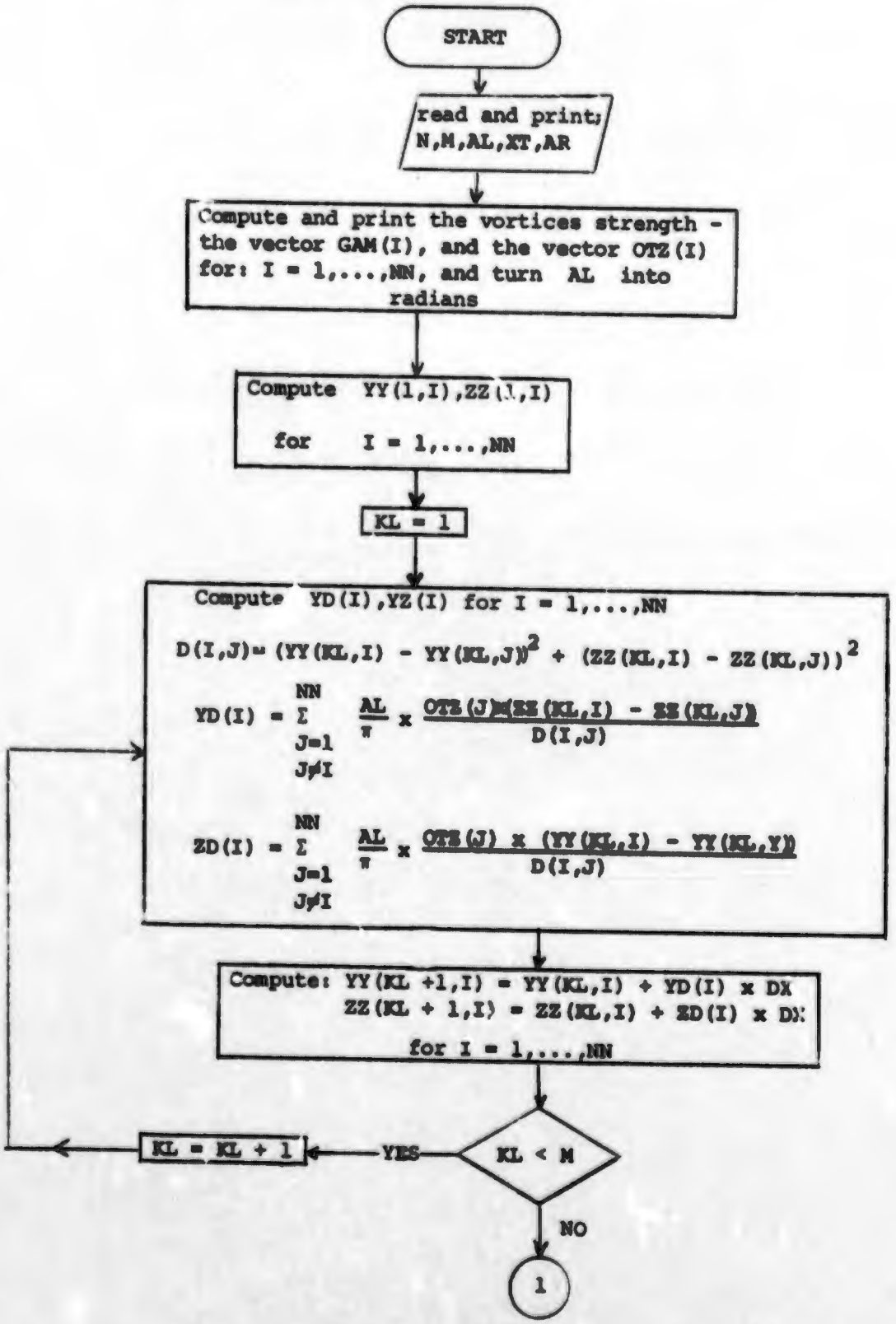

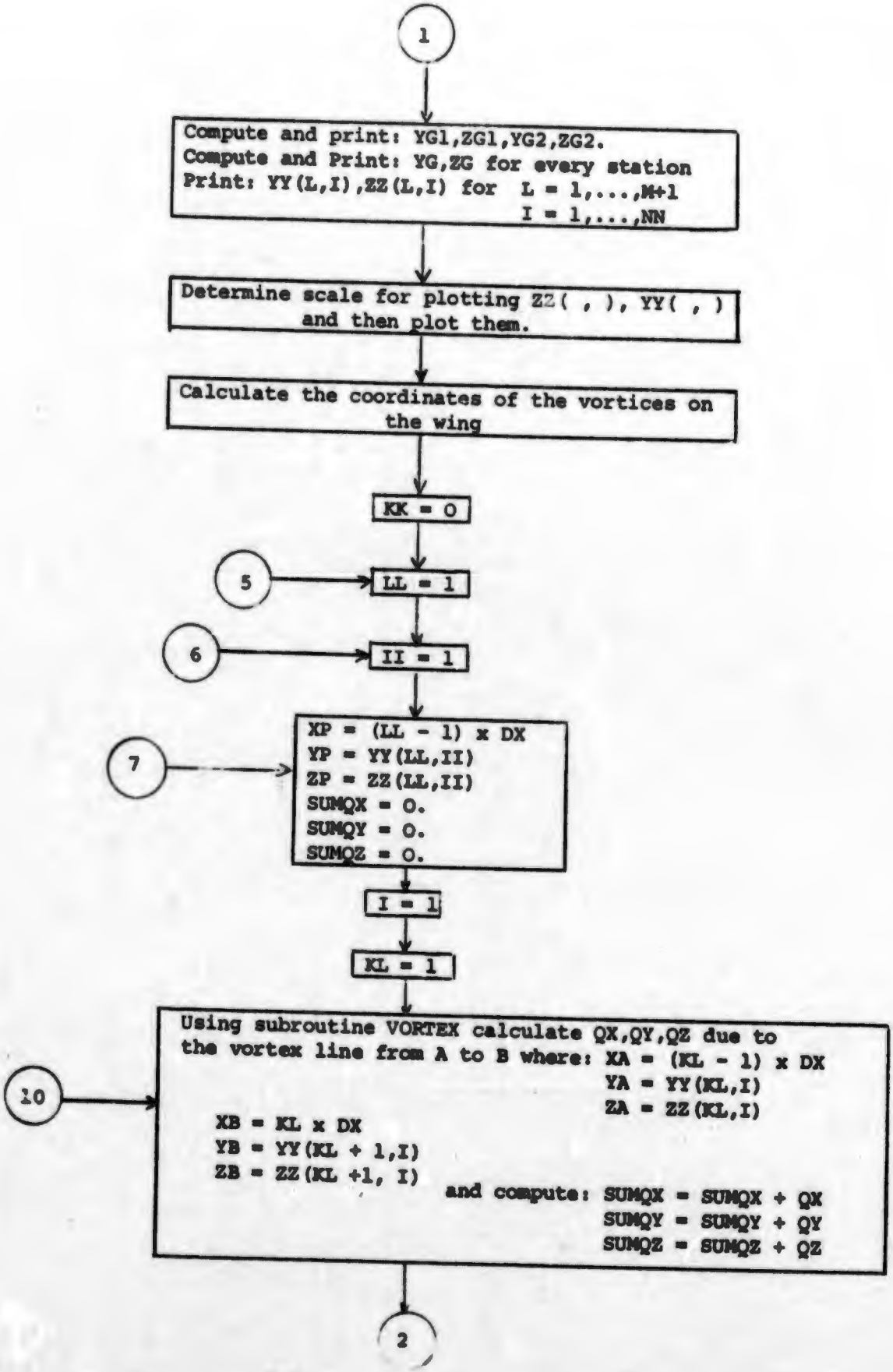
1
Compute and print: YG1,ZG1,YG2,ZG2.
Compute and Print: YG,ZG for every station
Print: YY(L,I),ZZ(L,I) for L = 1,...,M+1
I = 1,...,NN
Determine scale for plotting ZZ( , ), YY( , ) and then plot them.
Calculate the coordinates of the vortices on the wing
KK = 0
5
LL = 1
6
II = 1
7
XP = (LL - 1) x DX
YP = YY(LL,II)
ZP = ZZ(LL,II)
SUMQX = 0.
SUMQY = 0.
SUMQZ = 0.
I = 1
KL = 1
10
Using subroutine VORTEX calculate QX,QY,QZ due to the vortex line from A to B where: XA = (KL - 1) x DX
YA = YY(KL,I)
ZA = ZZ(KL,I)
XB = KL x DX
YB = YY(KL + 1,I)
ZB = ZZ(KL +1, I)
and compute: SUMQX = SUMQX + QX
SUMQY = SUMQY + QY
SUMQZ = SUMQZ + QZ
2

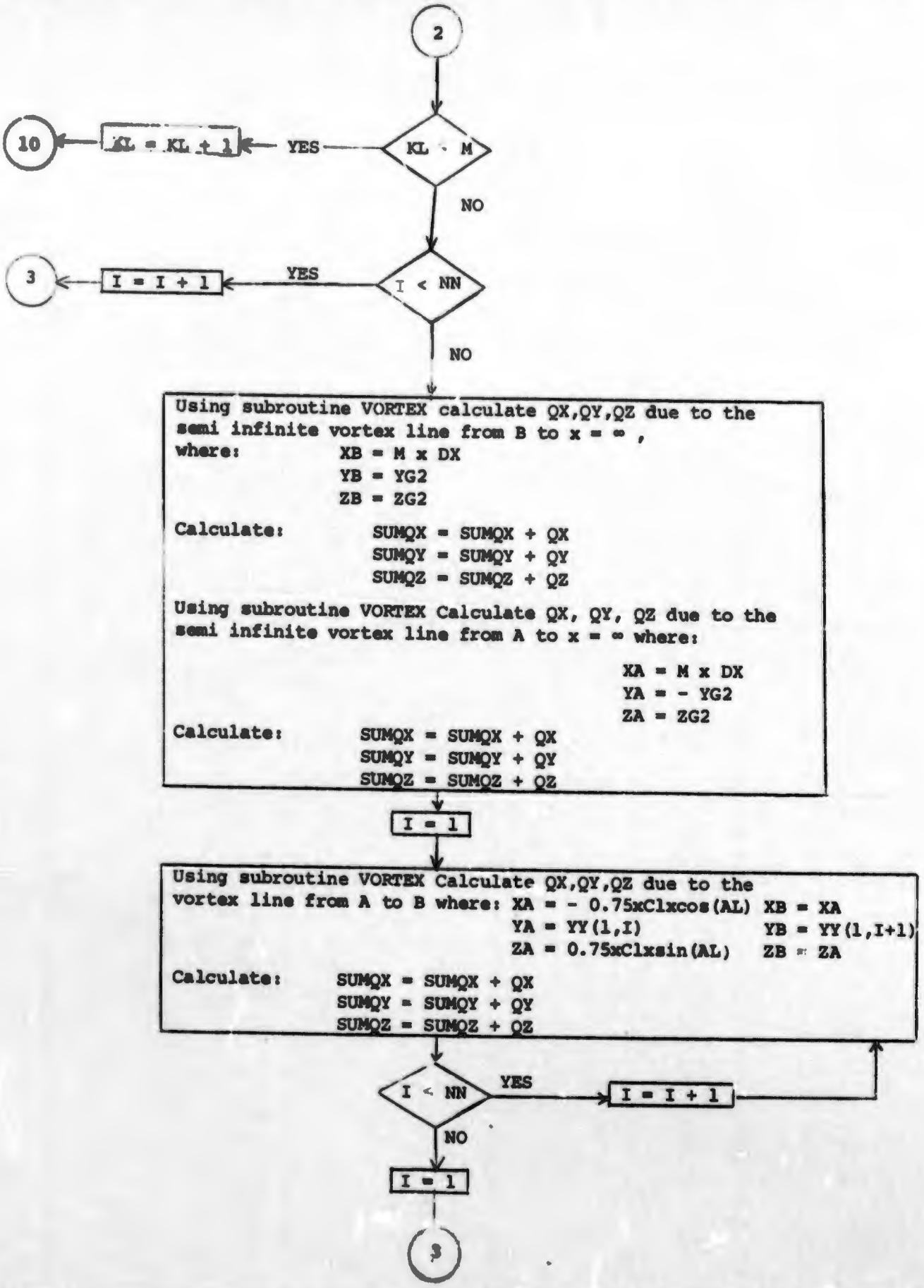
2
KL = M
YES
KL = KL + 1
10
NO
I < NN
YES
I = I + 1
3
NO
Using subroutine VORTEX calculate QX,QY,QZ due to the semi infinite vortex line from B to x = ∞ ,
where: XB = M x DX
YB = YG2
ZB = ZG2
Calculate: SUMQX = SUMQX + QX
SUMQY = SUMQY + QY
SUMQZ = SUMQZ + QZ
Using subroutine VORTEX Calculate QX, QY, QZ due to the semi infinite vortex line from A to x = ∞ where:
XA = M x DX
YA = - YG2
ZA = ZG2
Calculate: SUMQX = SUMQX + QX
SUMQY = SUMQY + QY
SUMQZ = SUMQZ + QZ
I = 1
Using subroutine VORTEX Calculate QX,QY,QZ due to the vortex line from A to B where: XA = - 0.75xC1xcos(AL) XB = XA
YA = YY(1,I) YB = YY(1,I+1)
ZA = 0.75xC1xsin(AL) ZB = ZA
Calculate: SUMQX = SUMQX + QX
SUMQY = SUMQY + QY
SUMQZ = SUMQZ + QZ
I < NN
YES
I = I + 1
NO
I = 1
3

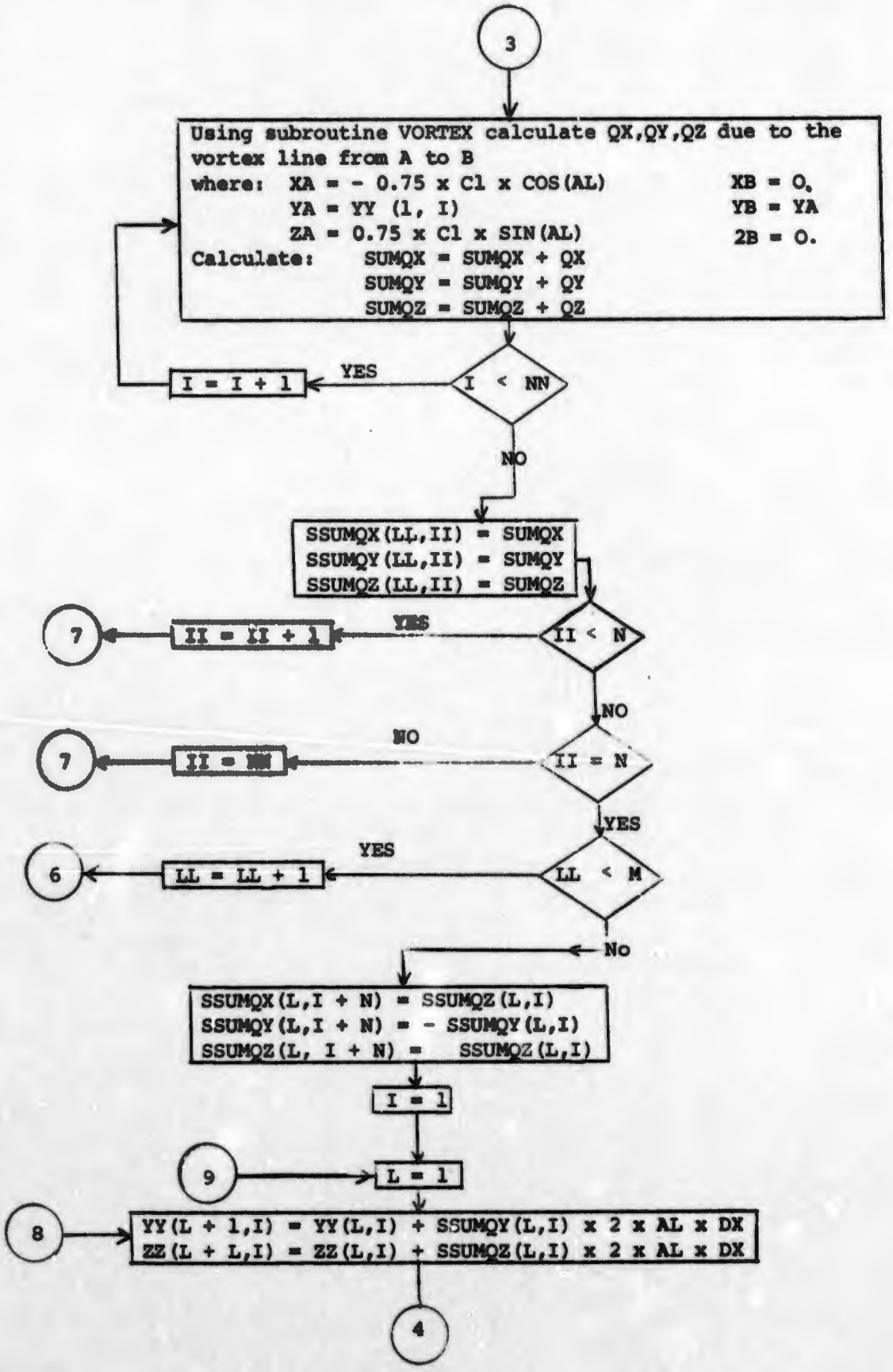
3
Using subroutine VORTEX calculate QX,QY,QZ due to the vortex line from A to B
where: XA = - 0.75 x C1 x COS(AL)
XB = 0.
YA = YY (1, I)
YB = YA
ZA = 0.75 x C1 x SIN(AL)
ZB = 0.
Calculate: SUMQX = SUMQX + QX
SUMQY = SUMQY + QY
SUMQZ = SUMQZ + QZ
I < NN
YES
I = I + 1
NO
SSUMQX(LL,II) = SUMQX
SSUMQY(LL,II) = SUMQY
SSUMQZ(LL,II) = SUMQZ
II < N
YES
II = II + 1
7
NO
II = N
NO
II = NN
7
YES
LL < M
YES
LL = LL + 1
6
No
SSUMQX(L,I + N) = SSUMQZ(L,I)
SSUMQY(L,I + N) = - SSUMQY(L,I)
SSUMQZ(L, I + N) = SSUMQZ(L,I)
I = 1
9
L = 1
8
YY(L + 1,I) = YY(L,I) + SSUMQY(L,I) x 2 x AL x DX
ZZ(L + L,I) = ZZ(L,I) + SSUMQZ(L,I) x 2 x AL x DX
4

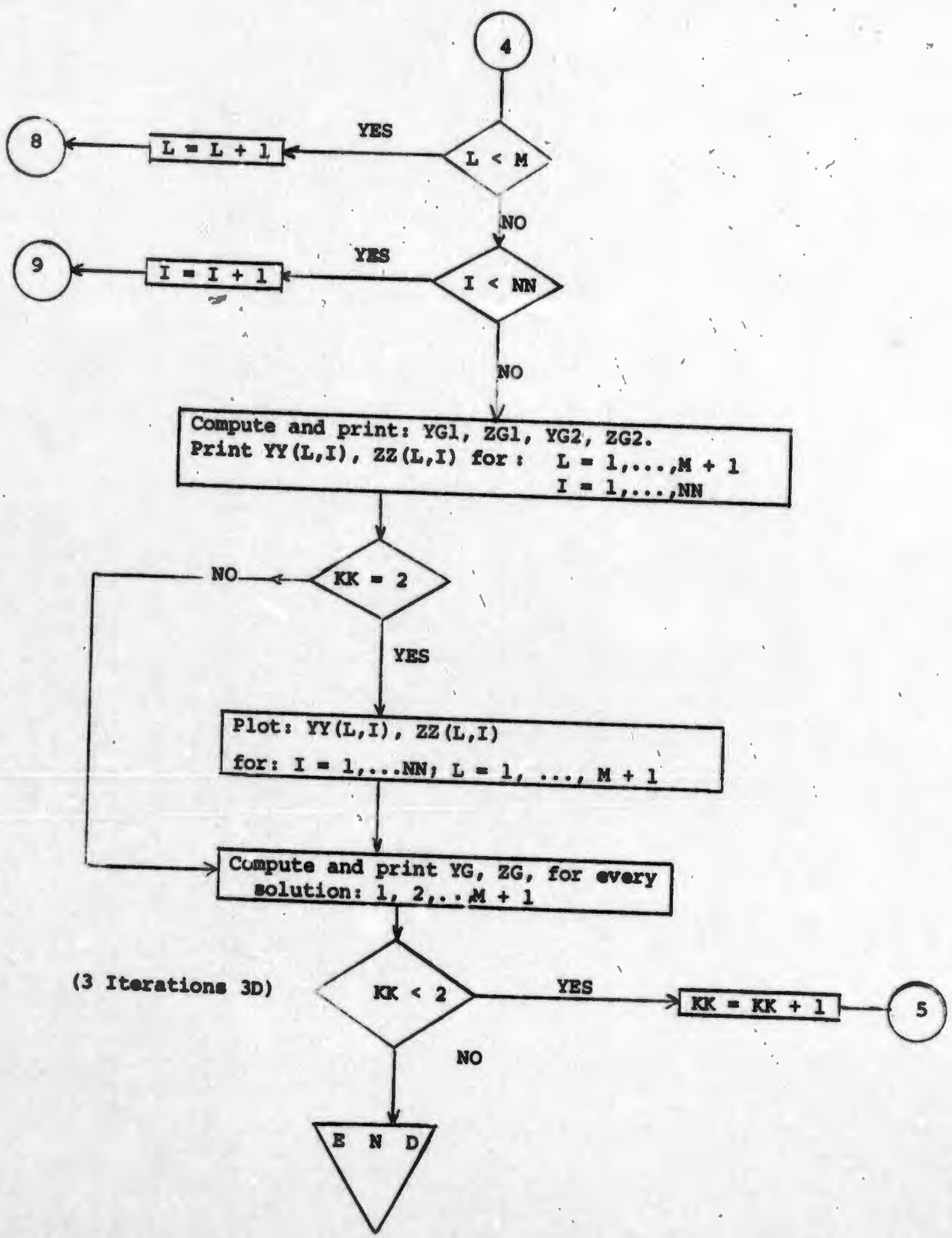
4
L < M
YES
L = L + 1
8
NO
I < NN
YES
I = I + 1
9
NO
Compute and print: YG1, ZG1, YG2, ZG2.
Print YY(L,I), ZZ(L,I) for : L = 1,...,M + 1
I = 1,...,NN
KK = 2
NO
YES
Plot: YY(L,I), ZZ(L,I)
for: I = 1,...NN; L = 1, ..., M + 1
Compute and print YG, ZG, for every solution: 1, 2,.. M + 1
(3 Iterations 3D)
KK < 2
YES
KK = KK + 1
5
NO
E N D

## APPENDIX B: FLOW CHART FOR PROGRAM OF ELLIPTIC DISTRIBUTION - EQUAL STRENGTH VORTICES

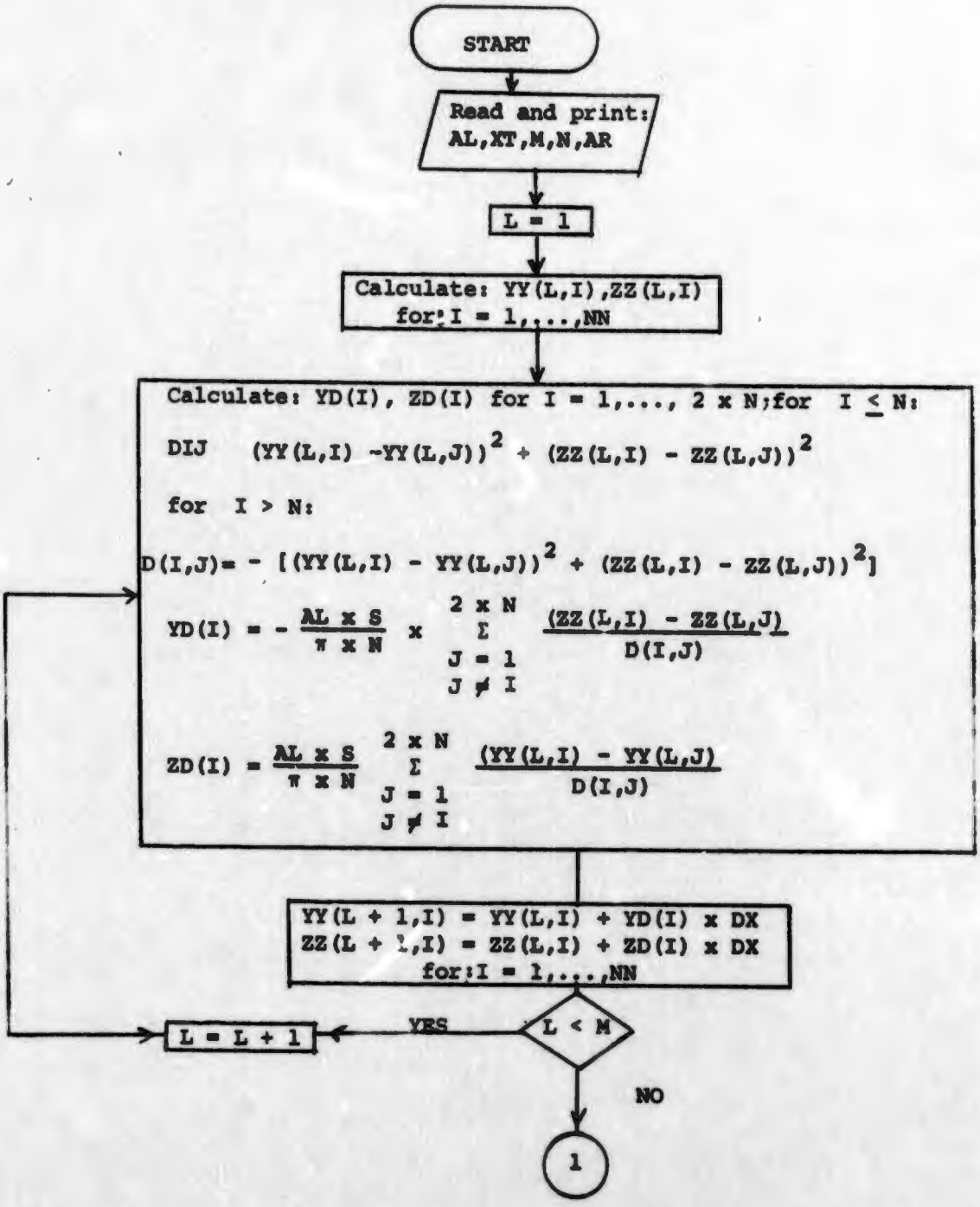

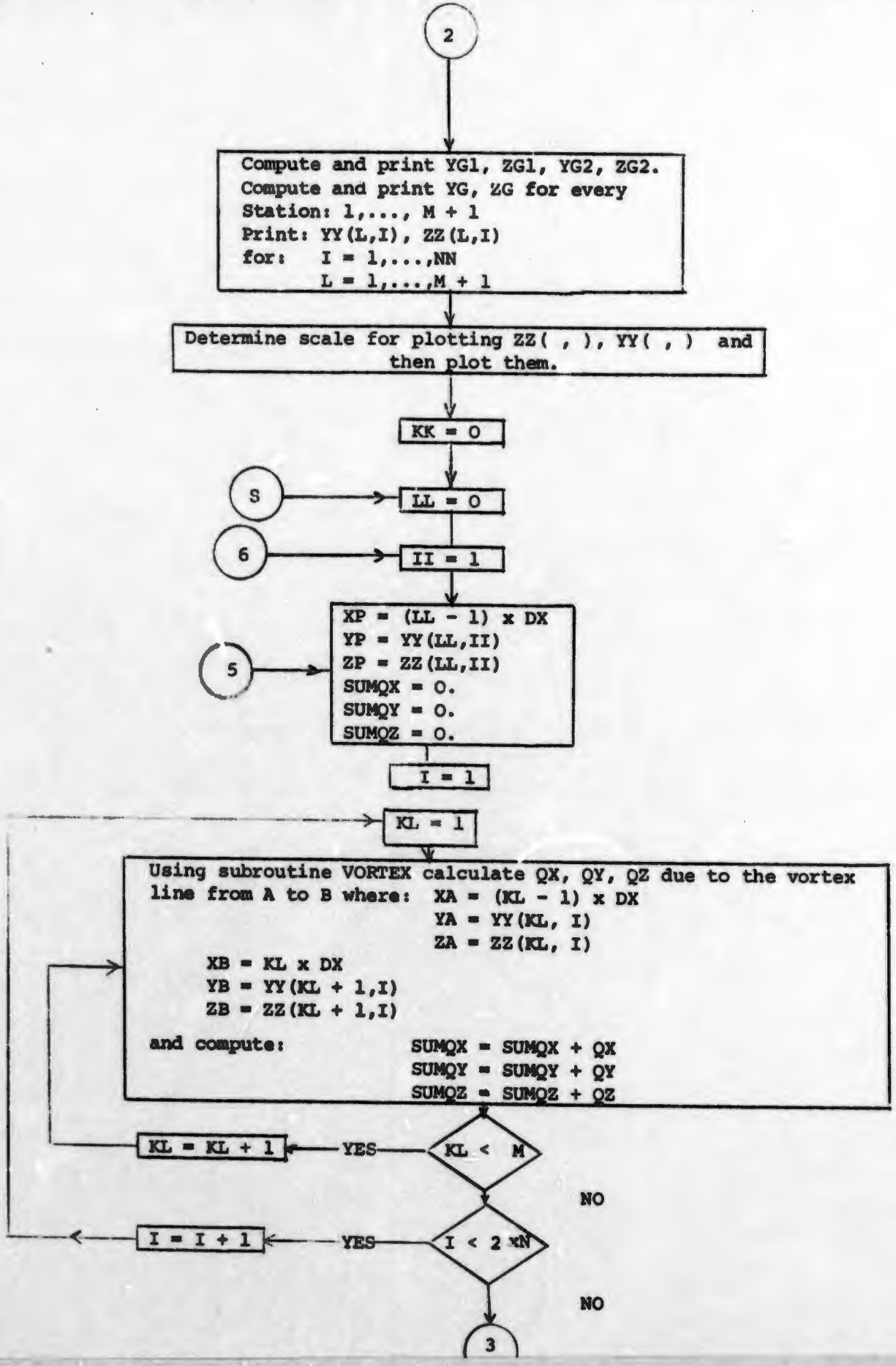
2
Compute and print YG1, ZG1, YG2, ZG2.
Compute and print YG, ZG for every
Station: 1,..., M + 1
Print: YY(L,I), ZZ(L,I)
for: I = 1,...,NN
L = 1,...,M + 1
Determine scale for plotting ZZ( , ), YY( , ) and then plot them.
KK = 0
S
LL = 0
6
II = 1
XP = (LL - 1) x DX
YP = YY(LL,II)
ZP = ZZ(LL,II)
SUMQX = 0.
SUMQY = 0.
SUMQZ = 0.
5
I = 1
KL = 1
Using subroutine VORTEX calculate QX, QY, QZ due to the vortex line from A to B where: XA = (KL - 1) x DX
YA = YY(KL, I)
ZA = ZZ(KL, I)
XB = KL x DX
YB = YY(KL + 1,I)
ZB = ZZ(KL + 1,I)
and compute: SUMQX = SUMQX + QX
SUMQY = SUMQY + QY
SUMQZ = SUMQZ + QZ
KL < M
YES
KL = KL + 1
NO
I < 2 xN
YES
I = I + 1
NO
3

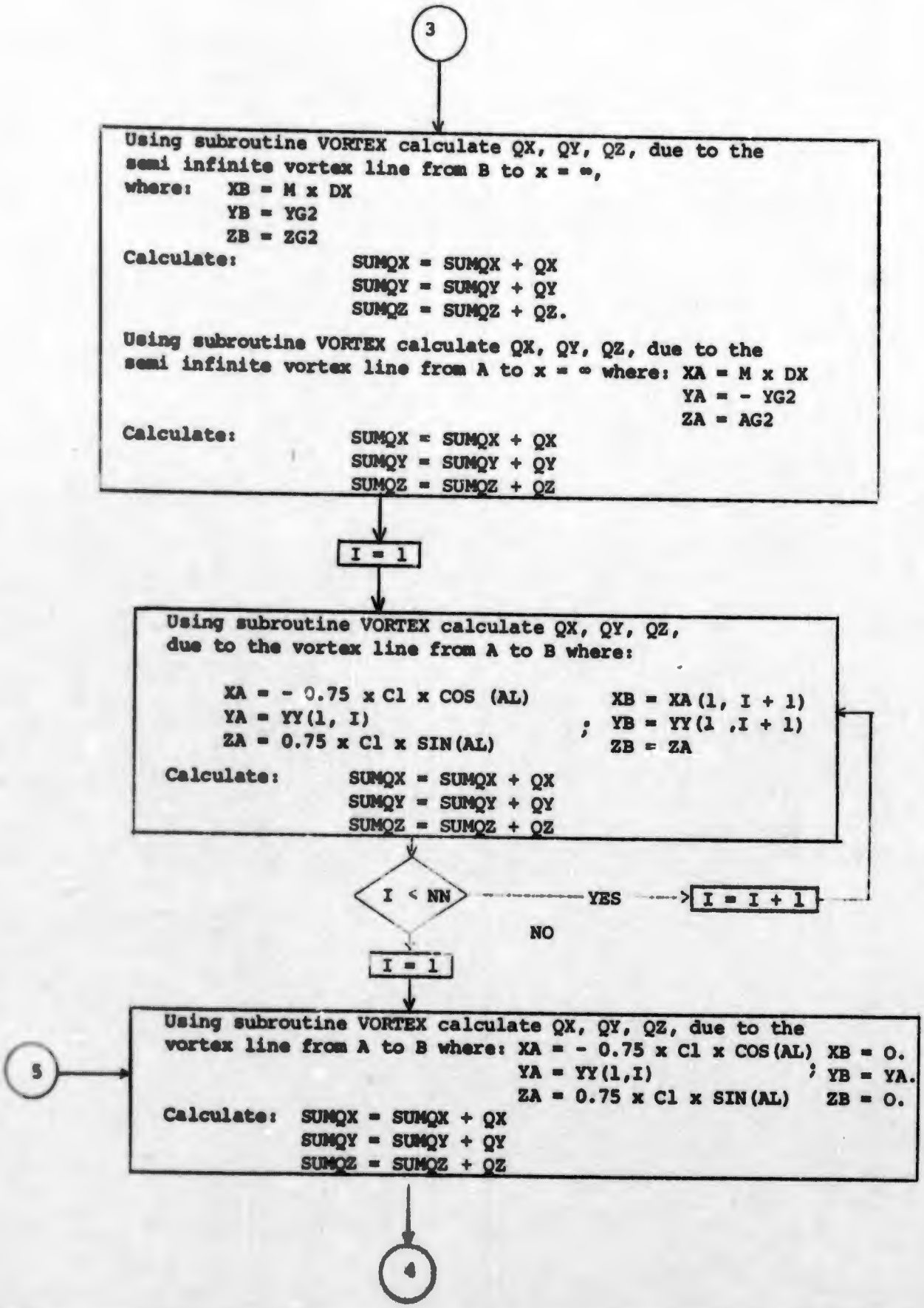
3
Using subroutine VORTEX calculate QX, QY, QZ, due to the semi infinite vortex line from B to x = ∞,
where: XB = M x DX
YB = YG2
ZB = ZG2
Calculate: SUMQX = SUMQX + QX
SUMQY = SUMQY + QY
SUMQZ = SUMQZ + QZ.
Using subroutine VORTEX calculate QX, QY, QZ, due to the semi infinite vortex line from A to x = ∞ where: XA = M x DX
YA = - YG2
ZA = AG2
Calculate: SUMQX = SUMQX + QX
SUMQY = SUMQY + QY
SUMQZ = SUMQZ + QZ
I = 1
Using subroutine VORTEX calculate QX, QY, QZ, due to the vortex line from A to B where:
XA = - 0.75 x C1 x COS (AL)
YA = YY(1, I)
ZA = 0.75 x C1 x SIN(AL)
XB = XA(1, I + 1)
; YB = YY(1 ,I + 1)
ZB = ZA
Calculate: SUMQX = SUMQX + QX
SUMQY = SUMQY + QY
SUMQZ = SUMQZ + QZ
I < NN
YES
I = I + 1
NO
I = 1
5
Using subroutine VORTEX calculate QX, QY, QZ, due to the vortex line from A to B where: XA = - 0.75 x C1 x COS(AL) XB = O.
YA = YY(1,I) ; YB = YA.
ZA = 0.75 x C1 x SIN(AL) ZB = O.
Calculate: SUMQX = SUMQX + QX
SUMQY = SUMQY + QY
SUMQZ = SUMQZ + QZ
4

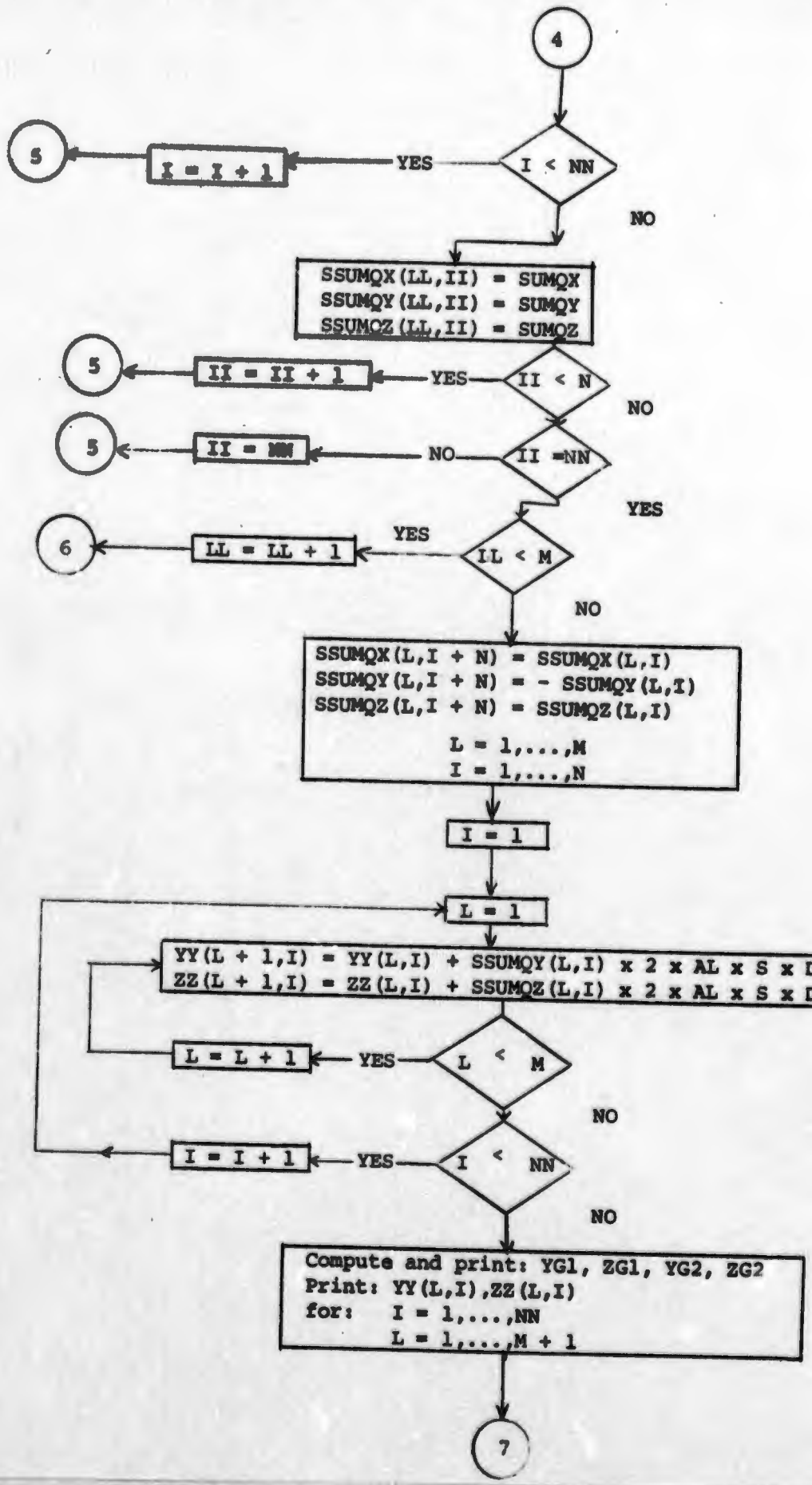
4
I < NN
YES
I = I + 1
5
NO
SSUMQX(LL,II) = SUMQX
SSUMQY(LL,II) = SUMQY
SSUMQZ(LL,II) = SUMQZ
II < N
YES
II = II + 1
5
NO
II = NN
NO
II = NN
5
YES
IL < M
YES
LL = LL + 1
6
NO
SSUMQX(L,I + N) = SSUMQX(L,I)
SSUMQY(L,I + N) = - SSUMQY(L,I)
SSUMQZ(L,I + N) = SSUMQZ(L,I)
L = 1,...,M
I = 1,...,N
I = 1
L = 1
YY(L + 1,I) = YY(L,I) + SSUMQY(L,I) x 2 x AL x S x DX/N
ZZ(L + 1,I) = ZZ(L,I) + SSUMQZ(L,I) x 2 x AL x S x DX/N
L < M
YES
L = L + 1
NO
I < NN
YES
I = I + 1
NO
Compute and print: YG1, ZG1, YG2, ZG2
Print: YY(L,I),ZZ(L,I)
for: I = 1,...,NN
L = 1,...,M + 1
7

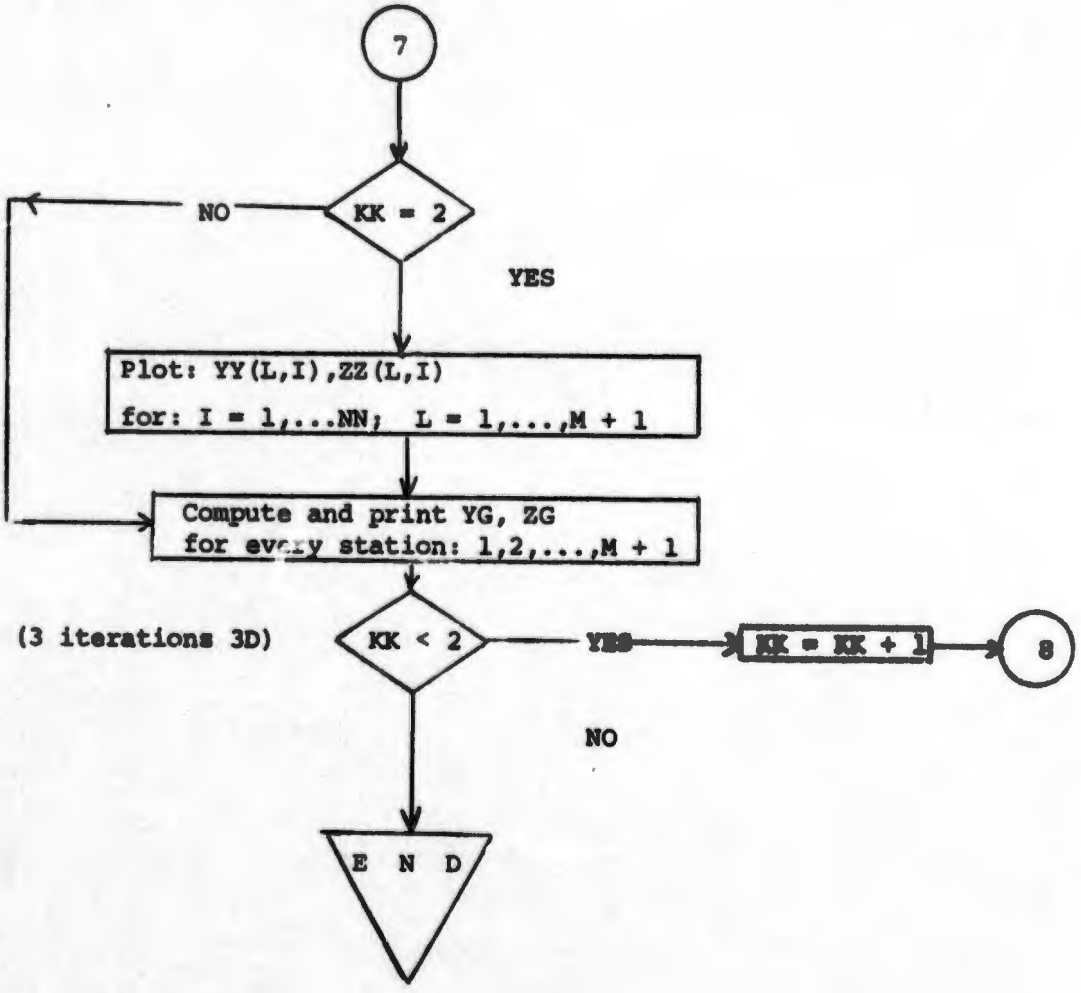
7
KK = 2
NO
YES
Plot: YY(L,I),ZZ(L,I)
for: I = 1,...NN; L = 1,...,M + 1
Compute and print YG, ZG
for every station: 1,2,...,M + 1
(3 iterations 3D)
KK < 2
YES
KK = KK + 1
8
NO
E N D

## APPENDIX C- FLOW CHART FOR THE VLM FOR THE CALCULATION OF THE AERODYNAMIC COEFFICIENTS

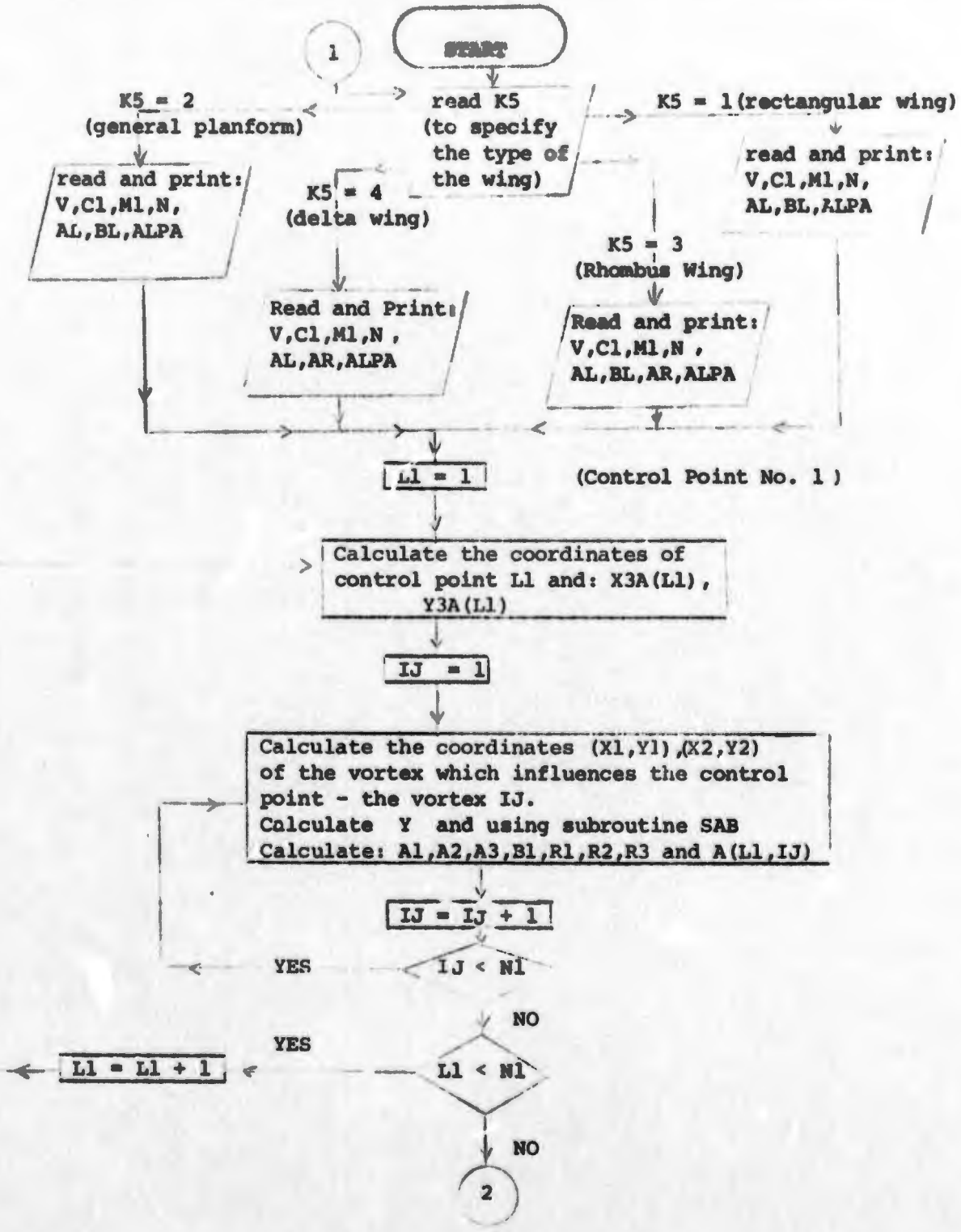

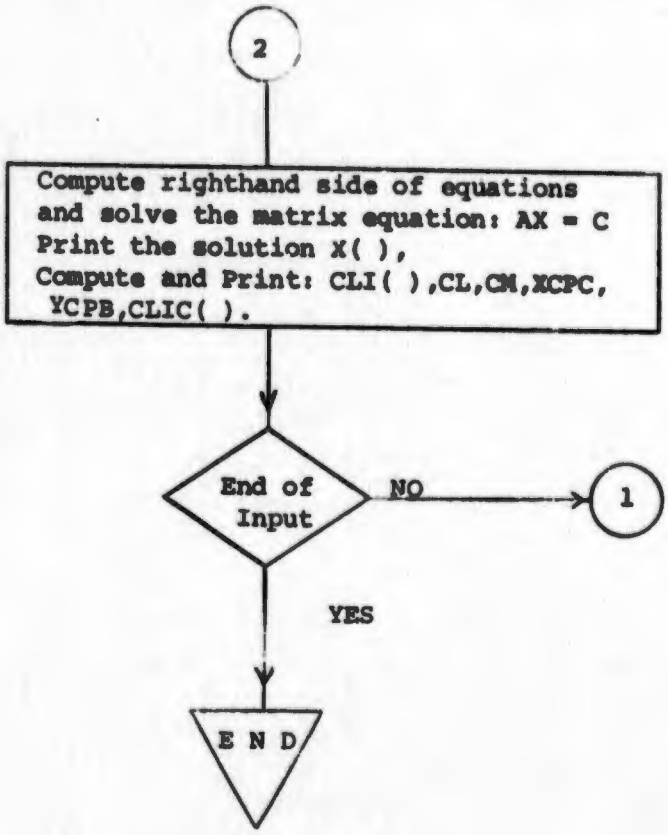
2
Compute righthand side of equations
and solve the matrix equation: AX = C
Print the solution X( ),
Compute and Print: CLI( ),CL,CM,XCPC,
YCPB,CLIC( ).
End of
Input
NO
1
YES
E N D

## APPENDIX D - FLOW CHART OF VLM-3D PROGRAM

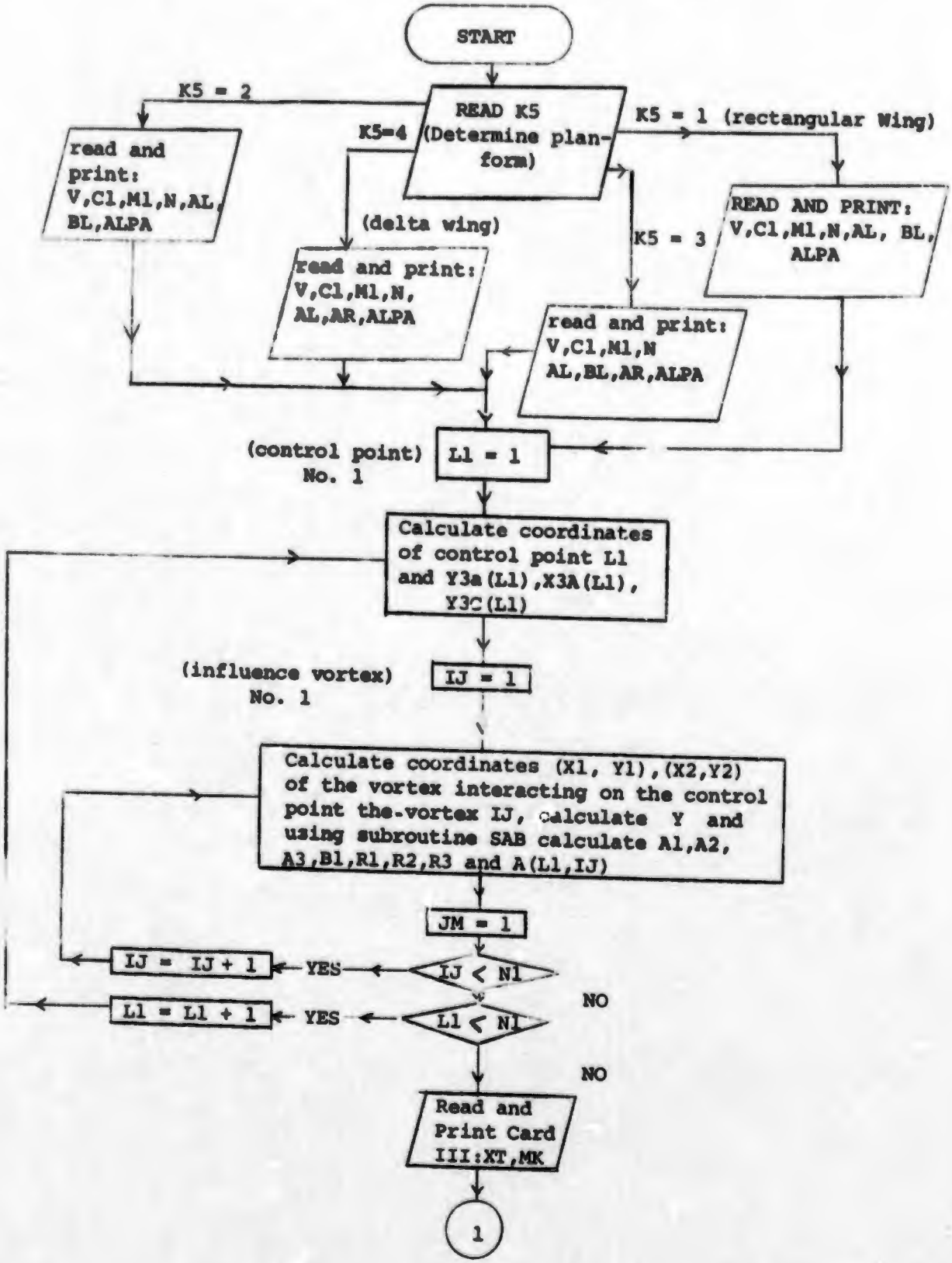

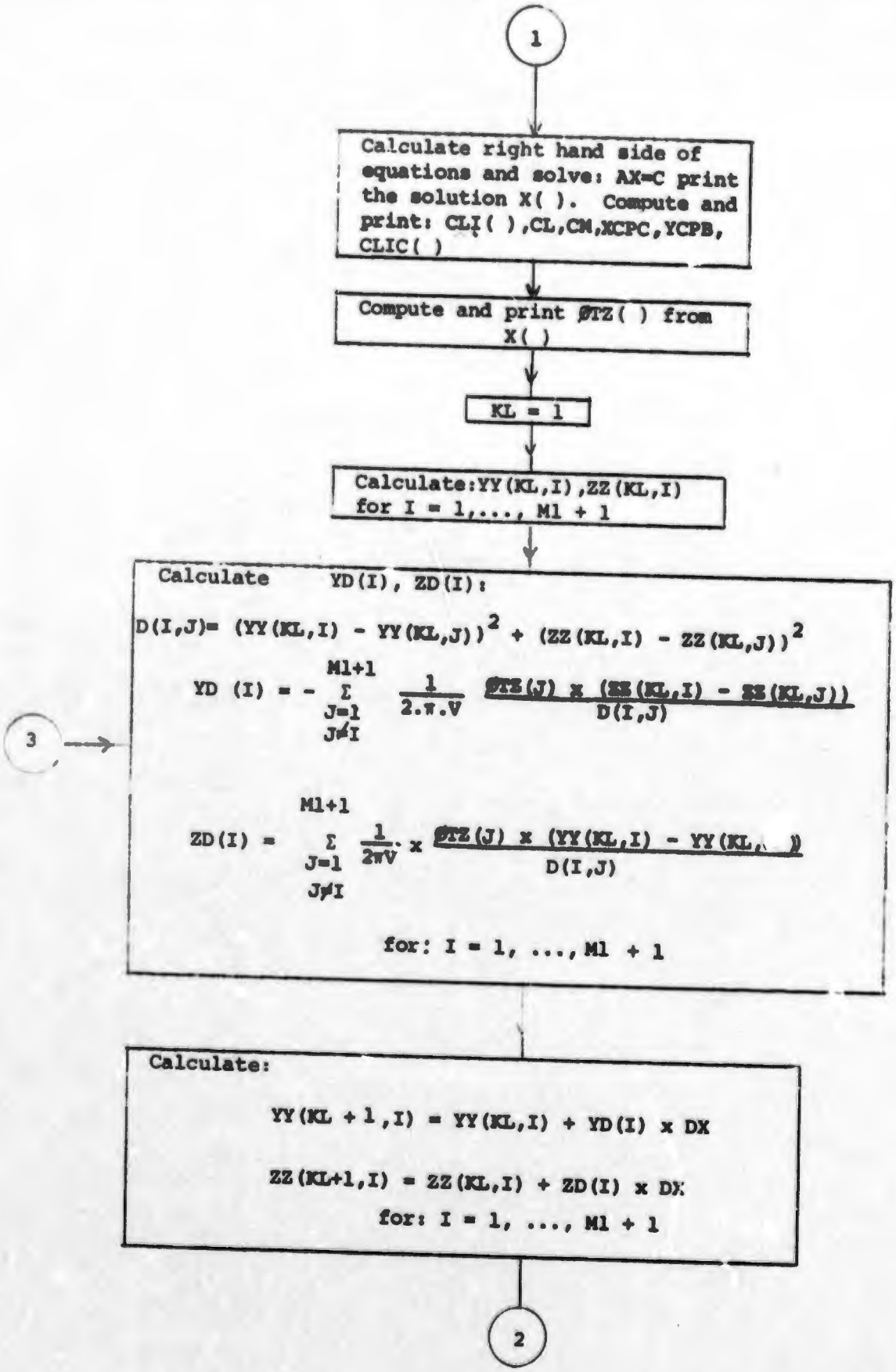
1
Calculate right hand side of equations and solve: AX=C print the solution X( ). Compute and print: CLI( ),CL,CM,XCPC,YCPB, CLIC( )
Compute and print ΦTZ( ) from X( )
KL = 1
Calculate:YY(KL,I),ZZ(KL,I) for I = 1,..., Ml + 1
Calculate YD(I), ZD(I):
D(I,J)= (YY(KL,I) - YY(KL,J))^2 + (ZZ(KL,I) - ZZ(KL,J))^2
YD (I) = - Σ (J=1, J≠I, Ml+1) 1/(2.π.V) ΦTZ(J) x (ZZ(KL,I) - ZZ(KL,J)) / D(I,J)
ZD(I) = Σ (J=1, J≠I, Ml+1) 1/(2πV) x ΦTZ(J) x (YY(KL,I) - YY(KL, )) / D(I,J)
for: I = 1, ..., Ml + 1
3
Calculate:
YY(KL + 1,I) = YY(KL,I) + YD(I) x DX
ZZ(KL+1,I) = ZZ(KL,I) + ZD(I) x DX
for: I = 1, ..., Ml + 1
2

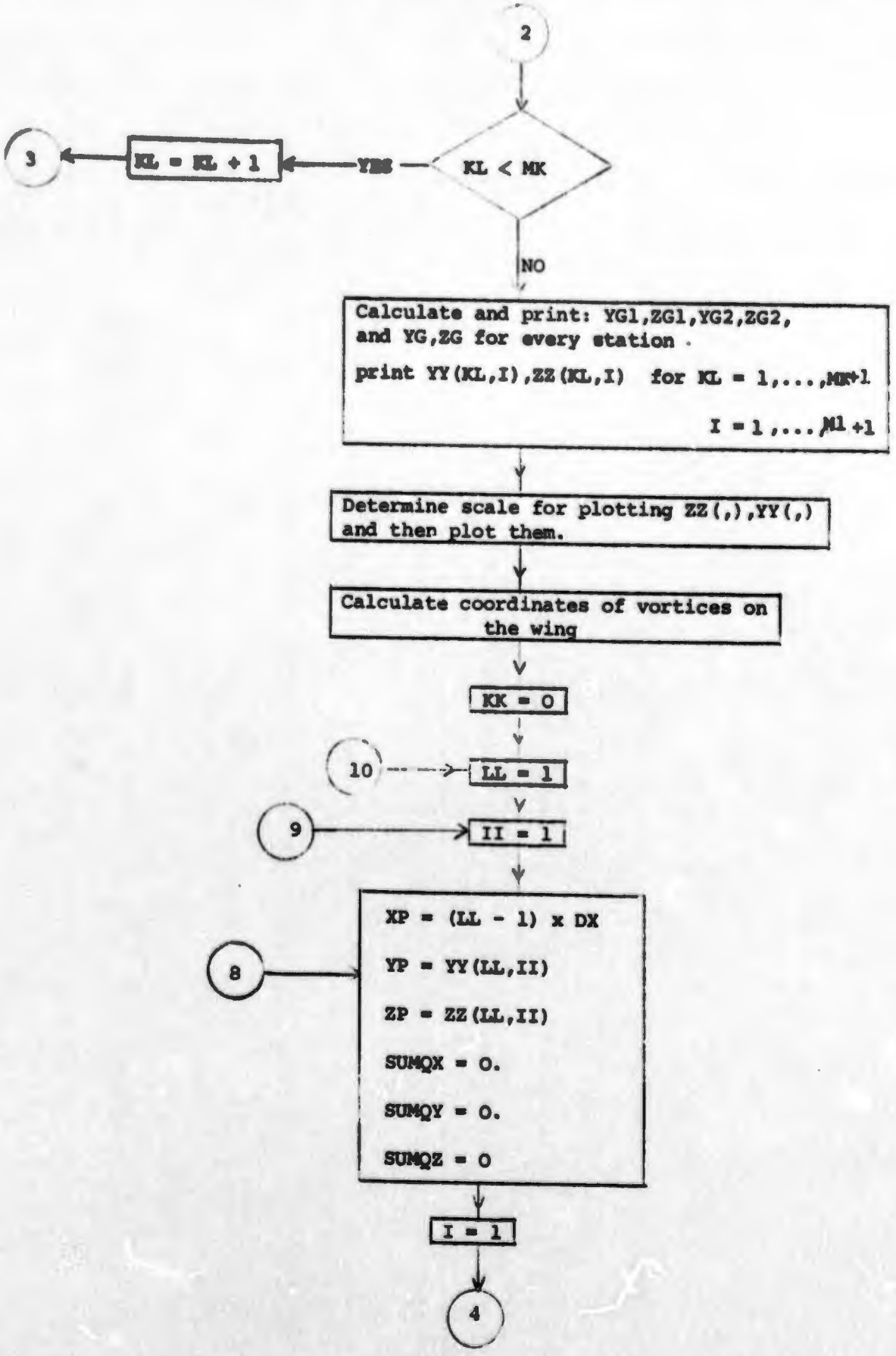
2
KL < MK
YES
KL = KL + 1
3
NO
Calculate and print: YG1,ZG1,YG2,ZG2,
and YG,ZG for every station .
print YY(KL,I),ZZ(KL,I) for KL = 1,...,MK+1
I = 1,...,M1+1
Determine scale for plotting ZZ(,),YY(,)
and then plot them.
Calculate coordinates of vortices on
the wing
KK = 0
10
LL = 1
9
II = 1
8
XP = (LL - 1) x DX
YP = YY(LL,II)
ZP = ZZ(LL,II)
SUMQX = 0.
SUMQY = 0.
SUMQZ = 0
I = 1
4

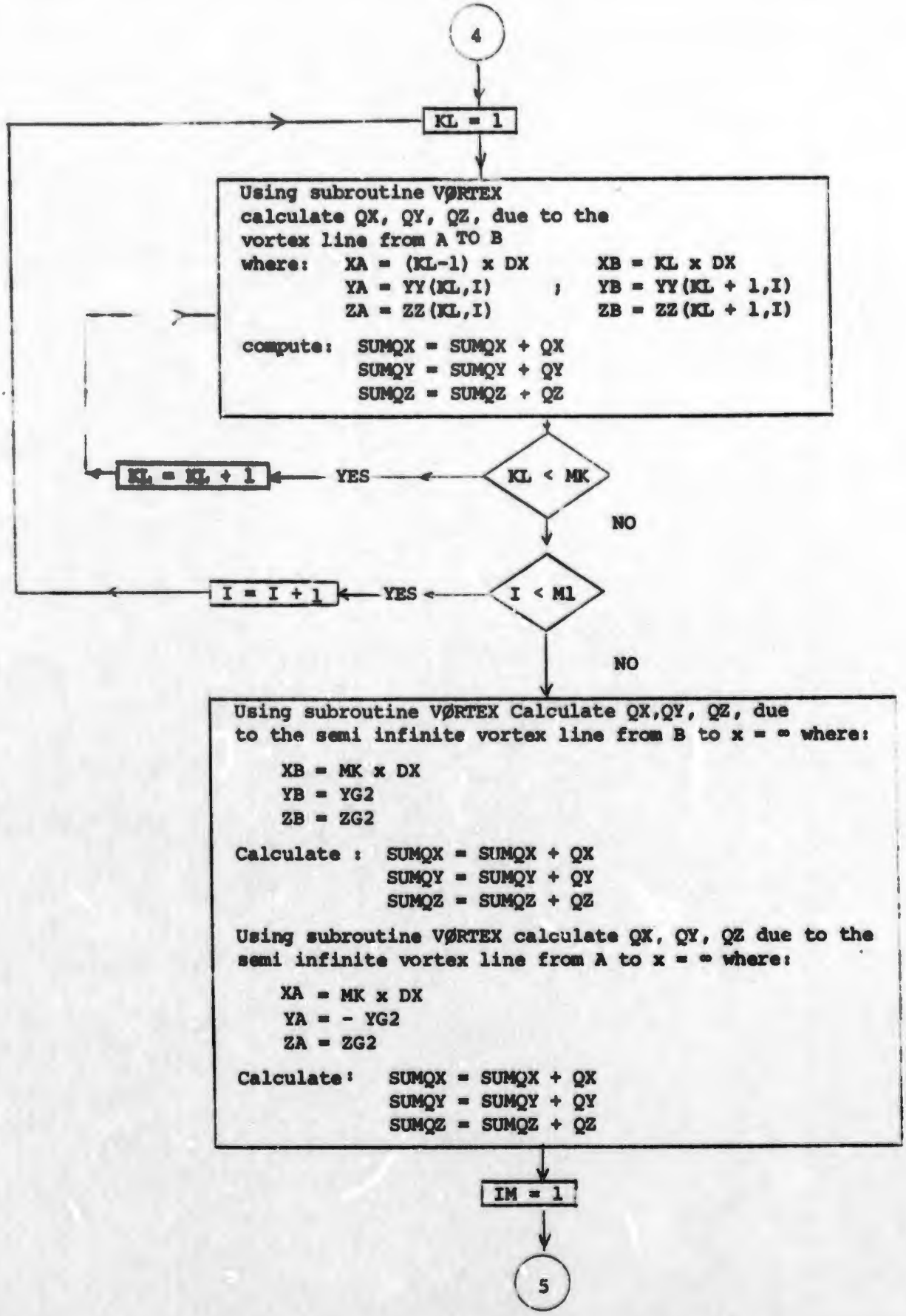
4
KL = 1
Using subroutine VØRTEX
calculate QX, QY, QZ, due to the
vortex line from A TO B
where: XA = (KL-1) x DX
YA = YY(KL,I)
ZA = ZZ(KL,I)
XB = KL x DX
YB = YY(KL + 1,I)
ZB = ZZ(KL + 1,I)
compute: SUMQX = SUMQX + QX
SUMQY = SUMQY + QY
SUMQZ = SUMQZ + QZ
KL < MK
YES
KL = KL + 1
NO
I < M1
YES
I = I + 1
NO
Using subroutine VØRTEX Calculate QX,QY, QZ, due
to the semi infinite vortex line from B to x = ∞ where:
XB = MK x DX
YB = YG2
ZB = ZG2
Calculate : SUMQX = SUMQX + QX
SUMQY = SUMQY + QY
SUMQZ = SUMQZ + QZ
Using subroutine VØRTEX calculate QX, QY, QZ due to the
semi infinite vortex line from A to x = ∞ where:
XA = MK x DX
YA = - YG2
ZA = ZG2
Calculate: SUMQX = SUMQX + QX
SUMQY = SUMQY + QY
SUMQZ = SUMQZ + QZ
IM = 1
5

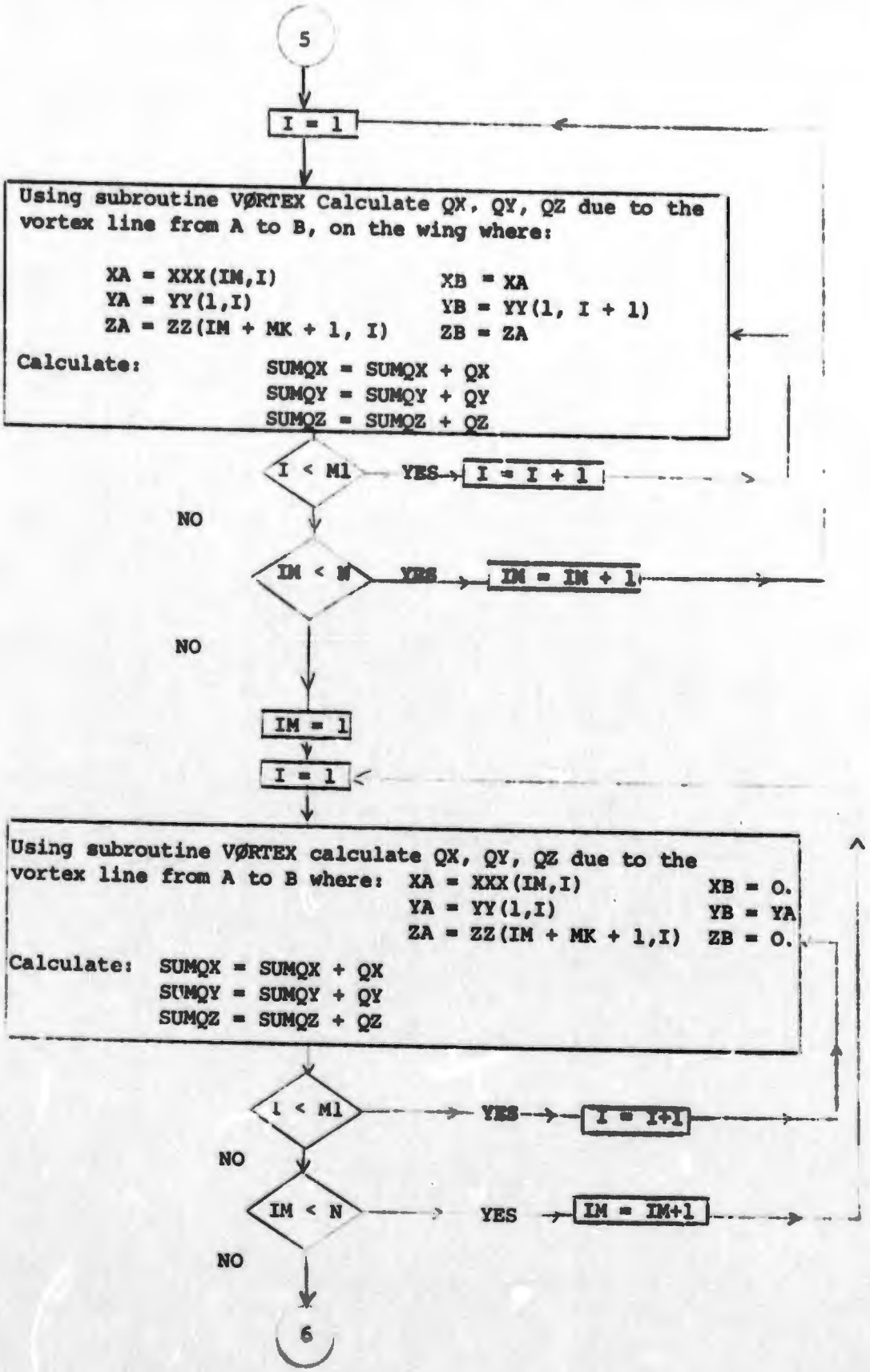
5
I = 1
Using subroutine VØRTEX Calculate QX, QY, QZ due to the vortex line from A to B, on the wing where:
XA = XXX(IM,I)
YA = YY(1,I)
ZA = ZZ(IM + MK + 1, I)
XB = XA
YB = YY(1, I + 1)
ZB = ZA
Calculate:
SUMQX = SUMQX + QX
SUMQY = SUMQY + QY
SUMQZ = SUMQZ + QZ
I < M1
YES
I = I + 1
NO
IM < N
YES
IM = IM + 1
NO
IM = 1
I = 1
Using subroutine VØRTEX calculate QX, QY, QZ due to the vortex line from A to B where:
XA = XXX(IM,I)
YA = YY(1,I)
ZA = ZZ(IM + MK + 1,I)
XB = O.
YB = YA
ZB = O.
Calculate:
SUMQX = SUMQX + QX
SUMQY = SUMQY + QY
SUMQZ = SUMQZ + QZ
I < M1
YES
I = I+1
NO
IM < N
YES
IM = IM+1
NO
6

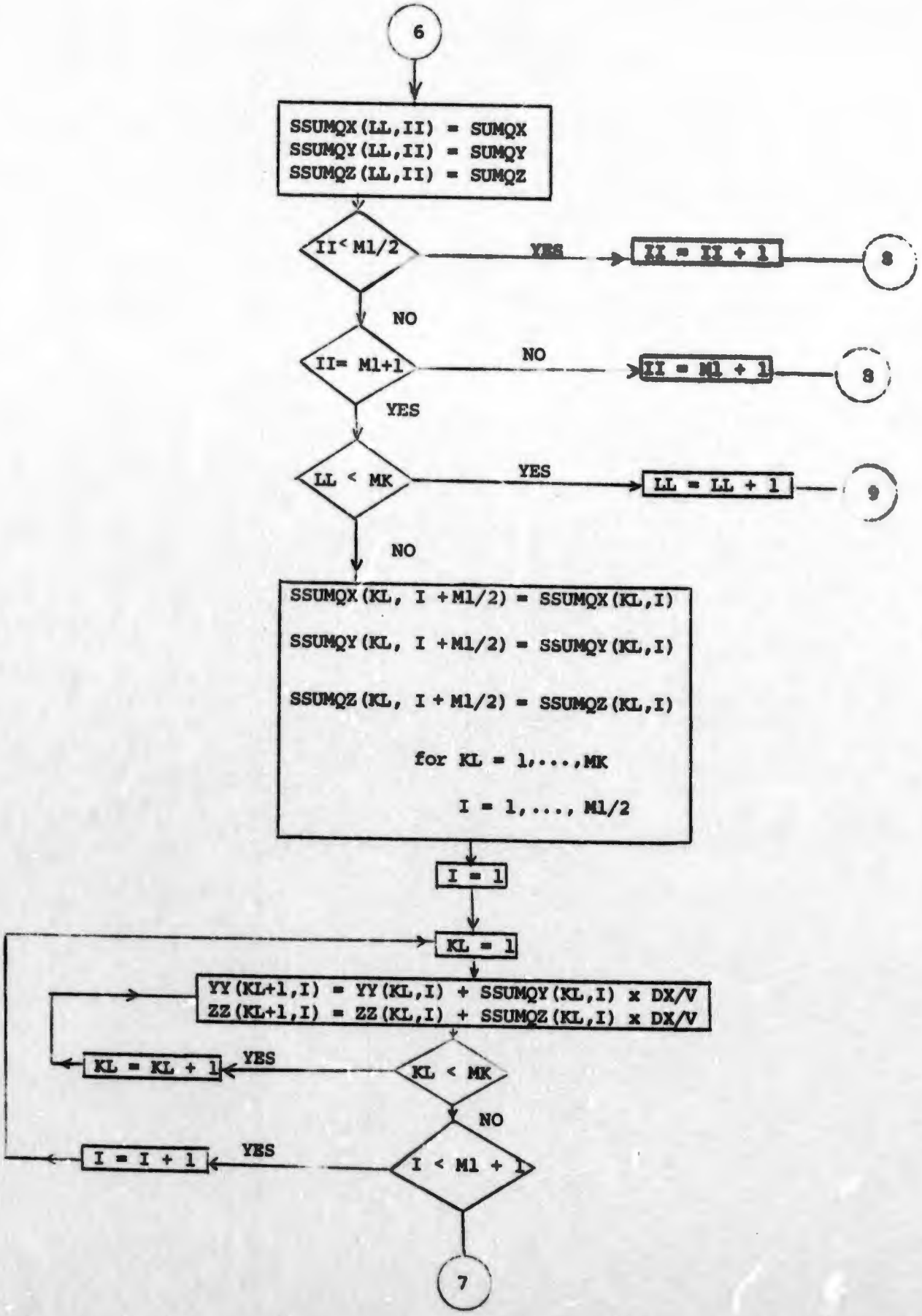
6
SSUMQX(LL,II) = SUMQX
SSUMQY(LL,II) = SUMQY
SSUMQZ(LL,II) = SUMQZ
II< M1/2
YES
II = II + 1
8
NO
II= M1+1
NO
II = M1 + 1
8
YES
LL < MK
YES
LL = LL + 1
9
NO
SSUMQX(KL, I +M1/2) = SSUMQX(KL,I)
SSUMQY(KL, I +M1/2) = SSUMQY(KL,I)
SSUMQZ(KL, I + M1/2) = SSUMQZ(KL,I)
for KL = 1,...,MK
I = 1,..., M1/2
I = 1
KL = 1
YY(KL+1,I) = YY(KL,I) + SSUMQY(KL,I) x DX/V
ZZ(KL+1,I) = ZZ(KL,I) + SSUMQZ(KL,I) x DX/V
KL = KL + 1
YES
KL < MK
NO
I = I + 1
YES
I < M1 + 1
7

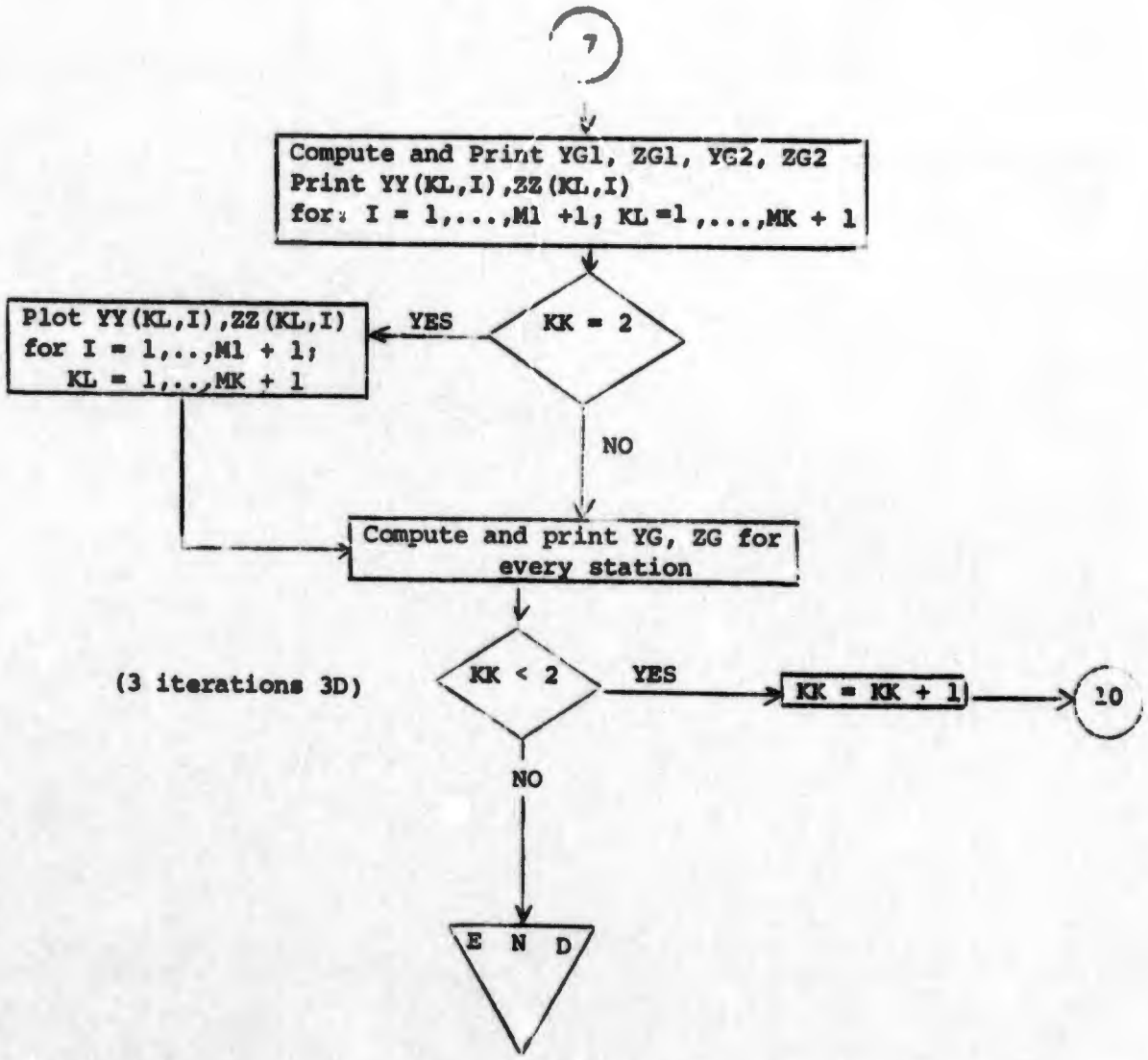
7
Compute and Print YG1, ZG1, YG2, ZG2
Print YY(KL,I),ZZ(KL,I)
for I = 1,...,M1 +1; KL =1,...,MK + 1
KK = 2
YES
Plot YY(KL,I),ZZ(KL,I)
for I = 1,..,M1 + 1;
KL = 1,..,MK + 1
NO
Compute and print YG, ZG for every station
(3 iterations 3D)
KK < 2
YES
KK = KK + 1
10
NO
E N D

## APPENDIX E : FLOW CHART FOR THE MVLM-3D PROGRAM

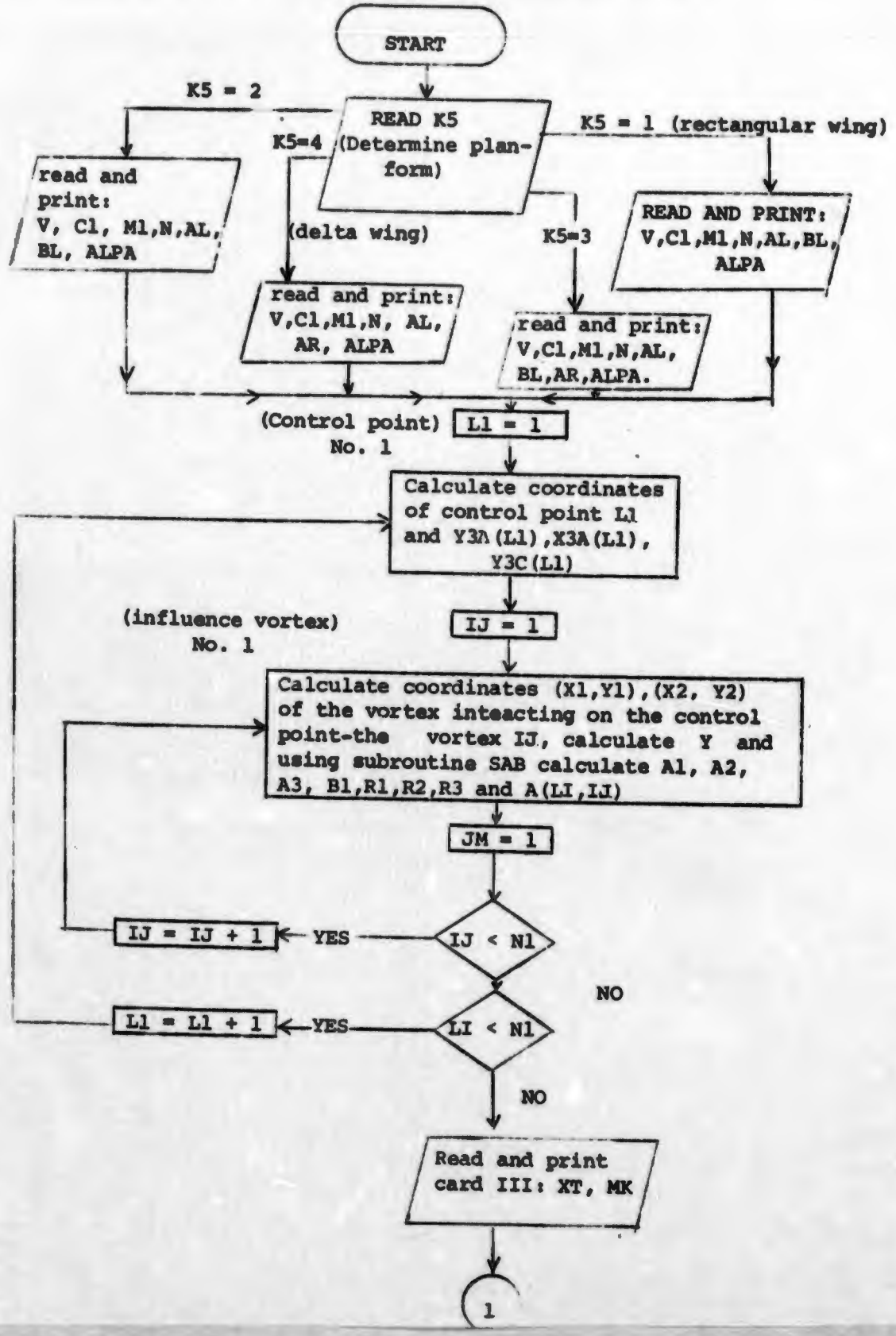

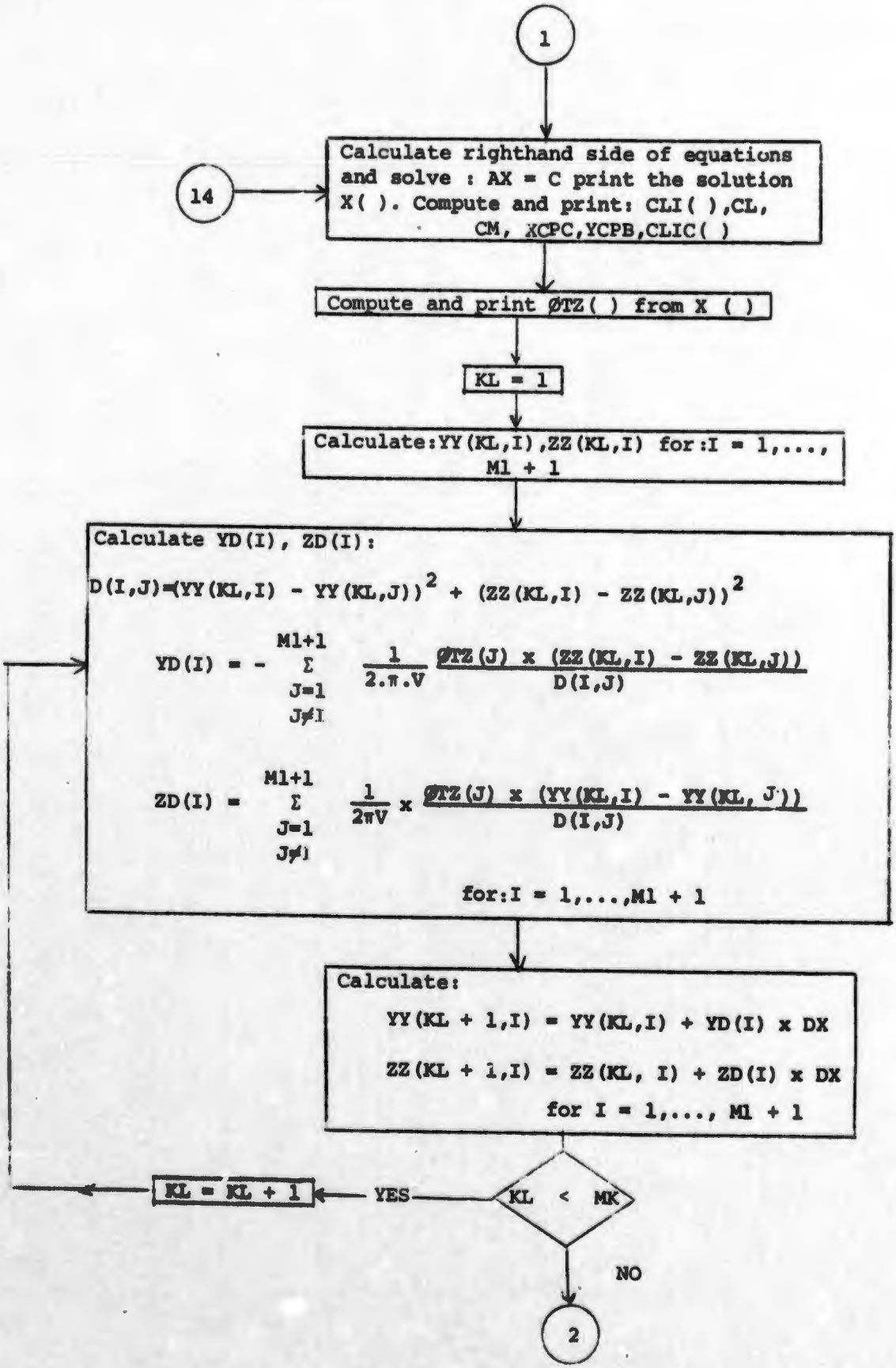
1
14
Calculate righthand side of equations and solve : AX = C print the solution X( ). Compute and print: CLI( ),CL, CM, XCPC,YCPB,CLIC( )
Compute and print ØTZ( ) from X ( )
KL = 1
Calculate:YY(KL,I),ZZ(KL,I) for:I = 1,..., Ml + 1
Calculate YD(I), ZD(I):
D(I,J)=(YY(KL,I) - YY(KL,J))^2 + (ZZ(KL,I) - ZZ(KL,J))^2
YD(I) = - Σ (J=1, J≠I, Ml+1) 1/(2.π.V) ØTZ(J) x (ZZ(KL,I) - ZZ(KL,J)) / D(I,J)
ZD(I) = Σ (J=1, J≠I, Ml+1) 1/2πV x ØTZ(J) x (YY(KL,I) - YY(KL,J)) / D(I,J)
for:I = 1,...,Ml + 1
Calculate:
YY(KL + 1,I) = YY(KL,I) + YD(I) x DX
ZZ(KL + 1,I) = ZZ(KL, I) + ZD(I) x DX
for I = 1,..., Ml + 1
KL < MK
YES
KL = KL + 1
NO
2

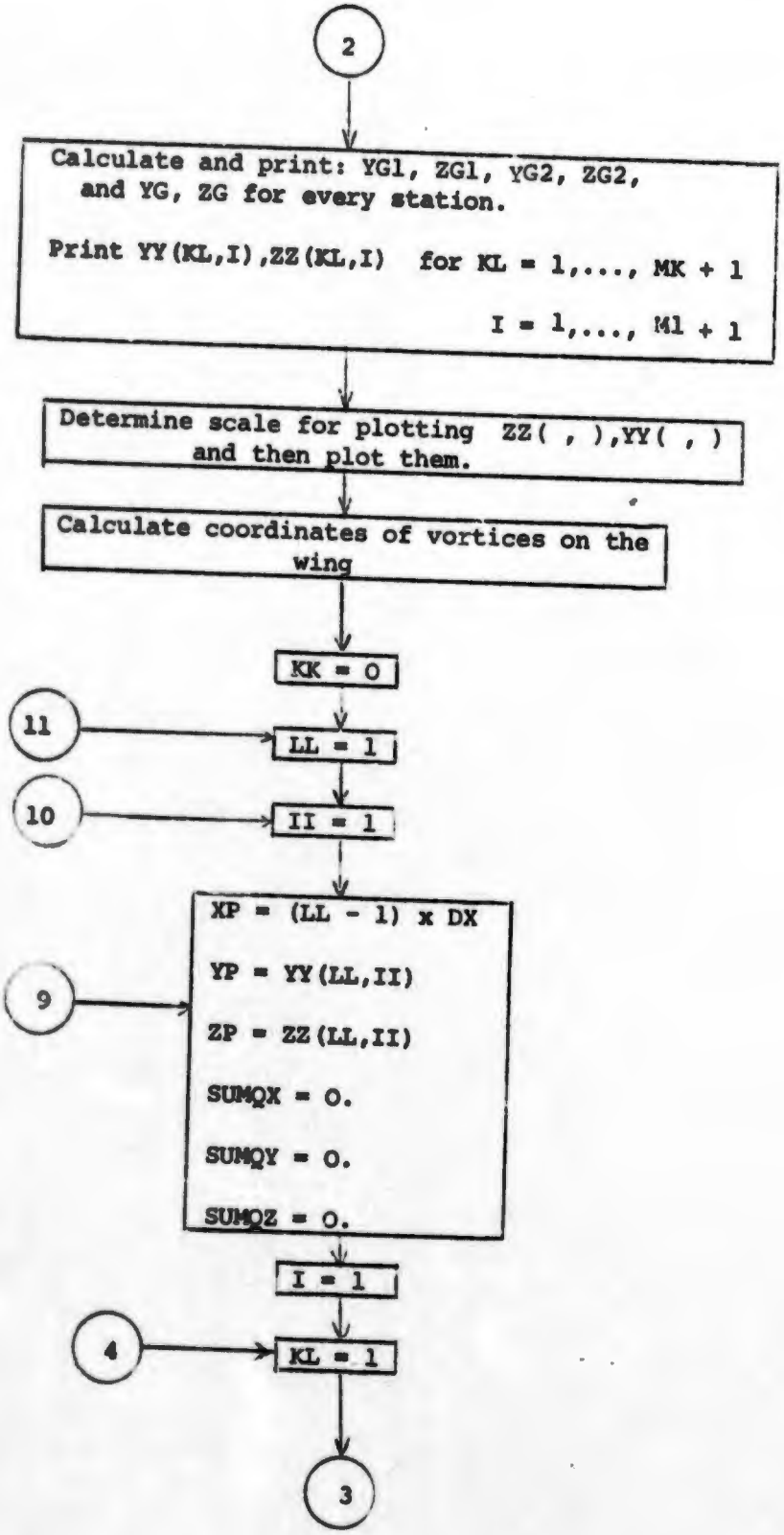
2
Calculate and print: YG1, ZG1, YG2, ZG2, and YG, ZG for every station.
Print YY(KL,I),ZZ(KL,I) for KL = 1,..., MK + 1
I = 1,..., M1 + 1
Determine scale for plotting ZZ( , ),YY( , ) and then plot them.
Calculate coordinates of vortices on the wing
KK = 0
11
LL = 1
10
II = 1
XP = (LL - 1) x DX
9
YP = YY(LL,II)
ZP = ZZ(LL,II)
SUMQX = 0.
SUMQY = 0.
SUMQZ = 0.
I = 1
4
KL = 1
3

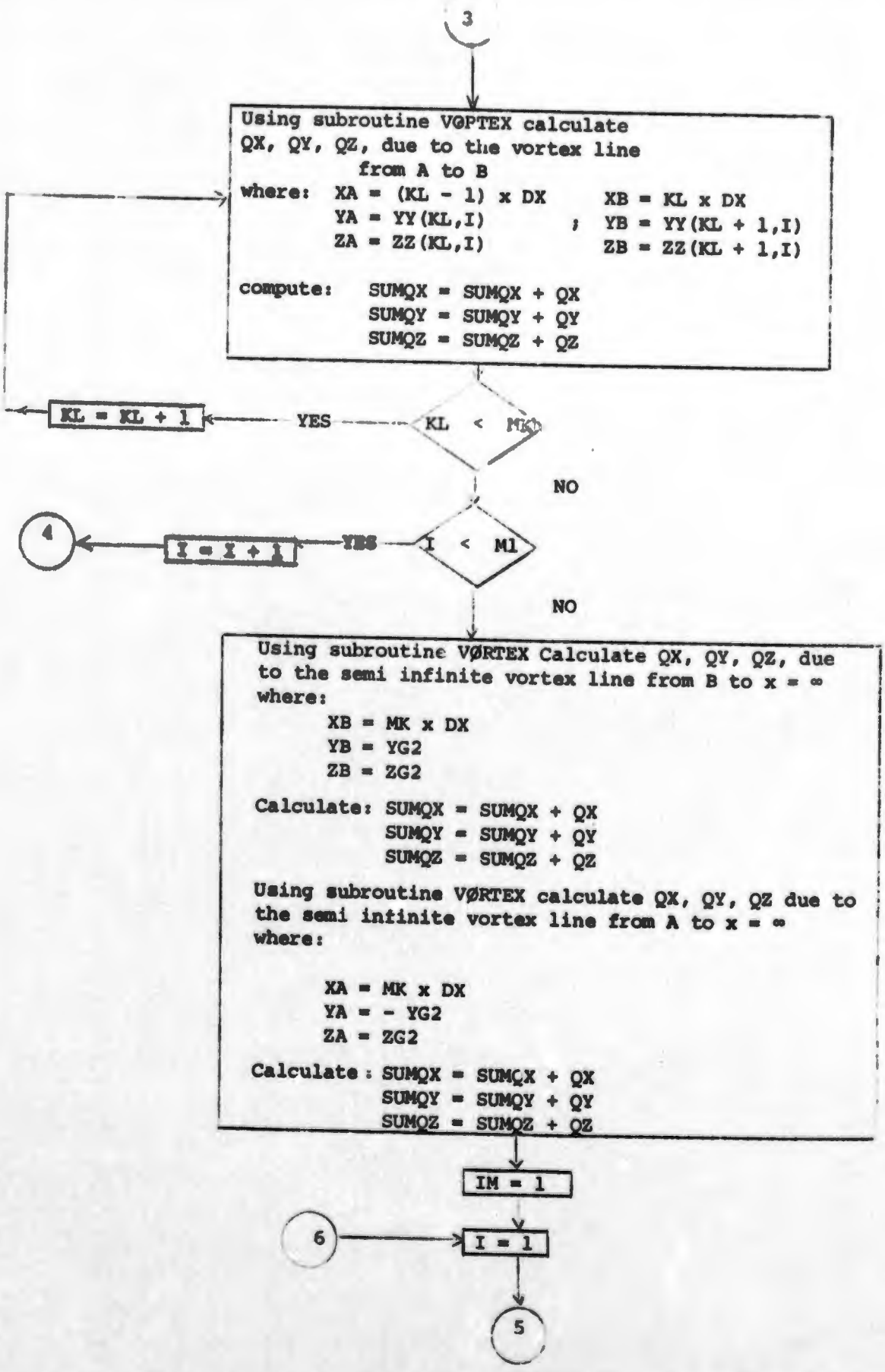
3
Using subroutine VØPTEX calculate
QX, QY, QZ, due to the vortex line
from A to B
where: XA = (KL - 1) x DX
YA = YY(KL,I)
ZA = ZZ(KL,I)
XB = KL x DX
; YB = YY(KL + 1,I)
ZB = ZZ(KL + 1,I)
compute: SUMQX = SUMQX + QX
SUMQY = SUMQY + QY
SUMQZ = SUMQZ + QZ
KL = KL + 1
YES
KL < MK
NO
4
I = I + 1
YES
I < M1
NO
Using subroutine VØRTEX Calculate QX, QY, QZ, due
to the semi infinite vortex line from B to x = ∞
where:
XB = MK x DX
YB = YG2
ZB = ZG2
Calculate: SUMQX = SUMQX + QX
SUMQY = SUMQY + QY
SUMQZ = SUMQZ + QZ
Using subroutine VØRTEX calculate QX, QY, QZ due to
the semi infinite vortex line from A to x = ∞
where:
XA = MK x DX
YA = - YG2
ZA = ZG2
Calculate : SUMQX = SUMQX + QX
SUMQY = SUMQY + QY
SUMQZ = SUMQZ + QZ
IM = 1
6
I = 1
5

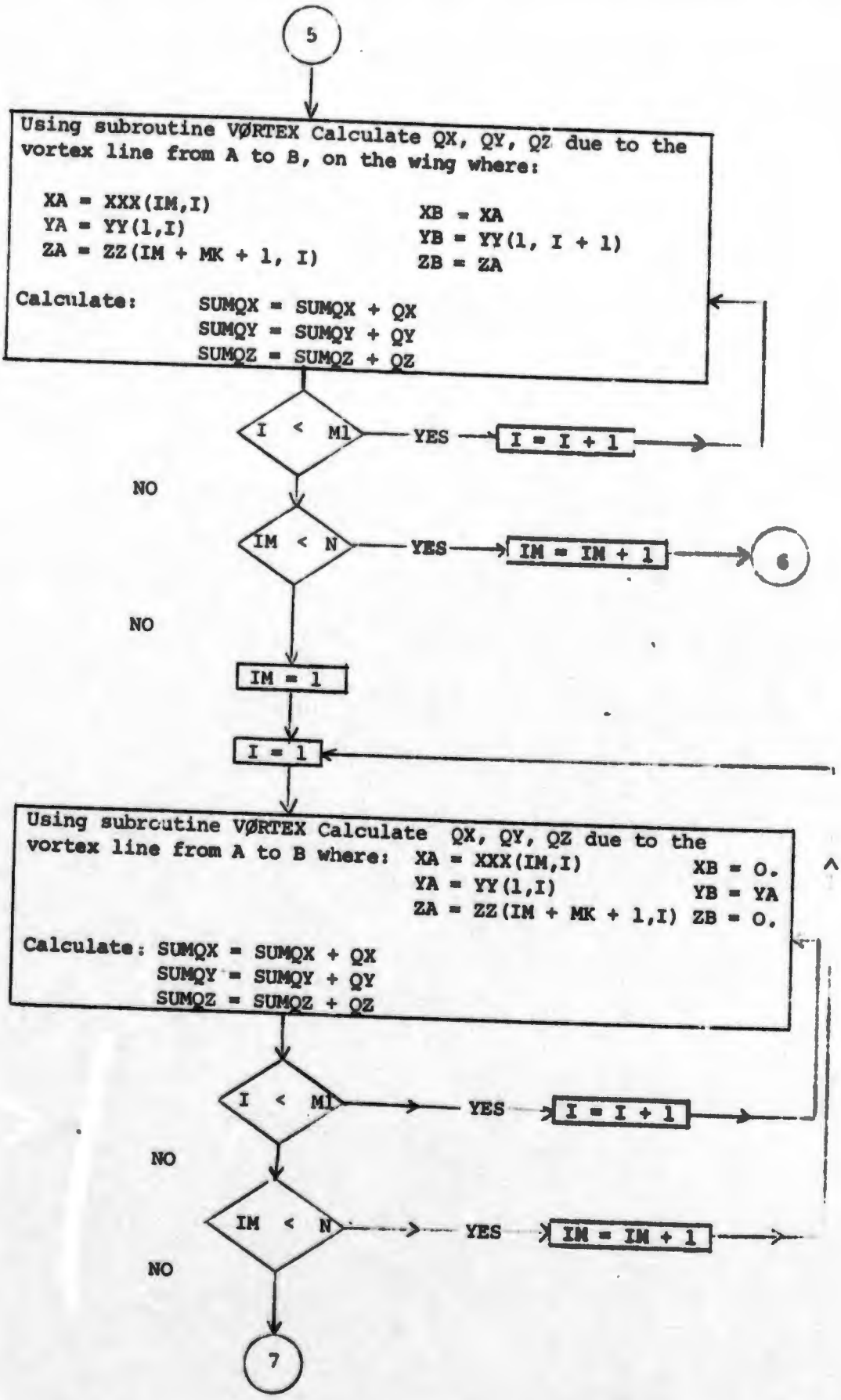
5
Using subroutine VØRTEX Calculate QX, QY, QZ due to the vortex line from A to B, on the wing where:
XA = XXX(IM,I)
YA = YY(1,I)
ZA = ZZ(IM + MK + 1, I)
XB = XA
YB = YY(1, I + 1)
ZB = ZA
Calculate: SUMQX = SUMQX + QX
SUMQY = SUMQY + QY
SUMQZ = SUMQZ + QZ
I < M1
YES
I = I + 1
NO
IM < N
YES
IM = IM + 1
6
NO
IM = 1
I = 1
Using subroutine VØRTEX Calculate QX, QY, QZ due to the vortex line from A to B where:
XA = XXX(IM,I)
YA = YY(1,I)
ZA = ZZ(IM + MK + 1,I)
XB = O.
YB = YA
ZB = O.
Calculate: SUMQX = SUMQX + QX
SUMQY = SUMQY + QY
SUMQZ = SUMQZ + QZ
I < M1
YES
I = I + 1
NO
IM < N
YES
IM = IM + 1
NO
7

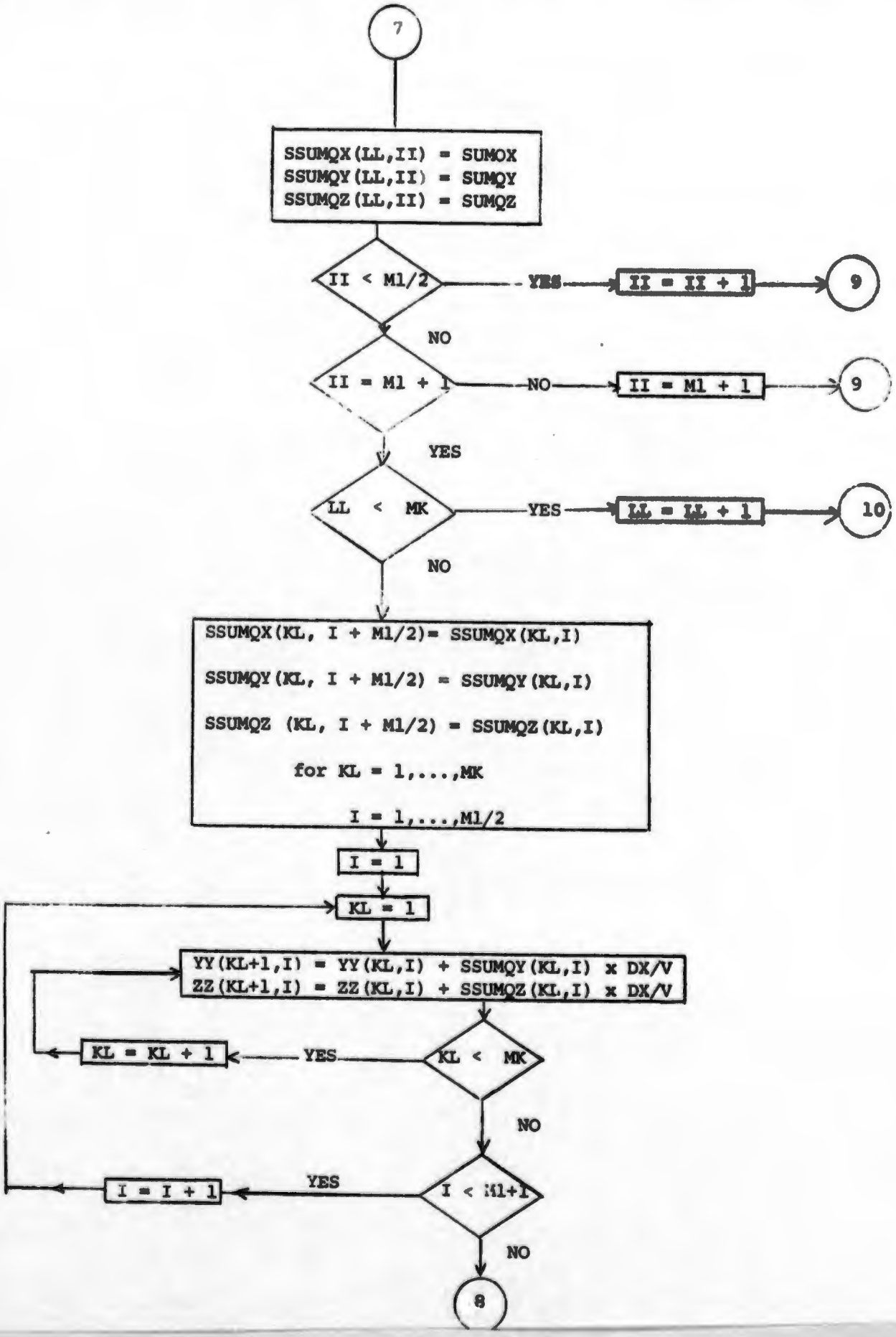
7
SSUMQX(LL,II) = SUMOX
SSUMQY(LL,II) = SUMQY
SSUMQZ(LL,II) = SUMQZ
II < M1/2
YES
II = II + 1
9
NO
II = M1 + 1
NO
II = M1 + 1
9
YES
LL < MK
YES
LL = LL + 1
10
NO
SSUMQX(KL, I + M1/2)= SSUMQX(KL,I)
SSUMQY(KL, I + M1/2) = SSUMQY(KL,I)
SSUMQZ (KL, I + M1/2) = SSUMQZ(KL,I)
for KL = 1,...,MK
I = 1,...,M1/2
I = 1
KL = 1
YY(KL+1,I) = YY(KL,I) + SSUMQY(KL,I) x DX/V
ZZ(KL+1,I) = ZZ(KL,I) + SSUMQZ(KL,I) x DX/V
KL = KL + 1
YES
KL < MK
NO
I = I + 1
YES
I < M1+1
NO
8

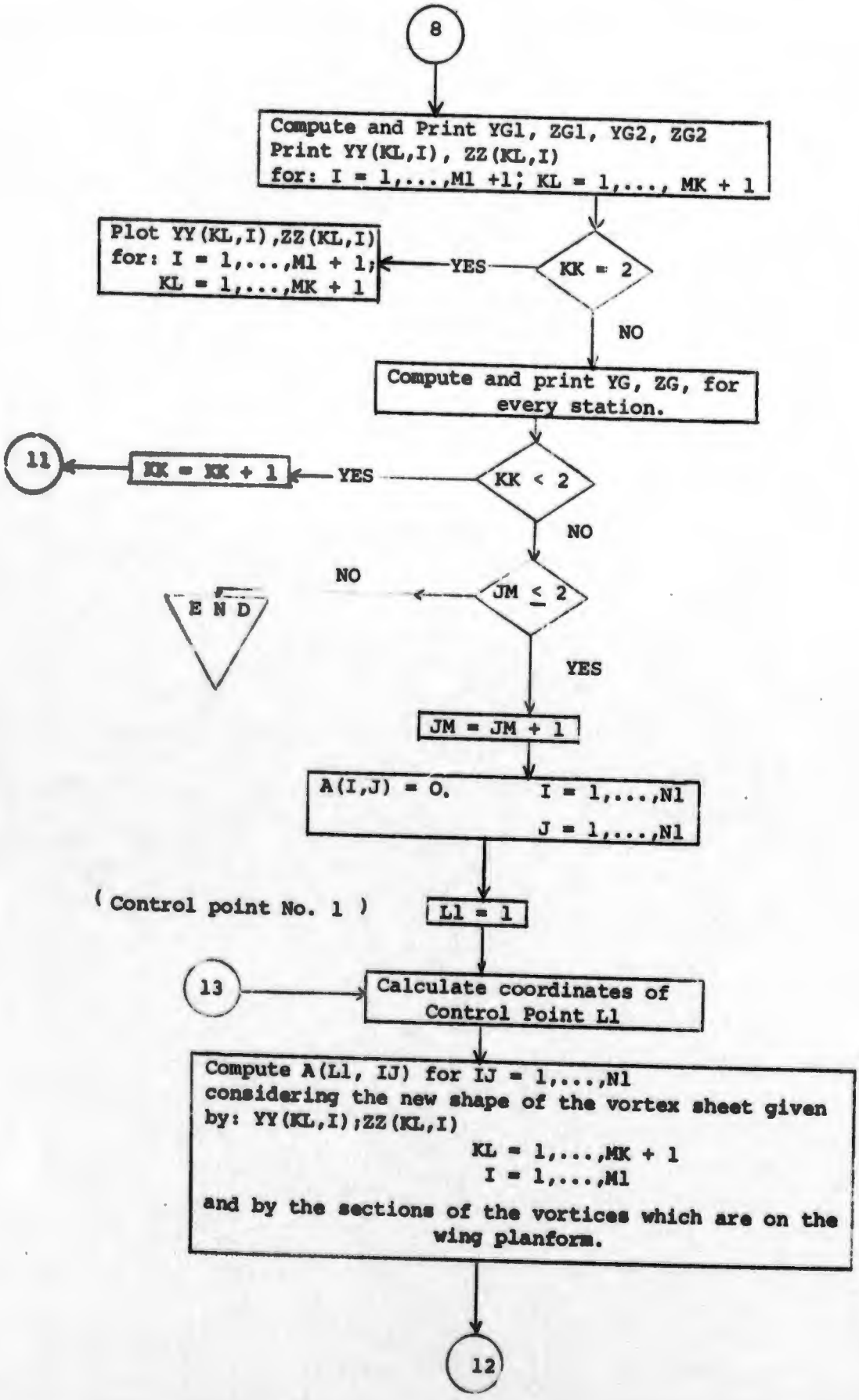
8
Compute and Print YG1, ZG1, YG2, ZG2
Print YY(KL,I), ZZ(KL,I)
for: I = 1,...,M1 +1; KL = 1,..., MK + 1
KK = 2
YES
Plot YY(KL,I),ZZ(KL,I)
for: I = 1,...,M1 + 1;
KL = 1,...,MK + 1
NO
Compute and print YG, ZG, for every station.
KK < 2
YES
KK = KK + 1
11
NO
JM ≤ 2
NO
E N D
YES
JM = JM + 1
A(I,J) = 0. I = 1,...,N1
J = 1,...,N1
( Control point No. 1 )
L1 = 1
13
Calculate coordinates of Control Point L1
Compute A(L1, IJ) for IJ = 1,...,N1
considering the new shape of the vortex sheet given by: YY(KL,I);ZZ(KL,I)
KL = 1,...,MK + 1
I = 1,...,M1
and by the sections of the vortices which are on the wing planform.
12

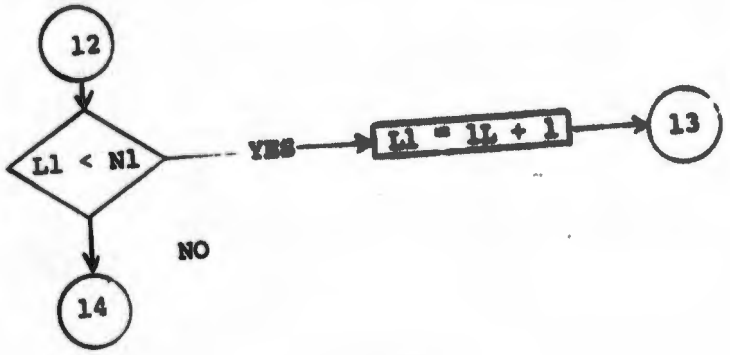
12
L1 < N1
YES
L1 = L1 + 1
13
NO
14

## APPENDIX F: FLOW CHART FOR NLVLM WITH STR . HT VORTICES FOR THE CALCULATION OF AERODYNAMIC COEFFICIENTS.

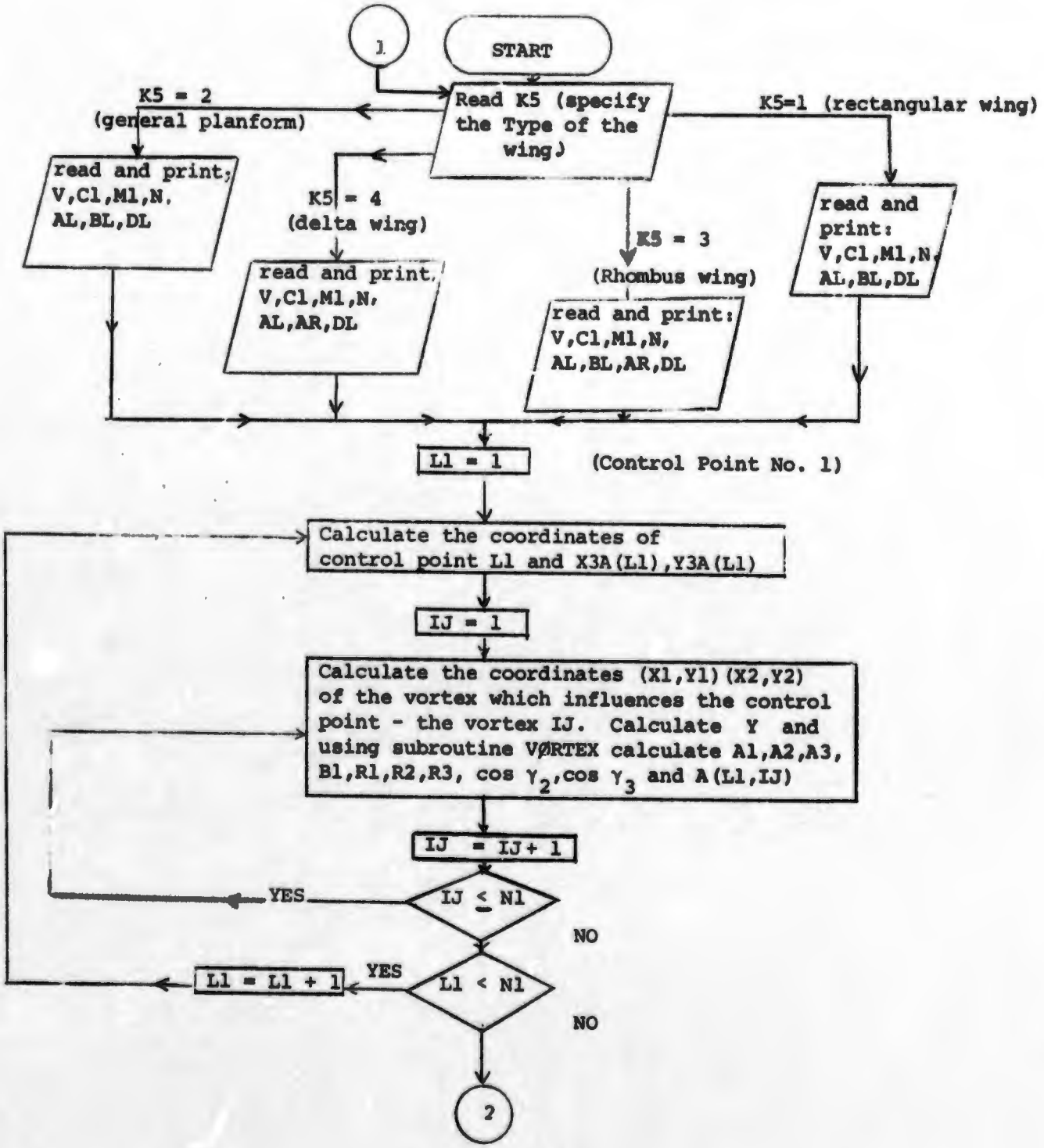

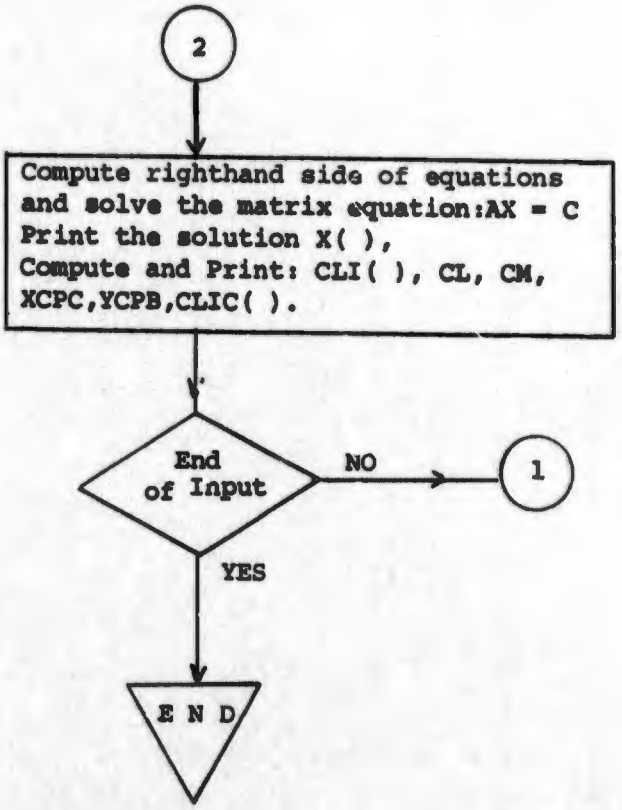
2
Compute righthand side of equations and solve the matrix equation:AX = C
Print the solution X( ),
Compute and Print: CLI( ), CL, CM, XCPC,YCPB,CLIC( ).
End of Input
NO
1
YES
E N D

TABLE Ia - CALCULATION OF THE LIFT COEFFICIENTS OF A RECTANGULAR WING of AR = 5.33 at $\alpha = 10^{\circ}$ FOR VARIOUS PLANFORM SUBDIVISIONS.

| $N_s$ \ $N_c$ | 1 | 2 | 3 | 4 |
|---|---|---|---|---|
| 5 | 0.4478 | 0.4480 | 0.4494 | 0.4495 |
| 10 | 0.4267 | 0.4291 | 0.4294 | 0.4295 |
| 15 | 0.4186 | 0.4212 | 0.4216 | 0.4218 |
| 20 | 0.4144 | 0.4170 | 0.4175 | |
| 40 | 0.4078 | 0.4105 | | |

TABLE Ib - CALCULATION OF THE LIFT COEFFICIENTS FOR RECTANGULAR WINGS OF ASPECT RATIO 0.5 to 6 at $\alpha = 10^{o}$ FOR VARIOUS PLANFORM SUBDIVISIONS.

| AR \ $N_c \times N_s$ | 2 x 20 | 4 x 20 |
|---|---|---|
| 0.5 | .1425 | 0.1429 |
| 1 | .2677 | 0.2689 |
| 1.5 | .3697 | 0.3714 |
| 2 | .4518 | 0.4535 |
| 3 | .5731 | 0.5747 |
| 4 | .6571 | 0.6586 |
| 5 | .7185 | 0.7198 |
| 6 | .7652 | 0.7662 |

TABLE II - CALCULATIONS OF THE LIFT COEFFICIENTS OF DELTA WINGS OF ASPECT RATIOS 0.5 to 5 at $\alpha = 10^{\circ}$ FOR VARIOUS SUBDIVISIONS WITH PERPENDICULAR AND INCLINED BOUND VORTICES.

| | $N_c = 4$ $N_s = 5$ | | $N_c = 2$ $N_s = 10$ | | |
|---|---|---|---|---|---|
| AR | Rectangular | Inclined | Rectangular | Inclined | Exp. Results |
| 0.5 | 0.162 | 0.138 | 0.134 | 0.125 | 0.13 |
| 1 | 0.288 | 0.248 | 0.240 | 0.231 | 0.23<br>0.24 |
| 2 | 0.462 | 0.416 | 0.397 | 0.393 | 0.4 |
| 3 | | | .510 | | 0.51 |
| 4 | | | .597 | | 0.60 |
| 5 | 0.724 | 0.692 | .664 | | |

TABLE III - CALCULATION OF THE LIFT COEFFICIENTS OF A CROPPED DELTA WING OF AR = 3 at $\alpha = 10^{o}$ USING VARIOUS PLANFORM SUBDIVISIONS WITH PERPENDICULAR AND INCLINED BOUND VORTICES.

| $N_c = 2$ | $N_s = 10$ | $N_c = 4$ | $N_s = 10$ | $N_c = 4$ | $N_s = 20$ |
|---|---|---|---|---|---|
| Rectangular | Inclined | Rectangular | Inclined | Rectangular | Included |
| .557 | .564 | .5589 | .5640 | .5543 | .5423 |

TABLE IVa: VLM-3D CALCULATION OF THE LIFT COEFFICIENT AND VORTEX CENTER TRAJECTORIES FOR A RECTANGULAR WING OF AR = 3 $\alpha = 10^{o}$ WITH M = 16 ($N_c = 2$; $N_s = 20$)

| Station No. | $Y_{cg}$ | $Z_{cg}$ | X(*) |
|---|---|---|---|
| 1 | 0.830026 | 0.0 | 0.0000 |
| 2 | 0.829882 | -0.033176 | 0.6250 |
| 3 | 0.828922 | -0.052121 | 1.2500 |
| 4 | 0.828492 | -0.068751 | 1.8750 |
| 5 | 0.828260 | -0.084376 | 2.5000 |
| 6 | 0.828141 | -0.099475 | 3.1250 |
| 7 | 0.828091 | -0.114223 | 3.7500 |
| 8 | 0.828074 | -0.128698 | 4.3750 |
| 9 | 0.828071 | -0.142955 | 5.0000 |
| 10 | 0.828070 | -0.157035 | 5.6250 |
| 11 | 0.828072 | -0.170968 | 6.2500 |
| 12 | 0.828075 | -0.184779 | 6.8750 |
| 13 | 0.828080 | -0.198495 | 7.5000 |
| 14 | 0.828084 | -0.212141 | 8.1250 |
| 15 | 0.828088 | -0.225740 | 8.7500 |
| 16 | 0.828073 | -0.239314 | 9.3750 |
| 17 | 0.827874 | -0.252771 | 10.0000 |

Calculated $C_L = 0.5731$

(*) X is given in half span units.

TABLE IVb: VLM-3D CALCULATION OF THE LIFT COEFFICIENT AND VORTEX CENTER TRAJECTORIES FOR A RECTANGULAR WING OF AR = 3 at $\alpha = 10^{o}$ WITH M = 32 ($N_c$=2; $N_s$ = 20)

| Station No. | $Y_{cg}$ | $Z_{cg}$ | $X^{(*)}$ |
|---|---|---|---|
| 1 | 0.830026 | 0.0 | 0.0 |
| 2 | 0.829906 | -0.016601 | 0.3125 |
| 3 | 0.829101 | -0.027971 | 0.6250 |
| 4 | 0.828617 | -0.037707 | 0.9375 |
| 5 | 0.828316 | -0.046624 | 1.2500 |
| 6 | 0.828123 | -0.055070 | 1.5625 |
| 7 | 0.827999 | -0.063207 | 1.8750 |
| 8 | 0.827925 | -0.071115 | 2.1875 |
| 9 | 0.827881 | -0.078842 | 2.5000 |
| 10 | 0.827849 | -0.086426 | 2.8125 |
| 11 | 0.827829 | -0.093895 | 3.1250 |
| 12 | 0.827812 | -0.101270 | 3.4375 |
| 13 | 0.827798 | -0.108567 | 3.7500 |
| 14 | 0.827786 | -0.115795 | 4.0625 |
| 15 | 0.827779 | -0.122964 | 4.3750 |
| 16 | 0.827771 | -0.130080 | 4.6875 |
| 17 | 0.827766 | -0.137151 | 5.0000 |
| 18 | 0.827761 | -0.144183 | 5.3125 |
| 19 | 0.827756 | -0.151184 | 5.6250 |
| 20 | 0.827753 | -0.158160 | 5.9375 |
| 21 | 0.827750 | -0.165113 | 6.2500 |
| 22 | 0.827747 | -0.172050 | 6.5625 |
| 23 | 0.827747 | -0.178972 | 6.8750 |
| 24 | 0.827747 | -0.185882 | 7.1875 |
| 25 | 0.827748 | -0.192782 | 7.500 |

TABLE IVb - CONTINUED

| Station No. | $Y_{cg}$ | $Z_{cg}$ | $X^{(*)}$ |
|---|---|---|---|
| 26 | 0.827749 | -0.199674 | 7.8125 |
| 27 | 0.827749 | -0.206557 | 8.1250 |
| 28 | 0.827749 | -0.213434 | 8.4375 |
| 29 | 0.827745 | -0.220305 | 8.7500 |
| 30 | 0.827732 | -0.227169 | 9.0625 |
| 31 | 0.827692 | -0.234021 | 9.3750 |
| 32 | 0.827551 | -0.240825 | 9.6875 |
| 33 | 0.826783 | -0.247300 | 10.0000 |

Calculated $C_L$ = 0.5731

(*) X is given in half span units.

TABLE IVc - MVLM CALCULATION OF THE LIFT COEFFICIENT AND VORTEX CENTER TRAJECTORIES FOR A RECTANGULAR WING OF AR = 3 at $\alpha = 10^{o}$ WITH M = 16 ($N_c = 2$; $N_s = 20$)

| Station No. | $Y_{cg}$ | $Z_{cg}$ | $X^{(*)}$ |
|---|---|---|---|
| 1 | 0.830163 | 0.0 | 0.0000 |
| 2 | 0.830020 | -0.032751 | 0.6250 |
| 3 | 0.829077 | -0.051457 | 1.2500 |
| 4 | 0.828653 | -0.067872 | 1.8750 |
| 5 | 0.828424 | -0.083293 | 2.5000 |
| 6 | 0.828307 | -0.098197 | 3.1250 |
| 7 | 0.828258 | -0.112754 | 3.7500 |
| 8 | 0.828241 | -0.127044 | 4.3750 |
| 9 | 0.828236 | -0.141119 | 5.0000 |
| 10 | 0.828236 | -0.155020 | 5.6250 |
| 11 | 0.828238 | -0.168775 | 6.2500 |
| 12 | 0.828242 | -0.182412 | 6.8750 |
| 13 | 0.828245 | -0.195953 | 7.5000 |
| 14 | 0.828251 | -0.209424 | 8.1250 |
| 15 | 0.828254 | -0.222849 | 8.7500 |
| 16 | 0.828240 | -0.236246 | 9.3750 |
| 17 | 0.828041 | -0.249526 | 10.0000 |

Calculated $C_L = 0.5656$

(*) X is given in half span units.

TABLE IVd - MVLM CALCULATION OF THE LIFT COEFFICIENT AND VORTEX CENTER TRAJECTORIES FOR A RECTANGULAR WING OF AR = 3 at $\alpha = 10^{o}$ WITH M = 32 ($N_c = 2$; $N_s = 20$)

| Station No. | $Y_{cg}$ | $Z_{cg}$ | $X^{(*)}$ |
|---|---|---|---|
| 1 | 0.830137 | 0.0 | 0.0 |
| 2 | 0.830020 | -0.016388 | 0.3125 |
| 3 | 0.829225 | -0.027616 | 0.6250 |
| 4 | 0.828748 | -0.037225 | 0.9375 |
| 5 | 0.828451 | -0.046025 | 1.2500 |
| 6 | 0.828261 | -0.054359 | 1.5625 |
| 7 | 0.828138 | -0.062389 | 1.8750 |
| 8 | 0.828065 | -0.070194 | 2.1875 |
| 9 | 0.828021 | -0.077821 | 2.5000 |
| 10 | 0.827991 | -0.085307 | 2.8125 |
| 11 | 0.827970 | -0.092679 | 3.1250 |
| 12 | 0.827954 | -0.099960 | 3.4375 |
| 13 | 0.827939 | -0.107164 | 3.7500 |
| 14 | 0.827929 | -0.114300 | 4.0625 |
| 15 | 0.827920 | -0.121378 | 4.3750 |
| 16 | 0.827913 | -0.12840. | 4.6875 |
| 17 | 0.827908 | -0.135384 | 5.0000 |
| 18 | 0.827904 | -0.142327 | 5.3125 |
| 19 | 0.827898 | -0.149239 | 5.6250 |
| 20 | 0.827896 | -0.156124 | 5.9375 |
| 21 | 0.827892 | -0.162989 | 6.2500 |
| 22 | 0.827891 | -0.169836 | 6.5625 |
| 23 | 0.827891 | -0.176669 | 6.8750 |
| 24 | 0.827891 | -0.183490 | 7.1875 |
| 25 | 0.827892 | -0.190301 | 7.5000 |

TABLE IVd - CONTINUED

| Station No. | $Y_{cg}$ | $Z_{cg}$ | $X^{(*)}$ |
|---|---|---|---|
| 26 | 0.827893 | -0.197103 | 7.8125 |
| 27 | 0.827894 | -0.203897 | 8.1250 |
| 28 | 0.827893 | -0.210685 | 8.4375 |
| 29 | 0.827888 | -0.217466 | 8.7500 |
| 30 | 0.827876 | -0.224241 | 9.0625 |
| 31 | 0.827837 | -0.231003 | 9.3750 |
| 32 | 0.827699 | -0.237717 | 9.6875 |
| 33 | 0.826941 | -0.244100 | 10.0000 |

Calculated $C_L$ = 0.5656.

(*) X is given in half span units.

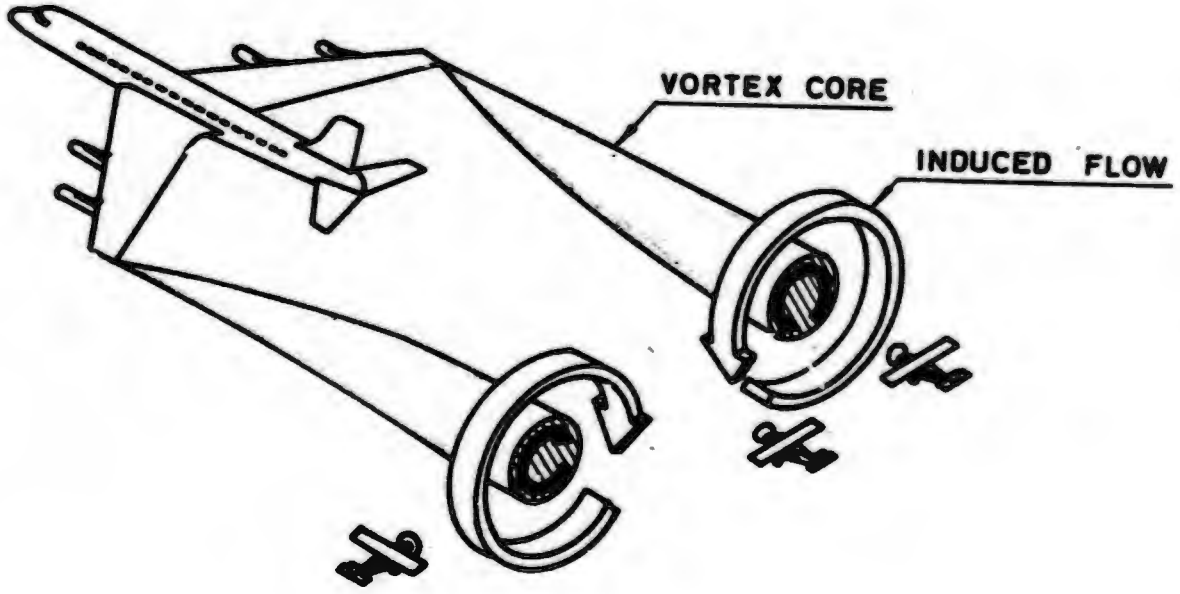


FIGURE 1 - ILLUSTRATION OF TRAILING VORTEX WAKE AND TYPES OF ENCOUNTER (From Ref. 1)

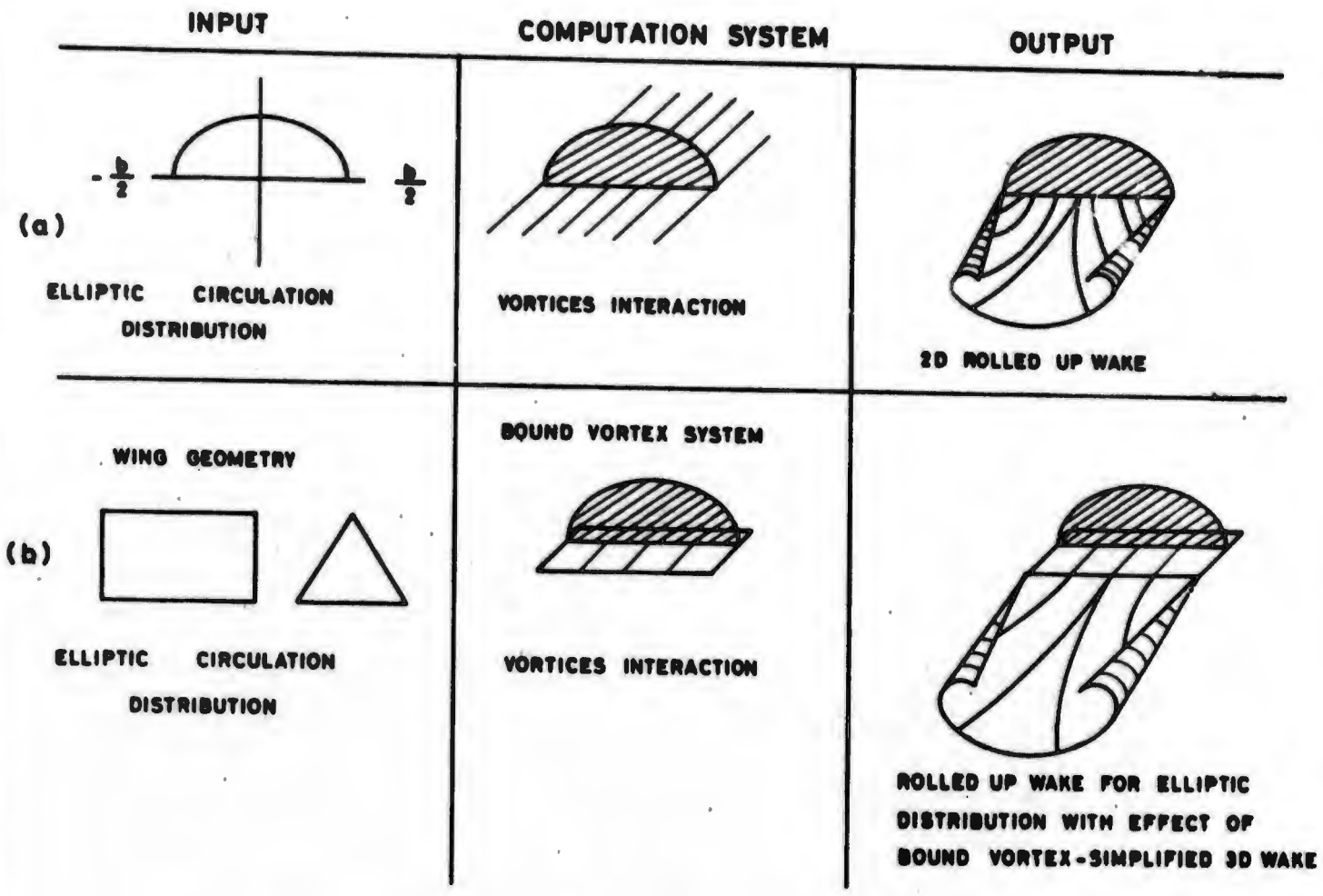


FIG 2 - ELLIPTIC LIFT, VORTEX WAKE CALCULATIONS

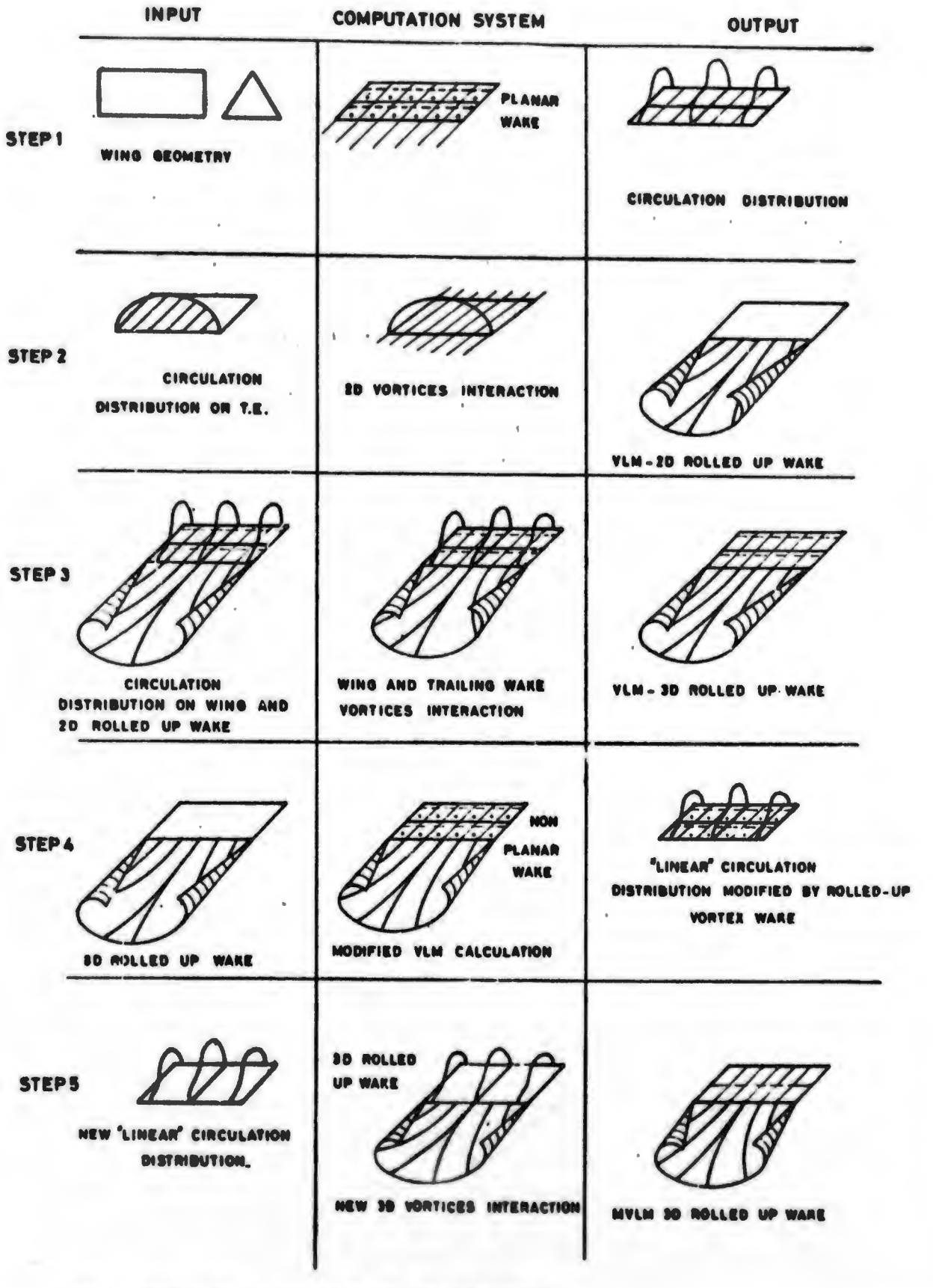


FIG 3 - VLM LIFT VORTEX WAKE CALCULATIONS

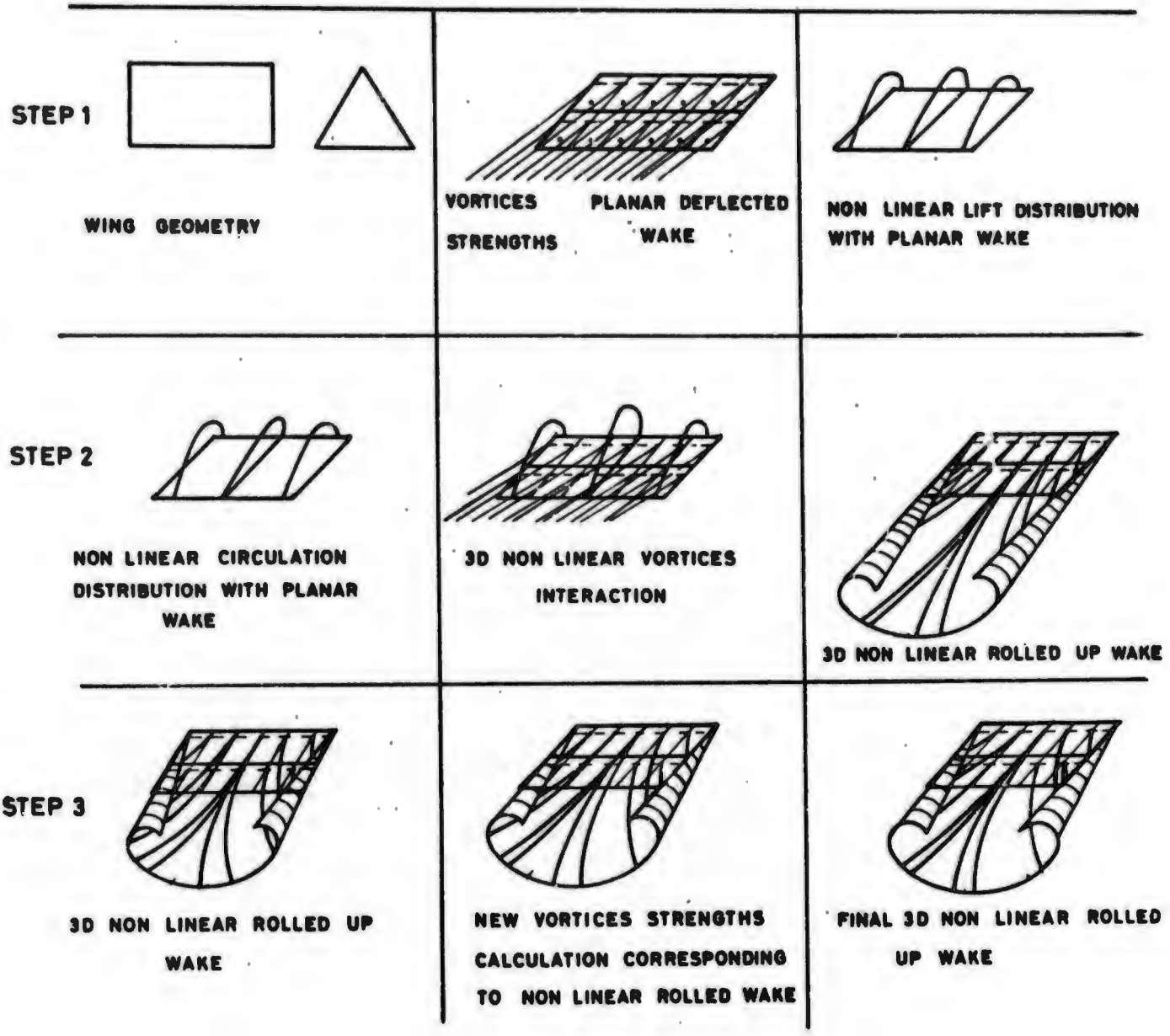


FIG 4 - NON LINEAR VORTEX WAKE CALCULATIONS

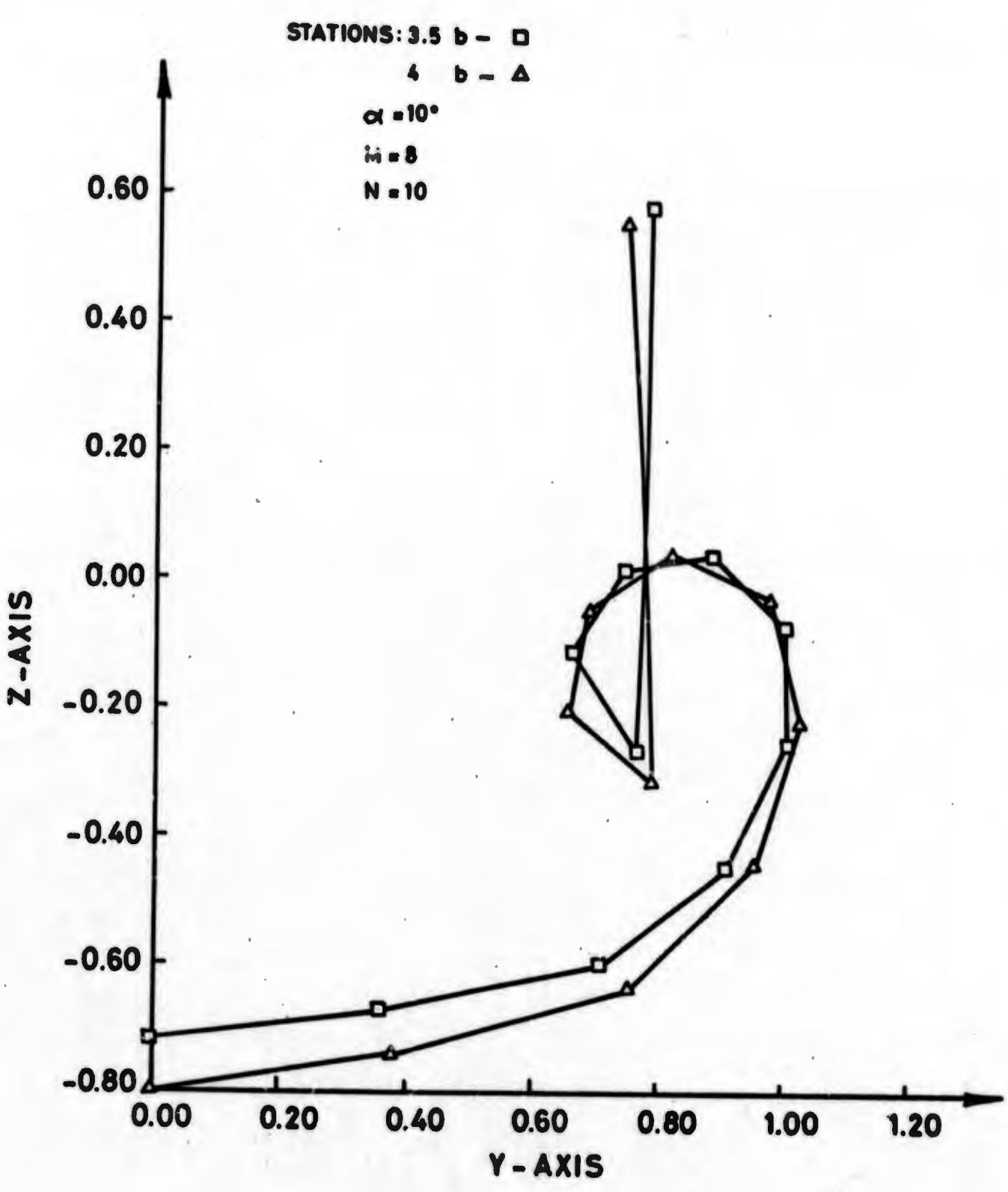


FIGURE 5 - PROBLEMS IN THE CALCULATIONS OF THE VORTEX SHEET ROLL-UP - "ESCAPE" OF THE "TIP" VORTEX.

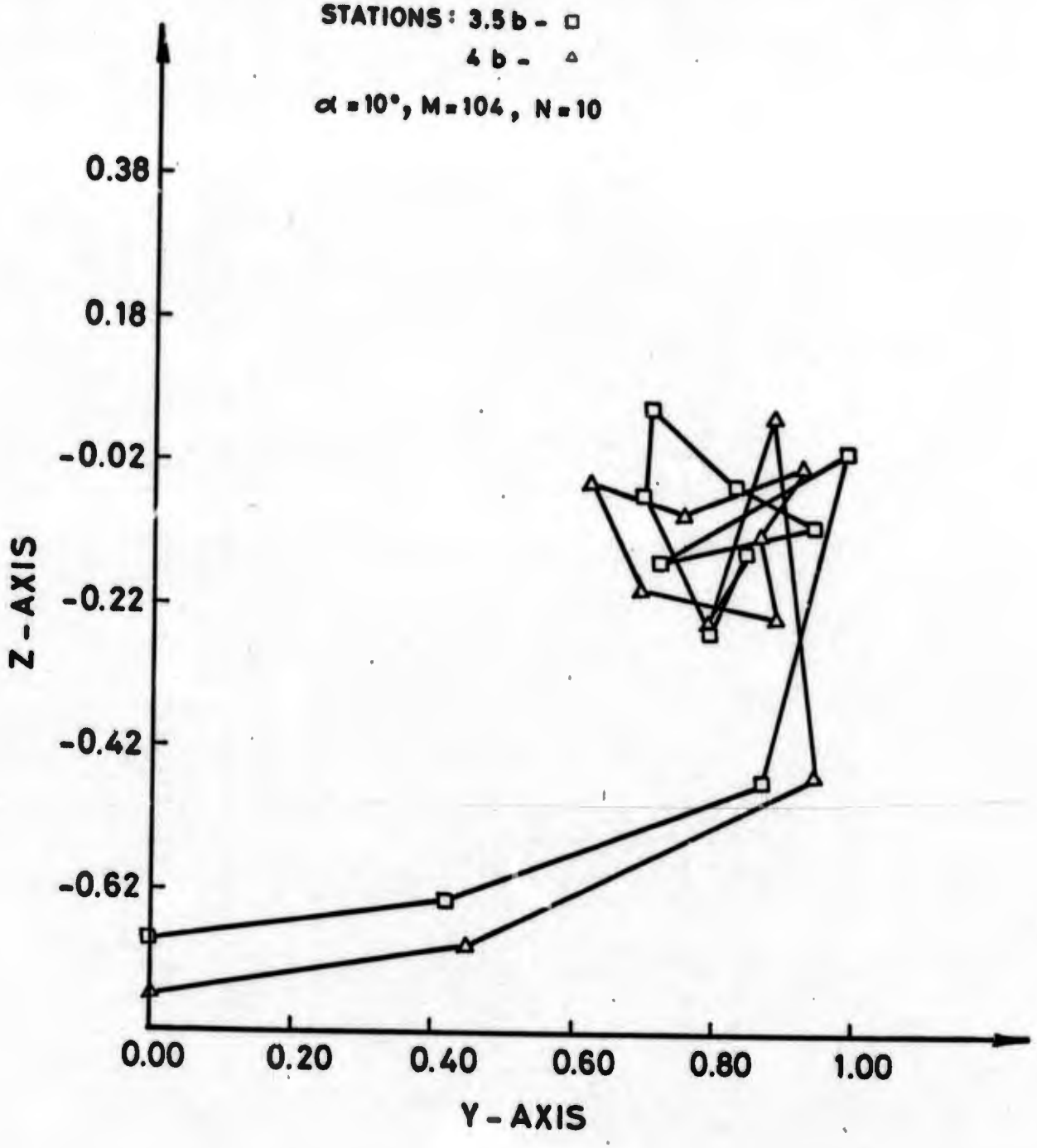


FIGURE 6 - PROBLEMS IN THE CALCULATIONS OF THE VORTEX SHEET ROLL-UP CROSS-OVER OF VORTEX LINES.

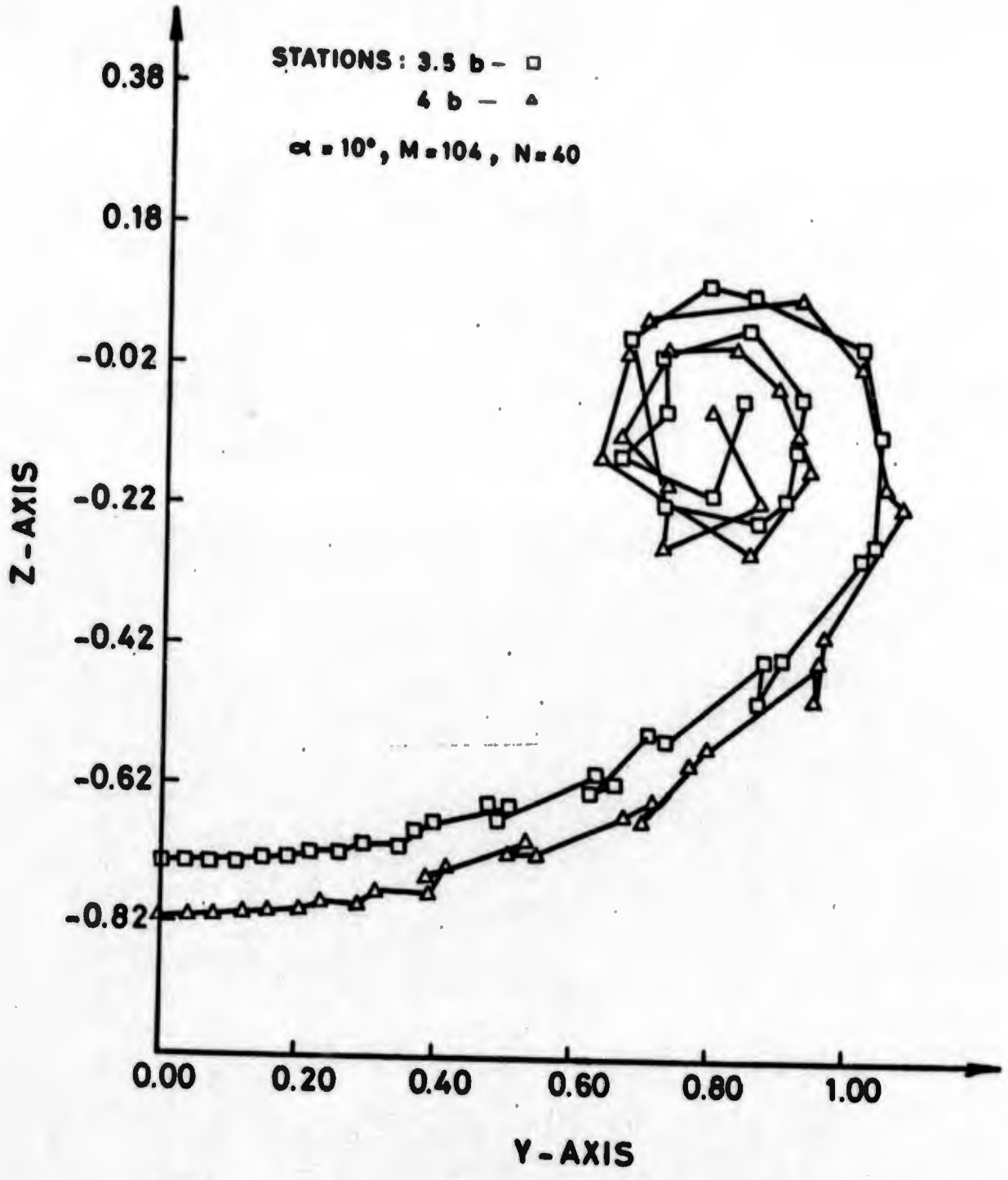


FIGURE 7 - PROBLEMS IN THE CALCULATIONS OF THE VORTEX SHEET ROLL UP - TOO MANY SUBDIVISIONS.

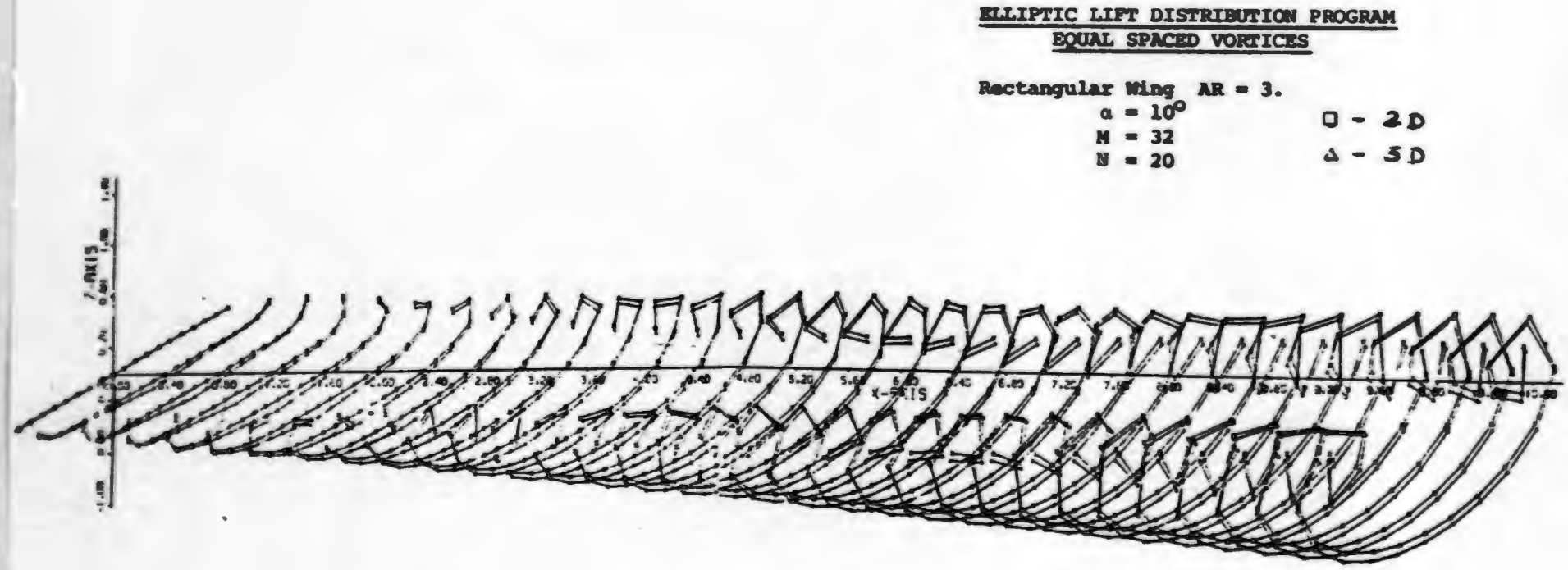


FIGURE 8 - THE TWO AND THREE DIMENSIONAL ROLLED UP WAKE SHAPES CALCULATED BY ELLIPTIC LIFT DISTRIBUTION PROCEDURE. (Figure Axes are given by Half Span Units).

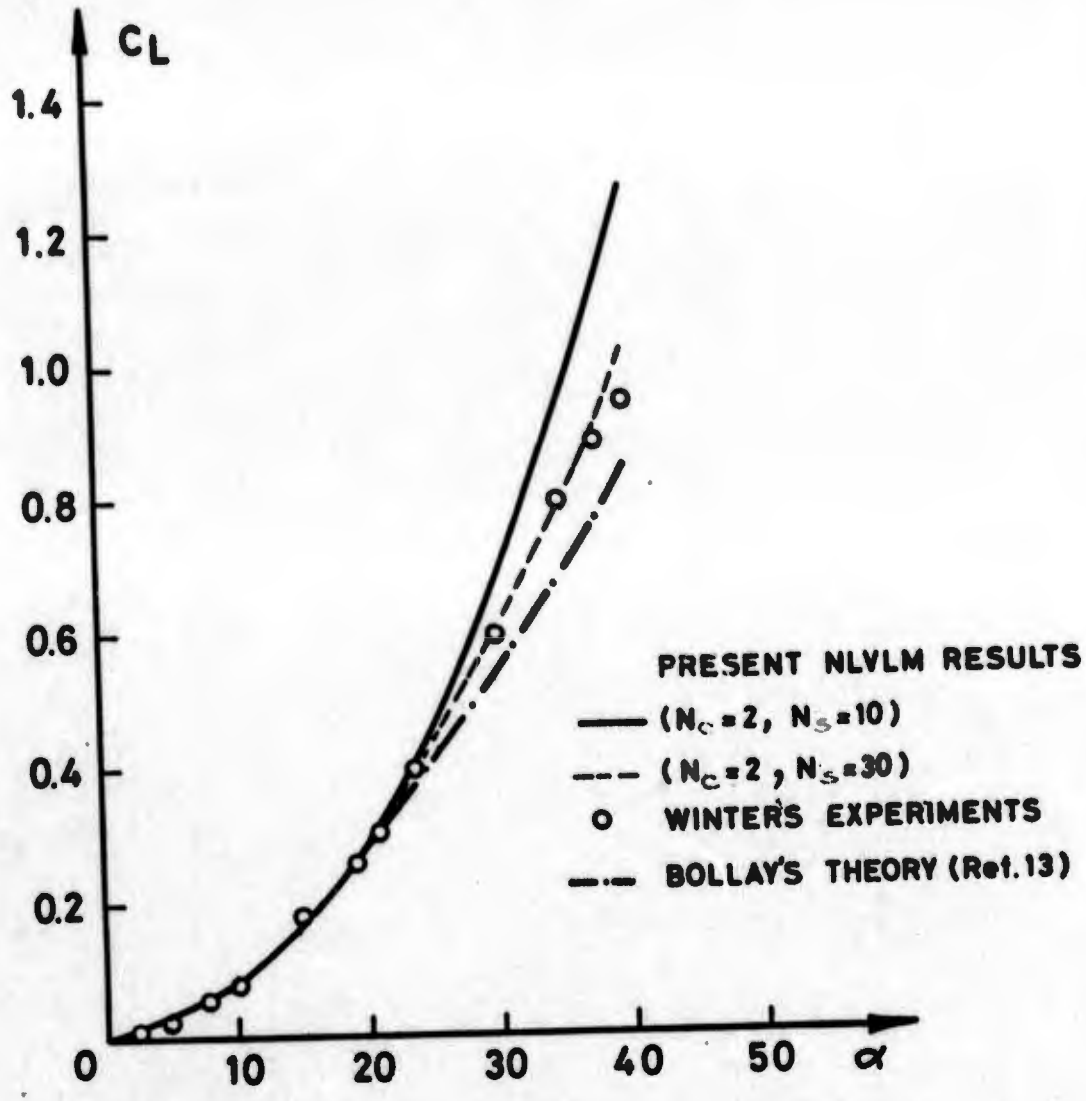


FIGURE 9 - THE LIFT COEFFICIENT CALCULATED BY THE NLVLM PROGRAM COMPARED WITH RESULTS PRESENTED IN REF. 13, FOR RECTANGULAR WING OF AR = 1/30.

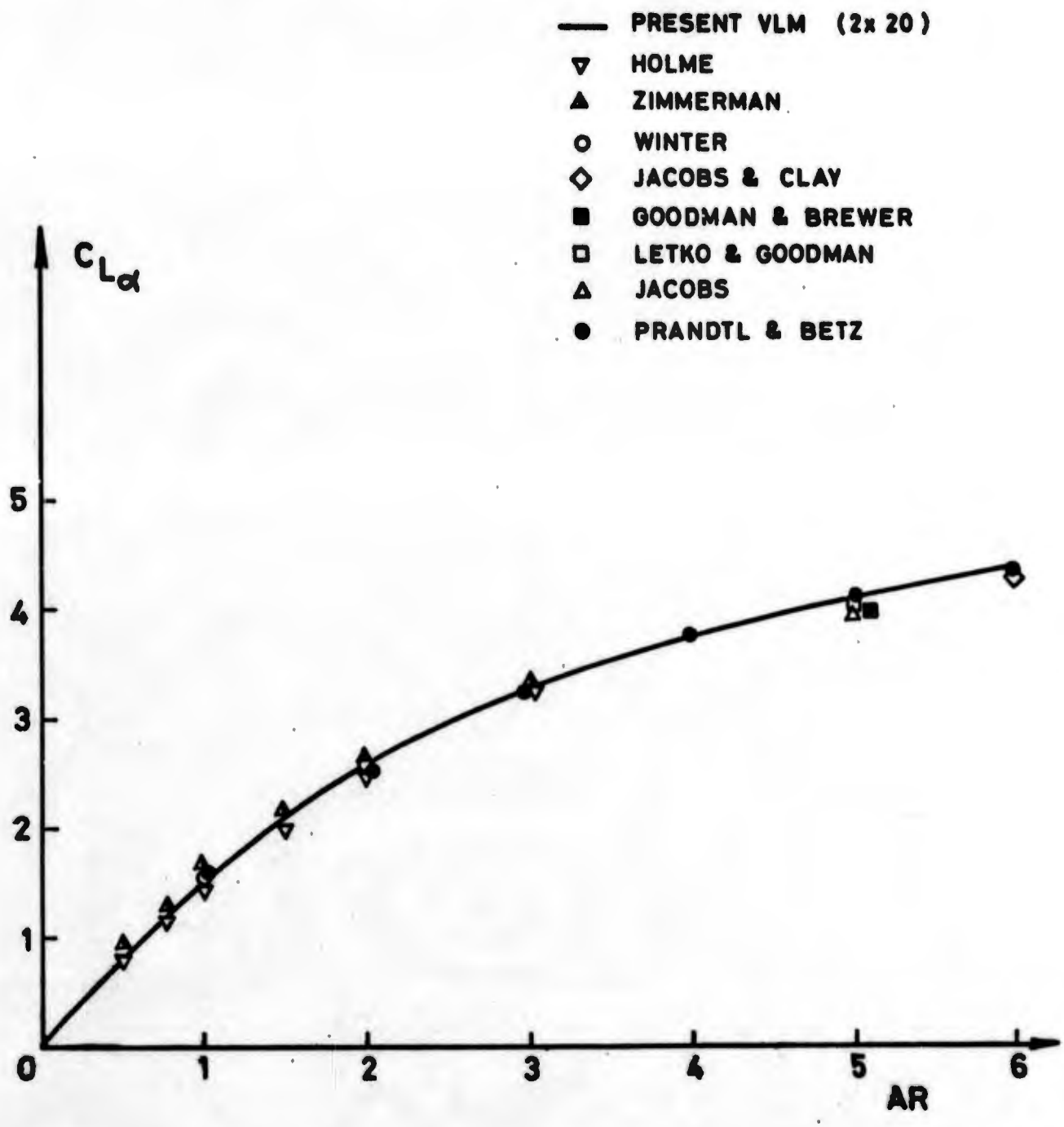


FIGURE 10 - THE LIFT CURVE SLOPE CALCULATED BY THE VLM PROGRAM, COMPARISON WITH EXPERIMENTAL RESULTS (REF. 31, 32) FOR RECTANGULAR WINGS.

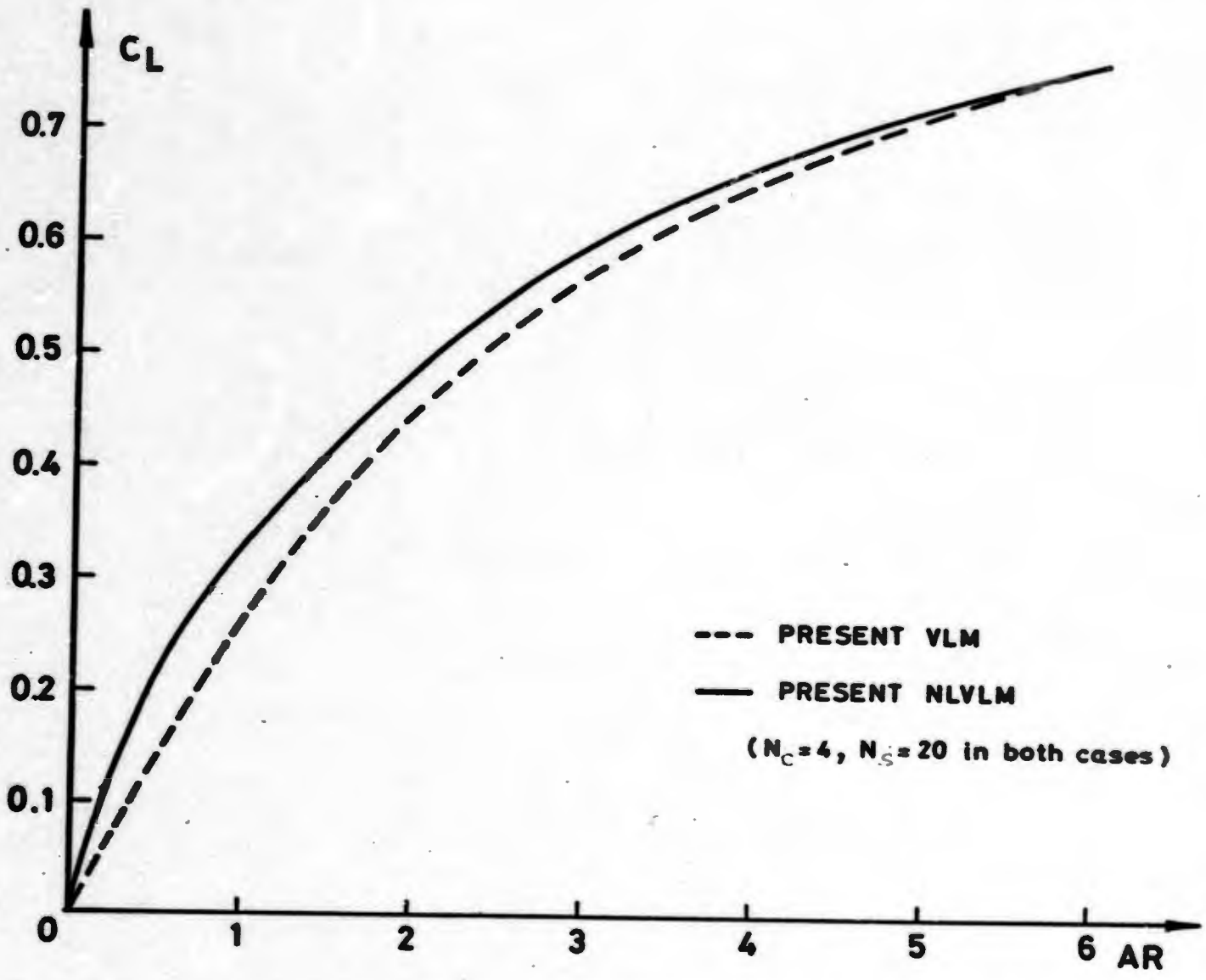


FIGURE 11 - COMPARISON OF THE LINEAR LIFT COEFFICIENT CALCULATED BY THE VLM PROGRAM AND THE NONLINEAR LIFT COEFFICIENT CALCULATED BY THE NLVLM PROGRAM FOR RECTANGULAR WINGS AT $\alpha = 10^{o}$

| | t/c | L.E. | Ref. |
|---|---|---|---|
| o | 0.092 | round | 34 |
| Δ | 0 | round | 34 |
| —PRESENT NLVLM ($N_c$=4, $N_s$=20) | | | |

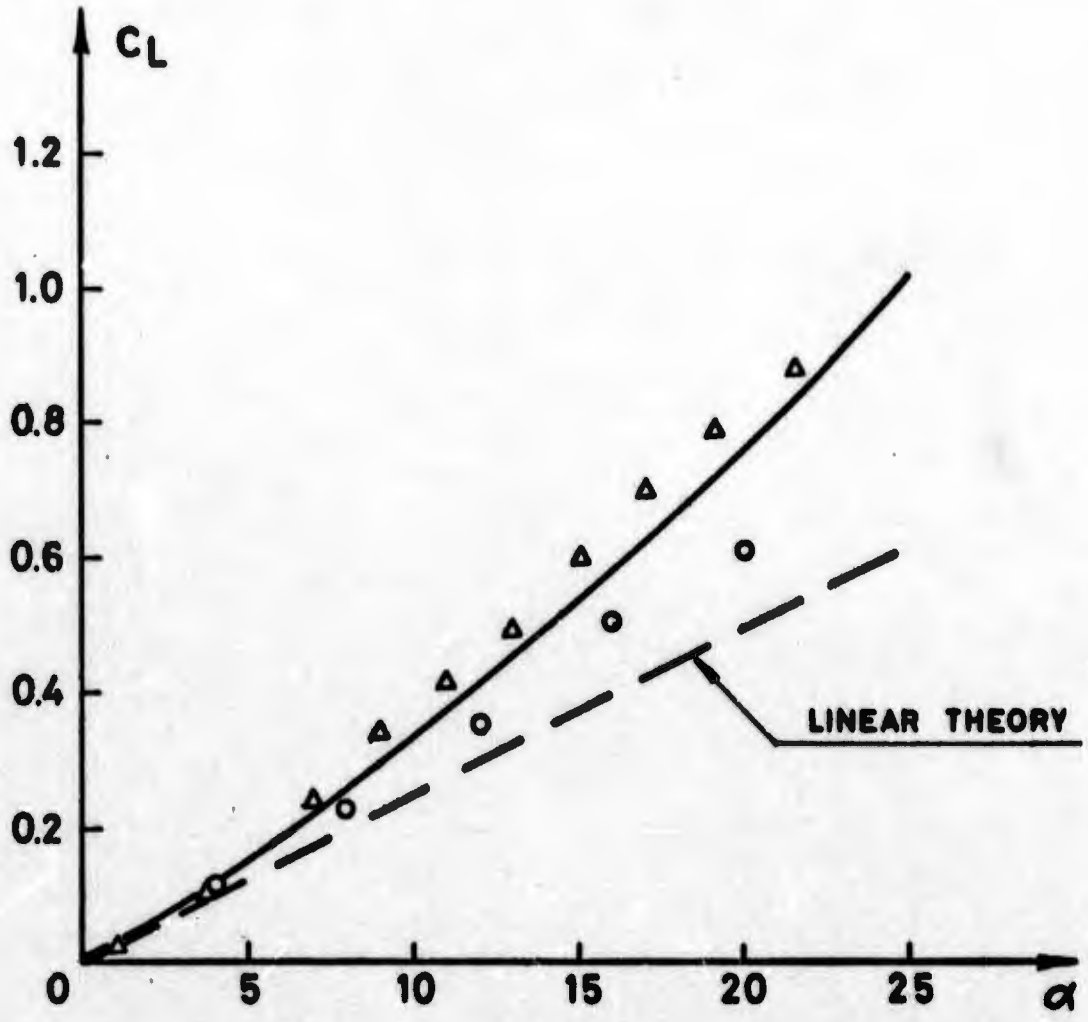


FIGURE 12a - THE LIFT COEFFICIENT OF A RECTANGULAR WING OF AR = 1.

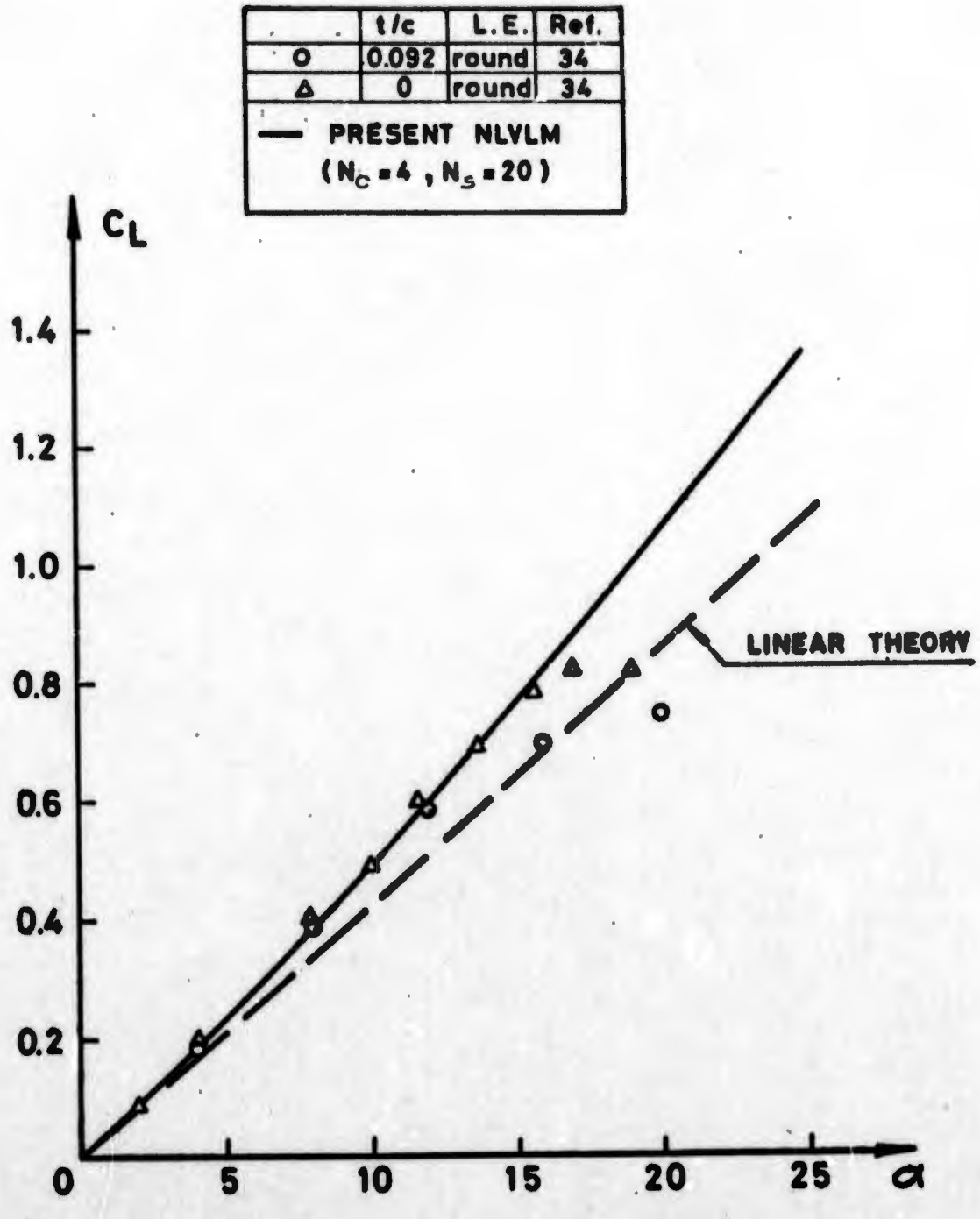


FIGURE 12b - THE LIFT COEFFICIENT OF A RECTANGULAR WING AR = 2.

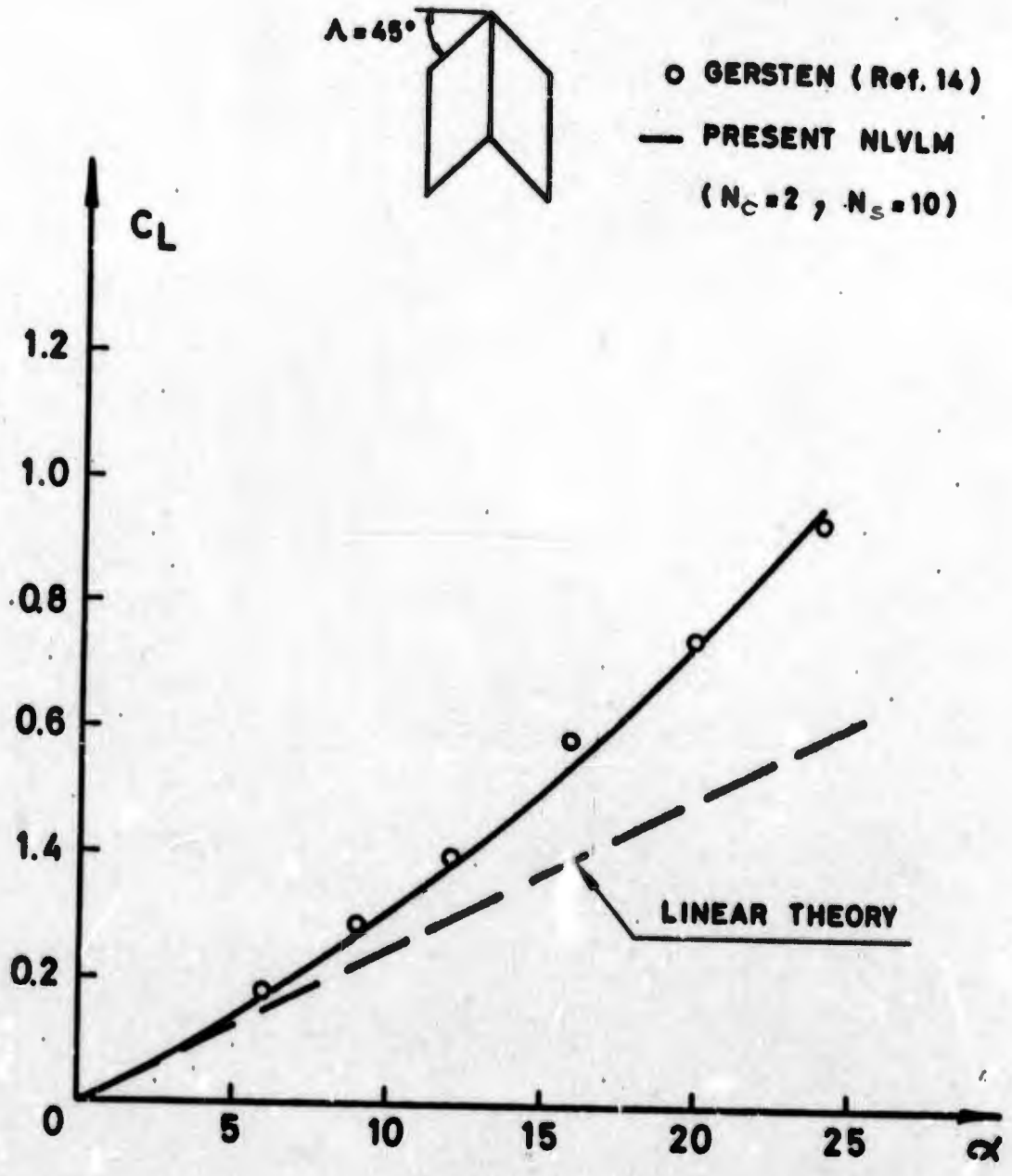


FIGURE 13a - THE LIFT COEFFICIENT OF A SWEPT BACK RECTANGULAR WING OF AR = 1

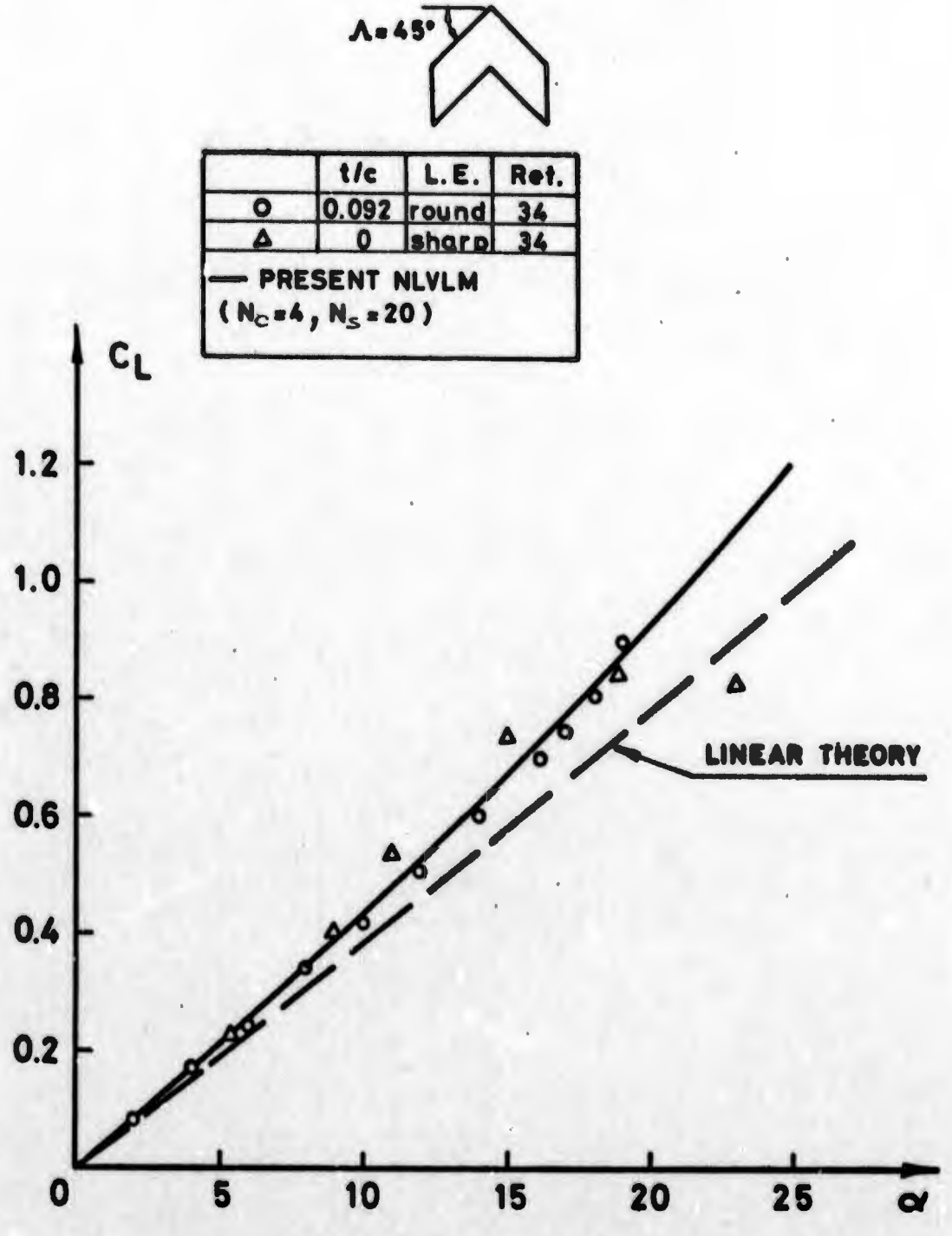


FIGURE 13 b - THE LIFT COEFFICIENT OF SWEPTBACK RECTANGULAR WING OF AR = 2.

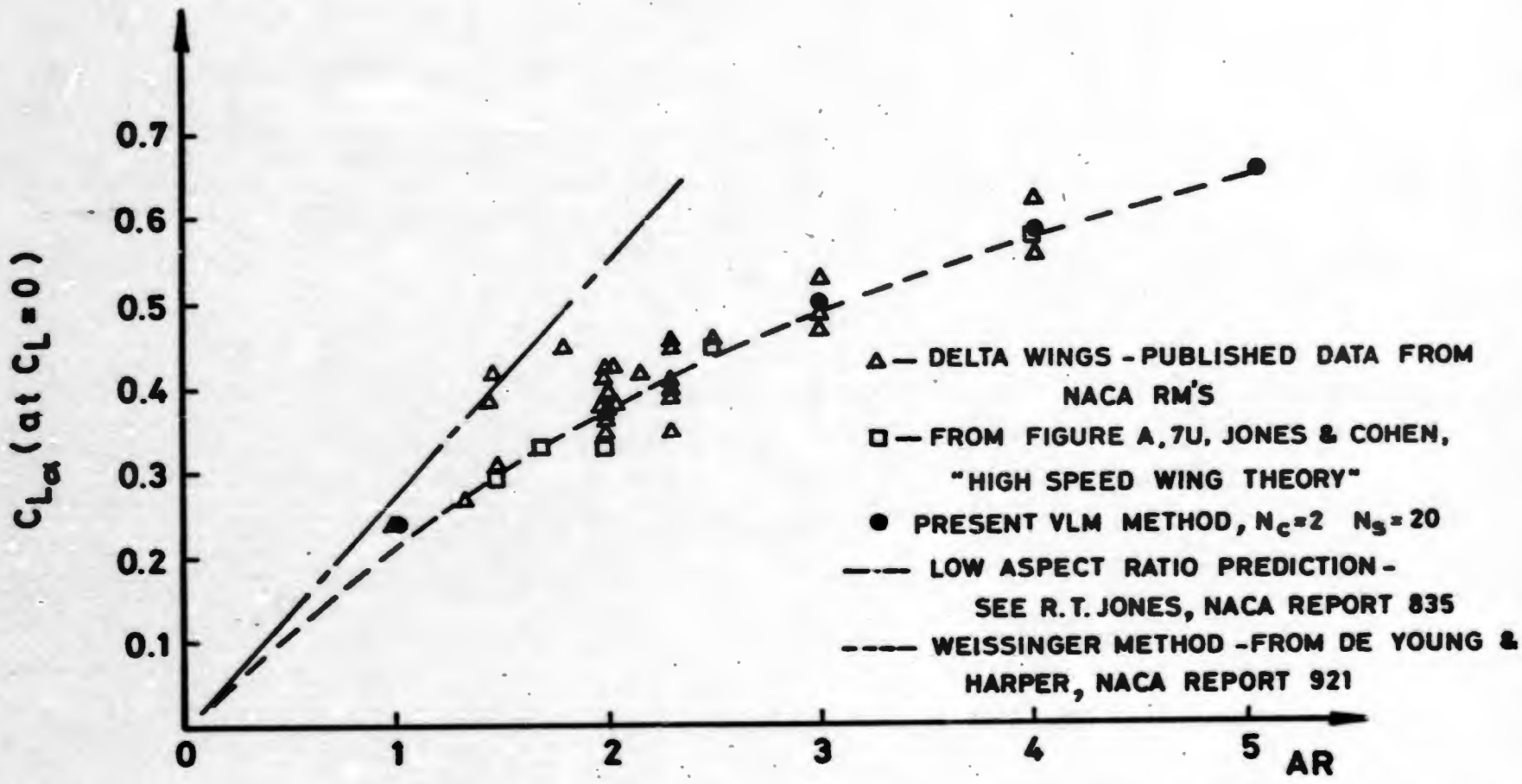


FIGURE 14 - CALCULATED VALUES OF $C_{L_\alpha}$ FOR DELTA WINGS BY THE VLM PROGRAM COMPARED WITH EXPERIMENTAL RESULTS OF REF. (41).

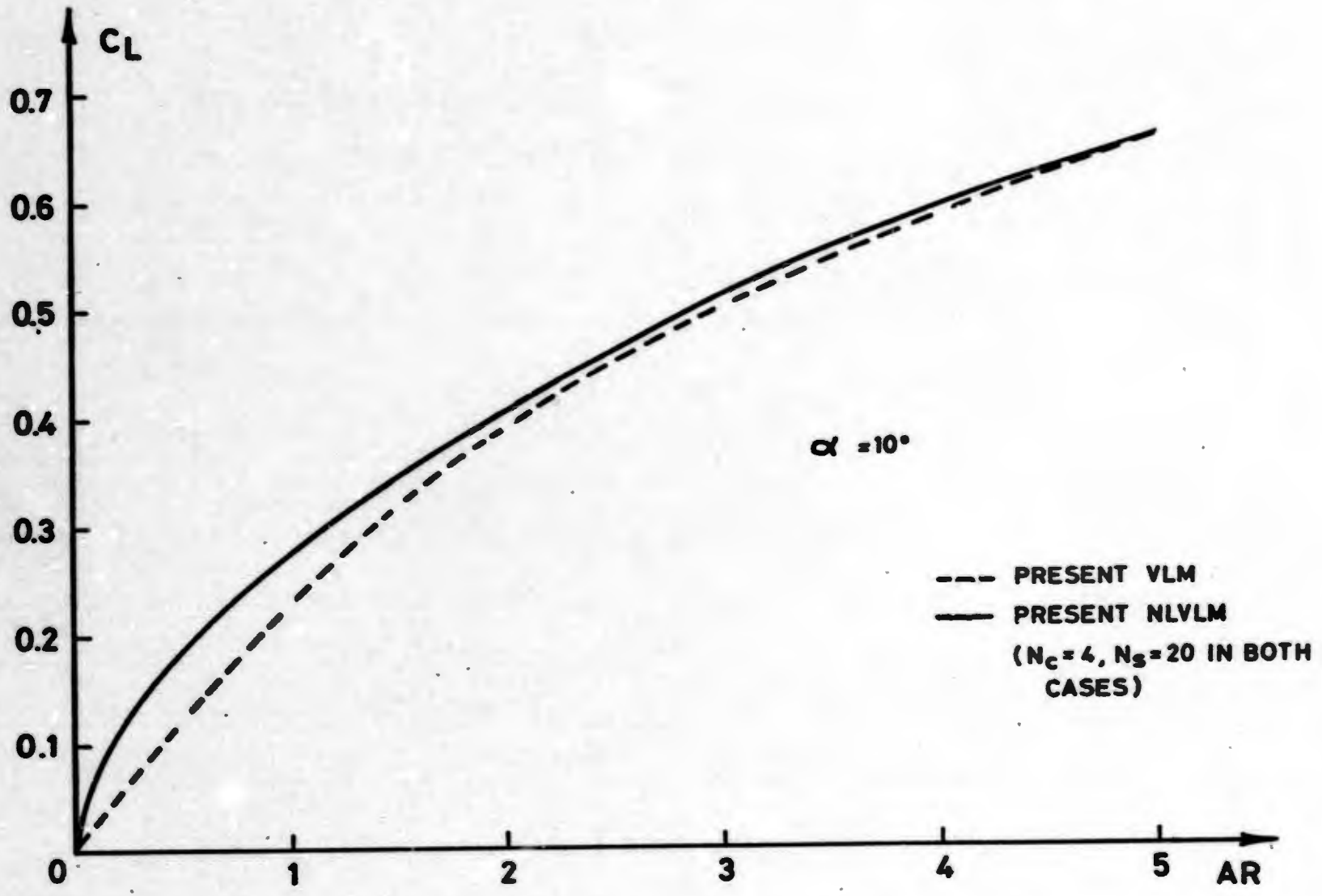


FIGURE 15 - COMPARISON OF THE LINEAR LIFT COEFFICIENT CALCULATED BY THE VLM PROGRAM AND THE NONLINEAR LIFT COEFFICIENT CALCULATED BY THE NLVLM PROGRAM FOR DELTA WINGS AT $\alpha = 10^{o}$

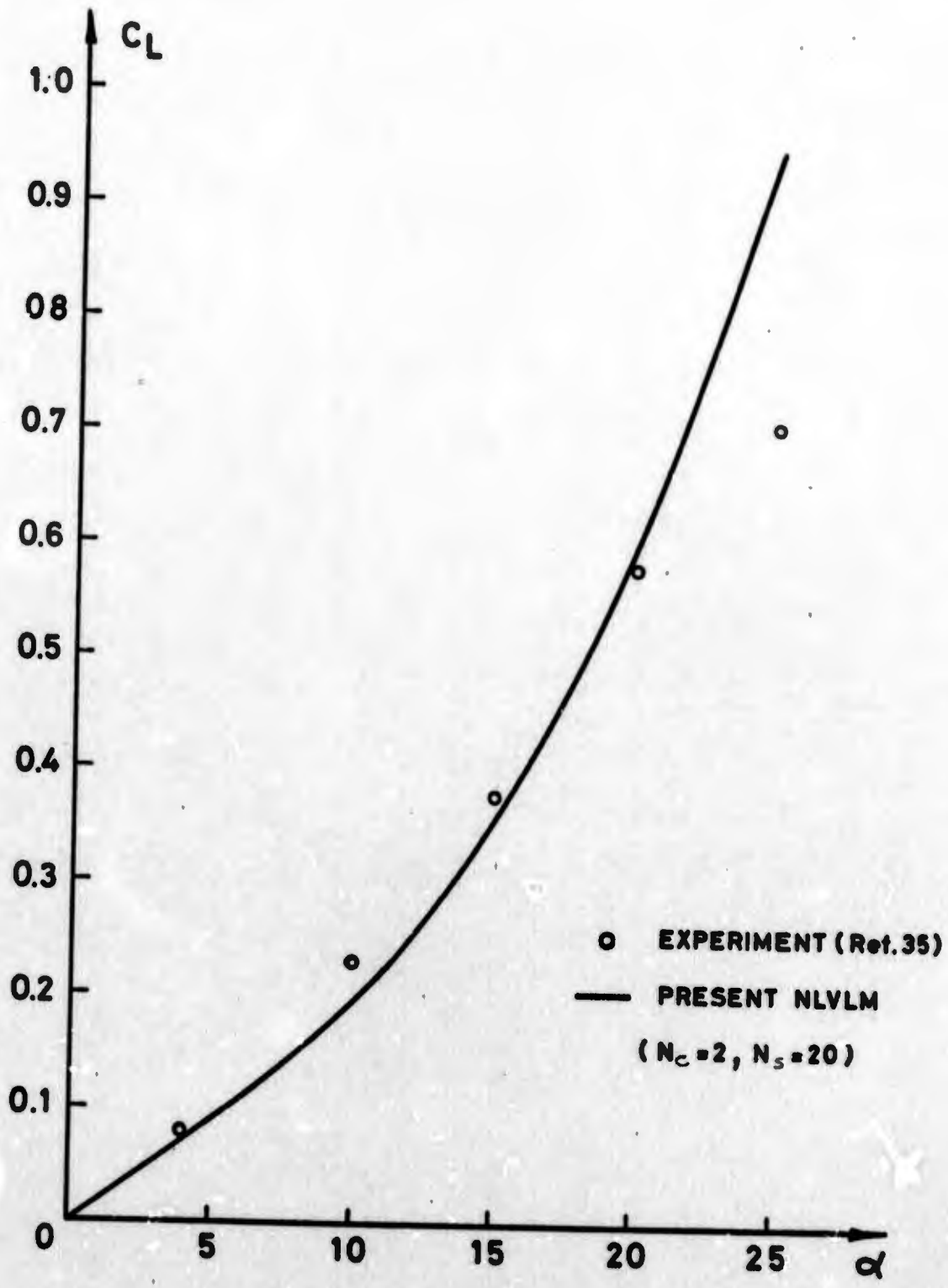


FIGURE 16a - THE LIFT COEFFICIENT OF A DELTA WING OF AR = 0.5.

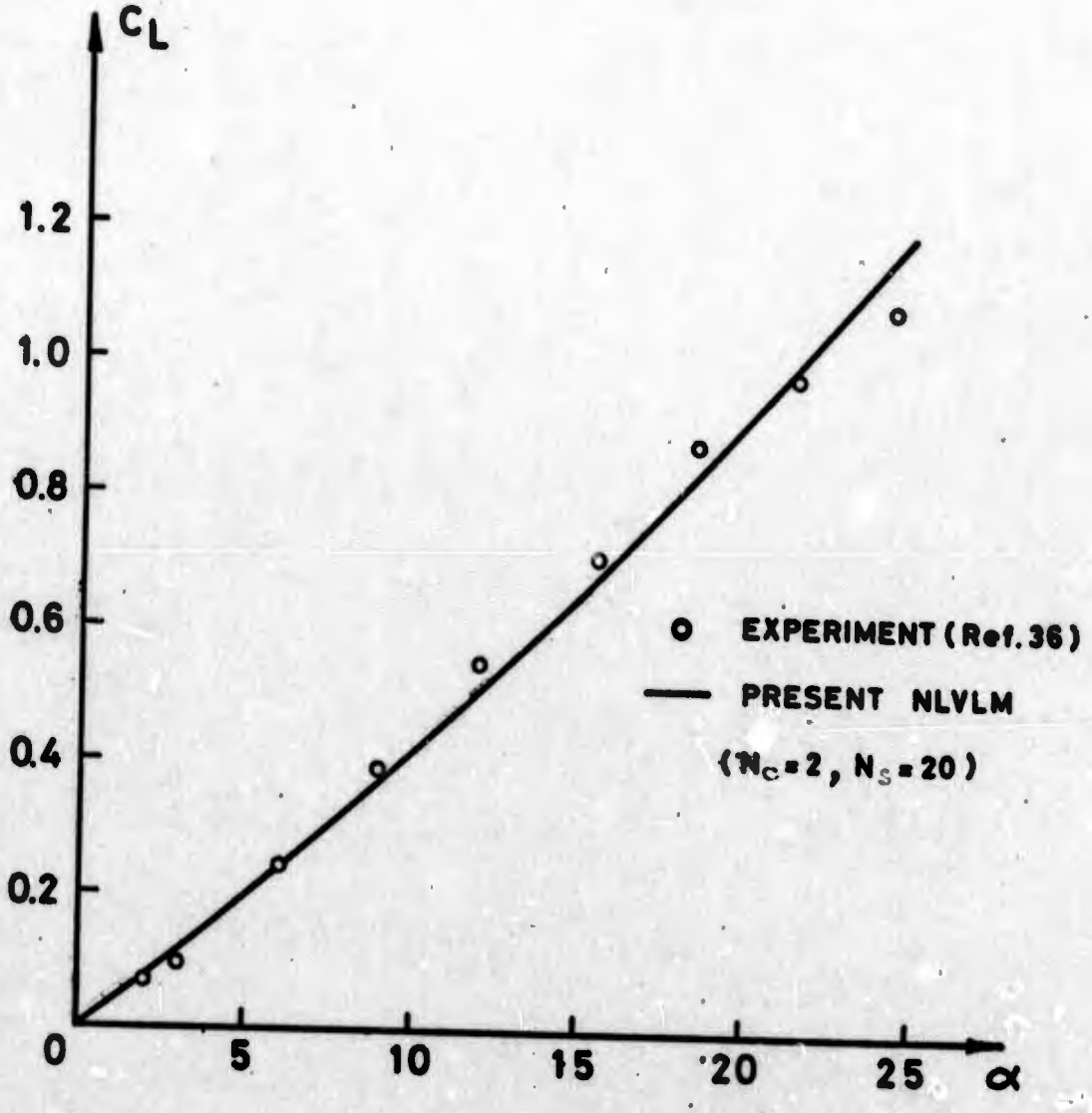


FIGURE 16b - THE LIFT COEFFICIENT OF A DELTA WING OF AR = 2.0.

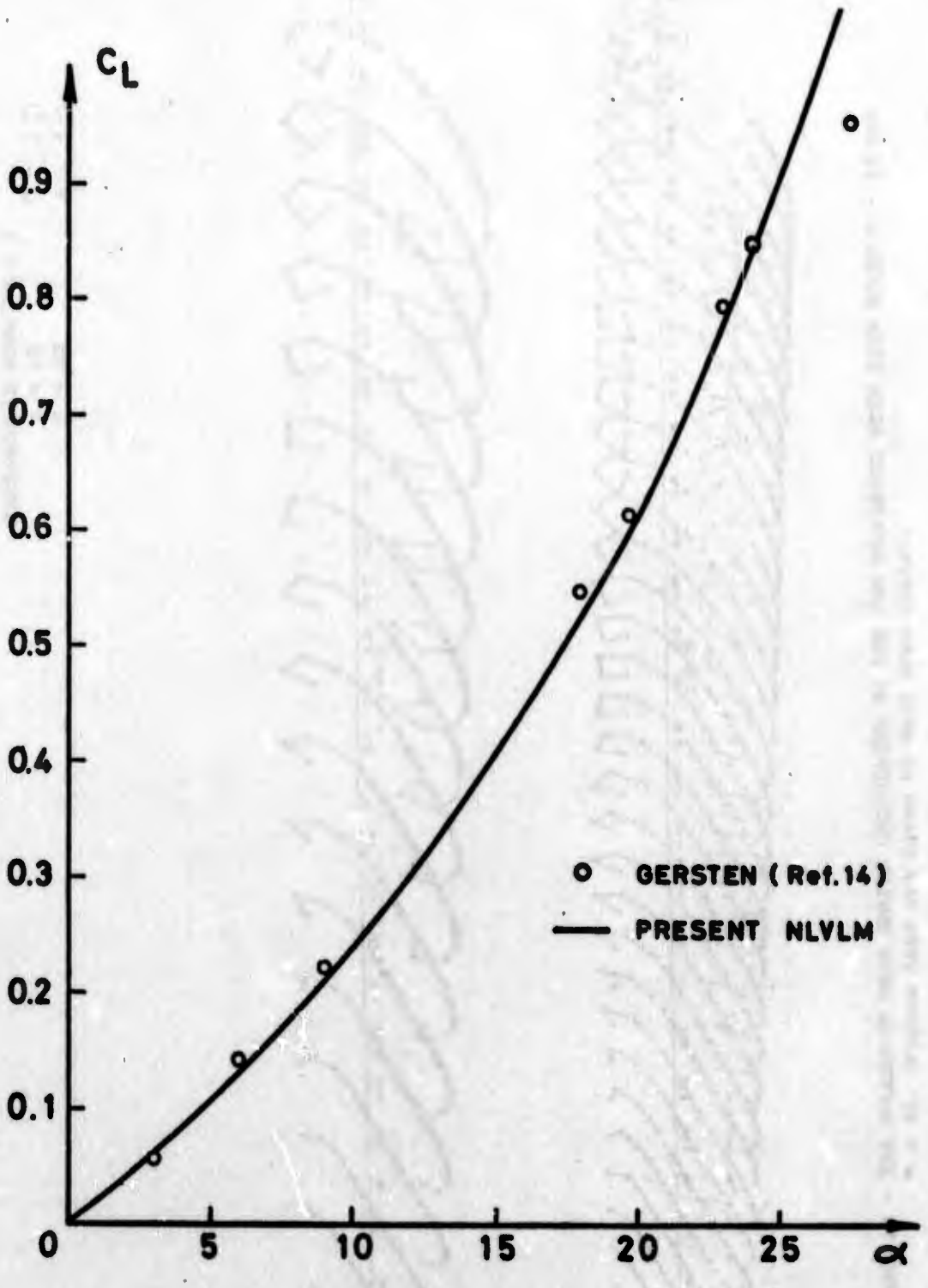


FIGURE 17 - THE LIFT COEFFICIENT OF A CROPPED DELTA WING OF AR = 0.78.

VLM PROGRAM

RECTANGULAR WING AR = 3
α = 10
N = 20

□ - 2D
Δ - 3D

M = 16

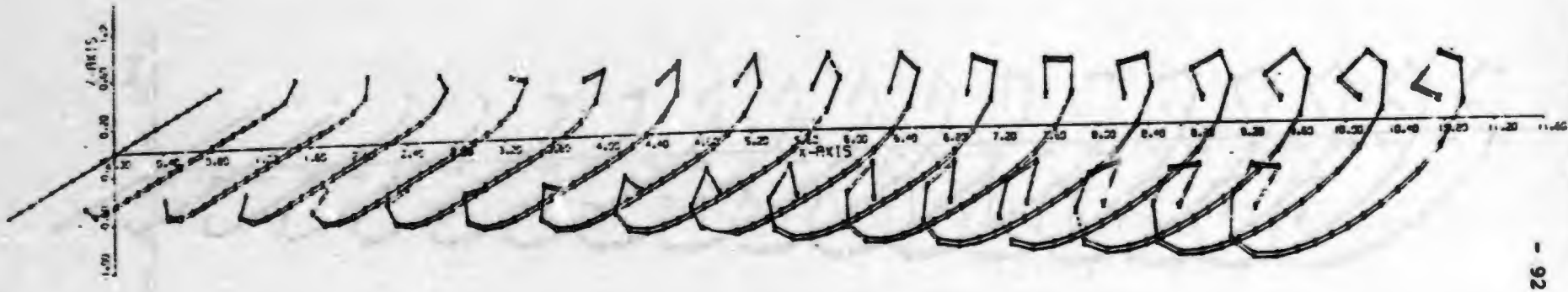


M = 32

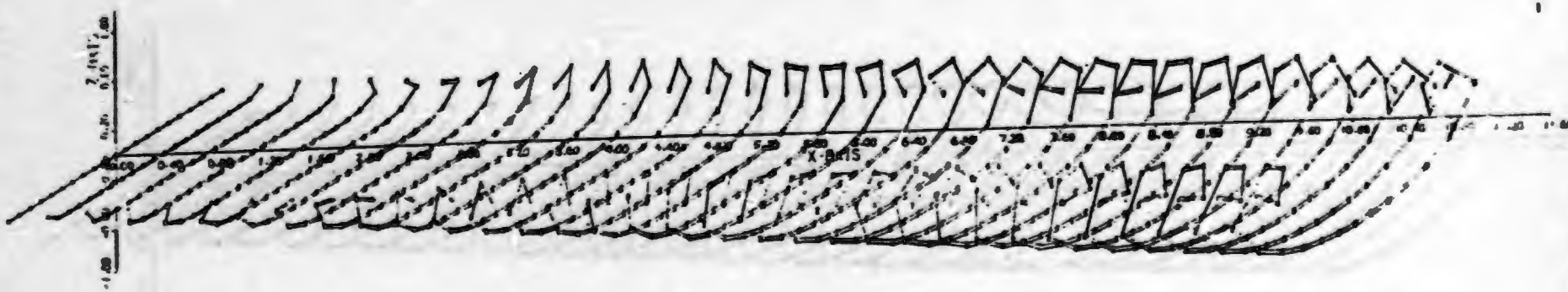


FIGURE 18 - THE ROLLED-UP WAKE SHAPES CALCULATED BY THE VLM PROCEDURE WITH STEP SIZES M = 16 AND M = 32. (Figure Axes are Given by Half Span Units).

MVLM PROGRAM
Rectangular Wing AR = 3
$\alpha = 10^{\circ}$
N = 20

□ – 2D
Δ – 3D

M=16

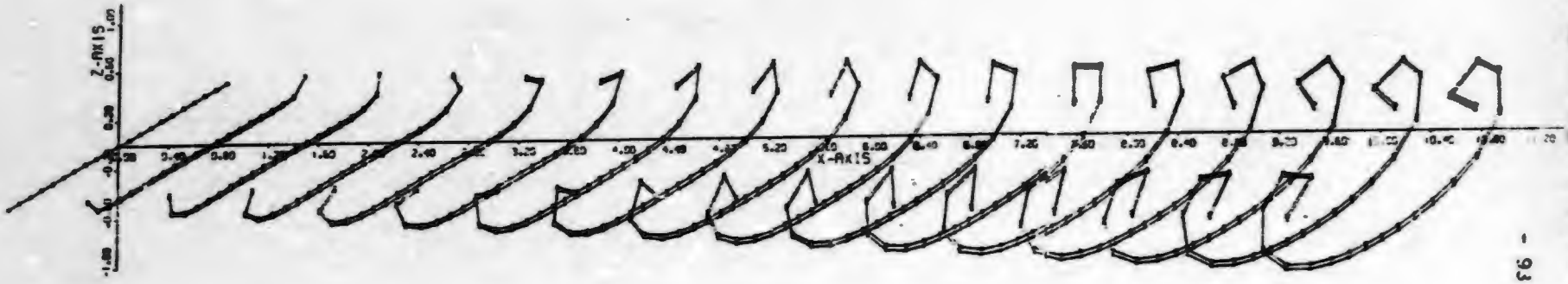


M = 32

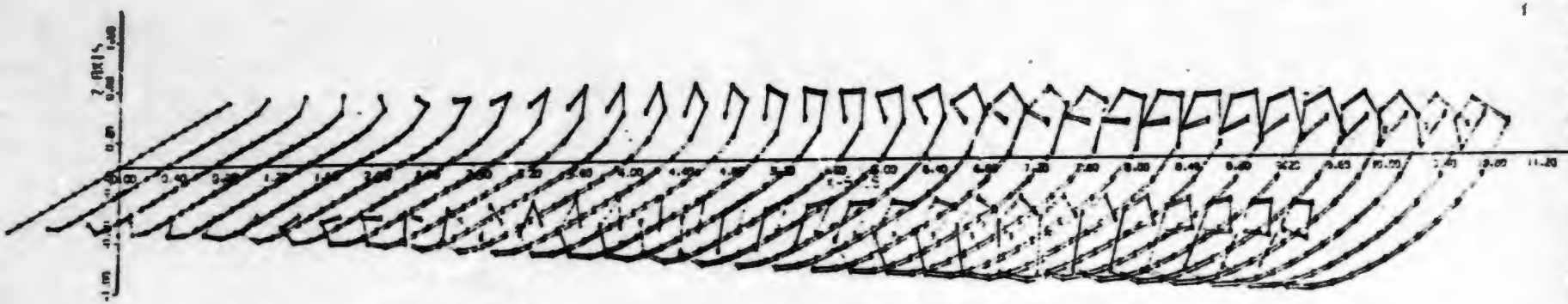


FIGURE 19 - THE ROLLED-UP WAKE SHAPES CALCULATED BY THE MVLM PROCEDURE WITH STEP SIZES M = 16 AND M = 32. (Figure Axes are given in Half Span Units).

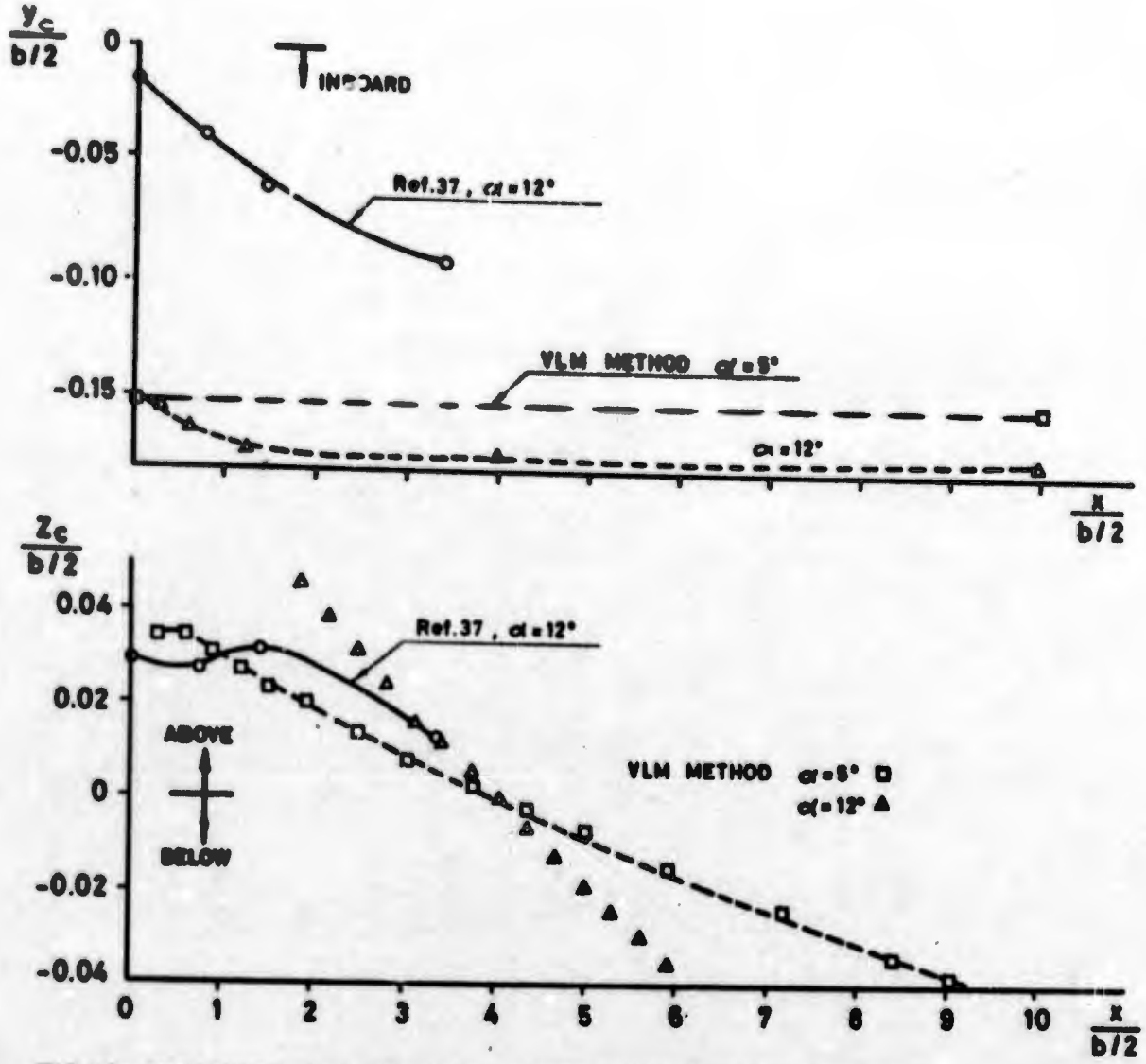


FIG.20 - SPANWISE AND NORMAL LOCATION OF VORTEX CENTER FOR RECTANGULAR WING - AR = 5.33